7-2005

Implications of Long-Term Global Warming and Tectonic Displacements at Buhne Hill, Humboldt County, California

William Page

IMPLICATIONS OF LONG-TERM GLOBAL WARMING AND TECTONIC DISPLACEMENTS AT BUHNE HILL, HUMBOLDT COUNTY, CALIFORNIA

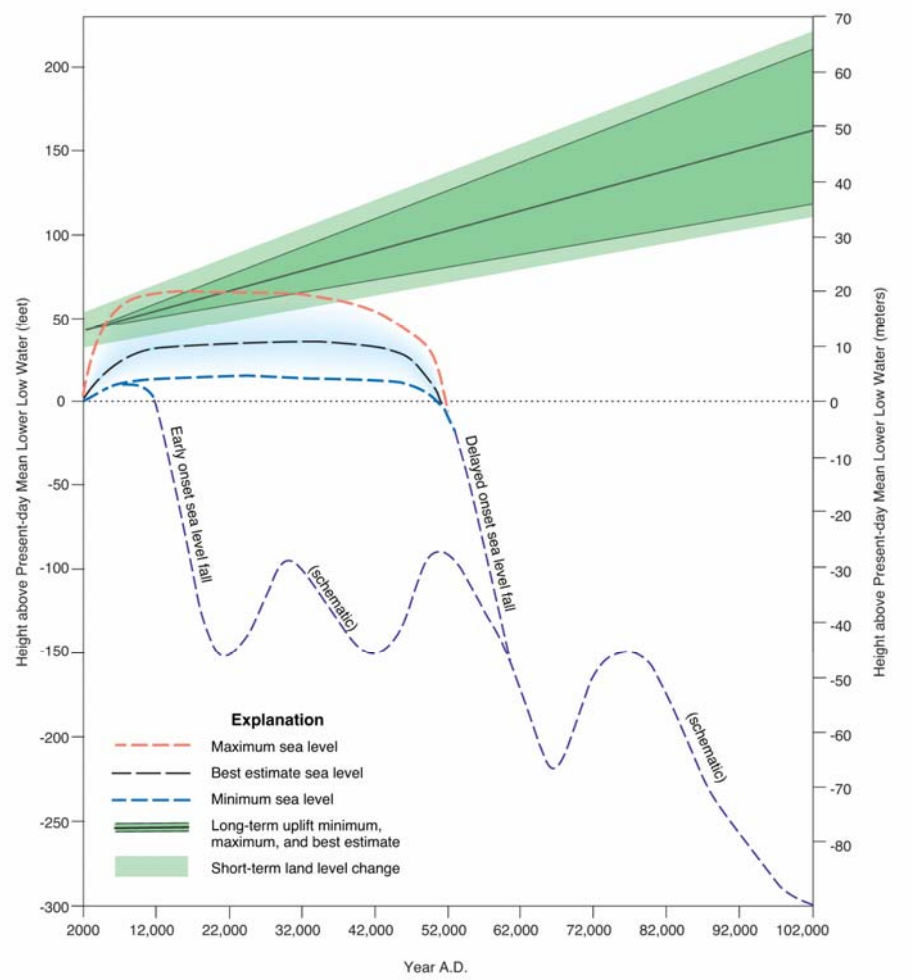

Report to the

California Coastal Commission
San Francisco

July 18, 2005

Prepared by

William D. Page, CEG No. 1432
PG&E Geosciences Department
San Francisco

TABLE OF CONTENTS

LIST OF FIGURES AND PHOTOS

IMPLICATIONS OF LONG-TERM GLOBAL WARMING AND TECTONIC DISPLACEMENTS AT BUHNE HILL, HUMBOLDT COUNTY, CALIFORNIA

SUMMARY

In response to the California Coastal Commission's request to analyze PG&E's proposed ISFSI site on Buhne Hill at Humboldt Bay for stability 'in perpetuity' (question #1) we have chosen scenarios up to 100,000 years in the future to model potential changes for two geologic hazards:

1. Surface faulting hazard, related to the tectonic movement of the Little Salmon fault zone, and
2. Coastal erosion hazard, related to projected sea level rise and Pacific storm variability in an environment of global warming and tectonic uplift of Buhne Hill.

The possible impacts of several scenarios are analyzed to assess the effectiveness of the coastal protection works that protect Buhne Hill from wave erosion.

The proposed ISFSI site is next to the PG&E Humboldt Bay Power Plant on Buhne Hill, a small promontory that is opposite the entrance to Humboldt Bay. The hill's bay-facing Red Bluff was severely eroded following the enhancement of the channel after the 1850s. The erosion stopped when the bluff was protected by a riprap berm placed in the 1950s. The ISFSI will consist of several robust canisters containing the waste that will be placed in a covered, reinforced concrete vault set below grade at elevation 44 feet (MLLW).

Surface Faulting

The ISFSI site is on the hanging wall (up-thrown side) of the Little Salmon fault zone, a major reverse fault connected to the Cascadia subduction zone. A secondary splay fault within the zone, the Buhne Point fault, dips beneath the ISFSI at a depth of 500 feet. Stratigraphic evidence proves the site has not had any surface displacement in the past 80,000 years. Applying models of movement on reverse faults, repeated displacement of 1 to 2 meters on the Buhne Point fault from large magnitude earthquakes on the Little Salmon fault zone will produce uplift and translation of the ISFSI site for the next tens of thousands of years. Surface faulting beneath the vault will be limited to fractures with small offsets of up to a few inches in the event that the translation of the site passes through a fault-bend-fold that projects to a bend in the fault at depth. If erosion is added to the model, the vault eventually will be translated to the bluff's edge, where it will be exposed to erosion. This eventuality would also take tens of thousands of years and tectonic uplift in this time period will raise the ISFSI high above sea level. The possibility of the Buhne Point fault changing geometry so that it might rupture directly beneath the ISFSI is not considered likely.

Effects of Global Warming

Analyses of the effect of global warming on relative sea level change and change in storminess of the Pacific entails several considerations. Relative sea level change results from both land level change and global sea level change. Land level change at Buhne Hill is dominated by long-term tectonic uplift at a rate of 1.2 ± 0.5 feet per thousand years (0.4 ± 0.1 mm/yr). Short-term land level change is dominated by elastic strain accumulation and release on the Cascadia subduction zone and Little Salmon fault zone. Estimates of current land level change at Buhne Hill are about 1.3 feet of uplift per hundred years (4 mm/yr) of interseismic uplift. Expected land level change during a major earthquake ranges from small amount of uplift or down dropping in one model to abrupt down dropping of about six feet (1.8 m) to a moderate amount of abrupt uplift in the other model; in either case, King Salmon, which is on the footwall of he fault will be down dropped several meters. The short-term pattern of interseismic and coseismic land level changes will result in long-term uplift of Buhne Hill.

Global warming over the next century and beyond will cause a rise in sea level and probably changed storm intensity and frequency. The context for evaluating sea level change over the very long term is an assumption that the earth's climate remains in the cycle of glacial and interglacial intervals that have persisted for the past 2.5 million years. During the Holocene, the current interglacial interval, sea level has risen steadily in response to melting of continental ice since the last glacial maximum, although sea-level rise has been slow and gradual for the past 3,000 years or so. Climate conditions and sea level during the Holocene are similar to but apparently less variable than conditions during past interglacial periods. Current emissions of greenhouse gasses, most notably carbon dioxide and methane, have produced higher atmospheric concentrations of those gasses than at any time in the past 420,000 years, and projected increase in temperature and rise in sea level are expected to occur at rates that are an order of magnitude or higher than rates typical of the past few thousand years. Changes in earth's orbit around the sun cause predictable variations in the solar insolation on earth, and these orbital variations closely correlate with glacial and interglacial cycles in the past. Current and projected solar insolation, combined with present day and near-future anthropogenic rise in greenhouse gasses, suggest that the earth may miss the next opportunity to enter the next glacial interval and hence global cooling may not start for another 50,000 years.

In our analysis we model the tectonic uplift of Buhne Hill and superimpose the potential range of sea level rise under several scenarios for time periods of 100, 1,000, 10,000 and 100,000 years. Over the next few hundred years sea level is expected to rise between less than one to as much as six feet, based on the 2001 report on climate change by the Intergovernmental Panel on Climate Change. In the thousand to ten thousand year time period sea level may rise and approach the ISFSI elevation with the extreme scenario of it being over topped. The maximum rate of sea level rise is not expected to exceed about 3.3 feet per century (10 mm/yr), the maximum rate of sea level rise recorded during an interglacial interval in the geologic record for the past 400,000 years. In the scenario forecasts that consider climate change over for tens of thousands of years, glacial intervals

are expected to resume with a corresponding drop in sea level. In all scenarios the long term tectonic uplift of the site tends to counter sea level rise.

Tsunami Potential

For the design of the ISFSI on Buhne Hill the site was chosen the 44 foot elevation to be above the estimated maximum tsunami runup of 36 feet (MLLW) from a near-source Cascadia earthquake. The runup was based on analysis of paleo-tsunamis in the past 3,000 years that showed runups did not exceed about 40 feet (MLLW) at the coast. Considering the potential rise in sea level from global warming discussed above, a Cascadia tsunami potentially may over top the ISFSI. Also in the time frames of tens of thousands to 100,000 years, a larger tsunami caused by an earthquake triggered submarine landslide offshore or a Sumatra type tsunami is possible.

Conclusions

Based on our analysis we form the following conclusions for the several aspects raised by the Coastal Commission's question #1.

Surface faulting - After many tens of thousands of years translation through a fault-bend-fold will subject the vault to tilting and small offsets at the base of the vault. Neither of these will damage the vault, and the tilting of the vault does not impact the integrity of the casks. After tens of thousands of years erosion may encroach on the ISFSI. In these scenarios PG&E would relocate the vault to a safer location on Buhne Hill before the ISFSI reached the area susceptible to bluff erosion.

Rise in sea level from global warming – Rise in sea level is a slow process (0.26 to 3.3 feet/100 years) and would be monitored. As the riprap protection at Buhne Hill was damaged, or possibly impacted, during increased storm activity and other changed conditions, additional riprap or other protection would be placed in front of Red Bluff and around Buhne Hill to insure the protection of the ISFSI. Over the next 100 years, barring a major earthquake on the Cascadia subduction zone, interseismic uplift will likely keep pace with sea level rise. However, a major earthquake on the Cascadia subduction zone would down drop King Salmon but may or may not cause abrupt coseismic subsidence of Buhne Hill of up to about six feet (two meters). In this occurrence, PG&E would evaluate the integrity of the coastal protection works following the event and place additional riprap or other protection in front of Red Bluff to insure the protection of the ISFSI. In the unlikely scenario that the sea level rose above the elevation of the ISFSI in several thousand years, the site would be moved to a safe location.

Tsunami impacts – If a tsunami overtops the ISFSI no damage is expected because the casks are designed to be submerged. The site is also set below grade so the potential impact from large objects, such as a ship, hitting the site is not a concern. Tsunamis undoubtedly would cause damage to the riprap protection at Buhne Hill and erode the hillslope around the site. The site is more than 50 feet from the edge of Red Bluff so any erosion from the limited number of runup surges impacting Buhne Hill would not reach the ISFSI even during an

extreme event. After the tsunami had subsided, the area would be assessed, coastal protection restored, and any erosion repaired.

1.0 INTRODUCTION

The California Coastal Commission in their letter from Mr. Tom Luster of April 19, 2005 to Mr. Roy Willis requested additional technical information to support the proposed ISFSI site at Buhne Hill adjacent to PG&E Humboldt Bay Power Plant. The information request #1 in their letter is abstracted below:

> 'We … request that you provide long-term analyses of the conditions of your proposed site and facility.' … because … 'there are no foreseeable alternative sites available for the spent fuel … the project would likely be at the site in perpetuity.' Please provide 'Analysis of geologic and coastal hazards for longer periods than the five to fifty years currently on the project application. These analyses should include the effects of seismic activity, coastal erosion, sea level rise, tsunami runup, and increased significant wave heights. We also request you to describe how the proposed project would be affected by those types of events and describe what changes would be necessary to the existing shoreline protective structure at the site to protect the project.'

This report responds to the above request that PG&E evaluate the safety of the Humboldt Bay ISFSI on Buhne Hill "in perpetuity." The request specifies that PG&E address the potential hazards from erosion caused by future sea level rise and changing wave heights and durations in response to projected global warming. A second part of the request asked for an analysis of the potential for surface faulting for time periods of tens of thousands of years.

Our response to the information request is based on analysis of the above issues following discussions with Dr. Mark Johnsson in May 2005. These discussions were held during a field review of the ISFSI site, the coastal protection at Buhne Point, the Little Salmon fault zone investigation sites, and several tsunami investigation sites. The response addresses two separate hazards as two parts that are discussed below as separate sections of this report.

Section 2 Analysis of surface faulting potential, and
Section 3 Implication of future sea level changes at Buhne Hill

1.1 SETTING

The Humboldt Bay ISFSI lies directly east of the entrance to Humboldt Bay on the lee side of Red Bluff, the northwest facing side of Buhne Hill (also called Buhne Point) (Figure 1-1; Photo 1-1). Buhne Hill is a small topographic high that is bordered by marshes to the northeast and south and by the bay to the northwest. The village of King Salmon is built on the sand spit that projects to the southwest of Buhne Point and on artificial fill of the adjacent marsh. The hill's bay-facing Red Bluff was severely eroded following the enhancement of the bay entrance channel following development of Humboldt Bay as a major port on the West Coast in the late 1850s (Figure 1-2). The erosion was stopped when PG&E installed a riprap berm in front of the bluff in the 1950s (Figure 1-1 inset).

The proposed storage site will consist of a reinforced concrete vault (Figure 1-3) that contains six separate cells (Figure 1-4) into which the robust canisters containing the waste are placed. These fault cells will be capped with a bolted cover (Figure 1-5) and whose top will be at grade with the ground surface at an elevation of 44 feet (13 meters (m)) above mean lower-low water (MLLW) (Figure 1-6).

1.2 ACKNOWLEDGEMENTS

This report was prepared under the direction of Lloyd S. Cluff, PG&E Geosciences Department and Larry Pulley, Project Manager, Humboldt Bay ISFSI. William D. Page, PG&E Geosciences Department, prepared the report. Stephen Thompson and Rob Witter, William Lettis & Associates, Inc., contributed the long-term projections of relative sea level change and the analysis of the tectonic uplift at Buhne Point in consultation with Gary Carver, Consultant, Kodiak, Alaska. Ron Flick, San Diego State University, provided the information on sea level rise and wave parameters for the near-term up to 100 year scenarios. Walter Crampton, Principal Engineer, TerraCosta Consulting Group, assessed the effectiveness of the coastal protection works and formulated the revised mitigation to counter sea level rise and changing wave patterns. Stuart Nishenko, PG&E Geosciences Department, assessed the impact of tsunami on Buhne Hill.

2.0 ANALYSIS OF SURFACE FAULTING POTENTIAL

2.1 INTRODUCTION

The analysis of the potential for surface faulting is presented in PG&E (2003). It concludes that the potential for surface faulting at the ISFSI site is very low. The ISFSI site is on the hanging wall (up-thrown side) of the Little Salmon fault zone (Figure 2-1), a fault zone that contains several separate faults including the Bay Entrance fault and the Buhne Point fault. Specifically, the site directly overlies a thrust ramp of the Buhne Point fault (Figures 2-2 and 2-3). Based on our kinematic model, the ground directly beneath the ISFSI moves vertically and laterally during earthquakes on the Little Salmon fault zone (including simultaneous rupture with the Cascadia subduction zone), but is not subjected to differential displacements from surface faulting. It essentially is taken for a ride as movement on the fault transports the hanging wall to the southwest. Supporting this argument is the fact that the 80,000-year-old (possibly 105,000-years-old) strata of the Hookton Formation are not faulted across the marine isotope-stage-5a terrace that caps Buhne Hill (Figure 2-4). This is well documented in the extensive trenches excavated across Buhne Hill and the ISFSI site (e.g., Figures 2-5 and 2-6). Earthquake recurrence on the Little Salmon fault, estimated from several detailed investigations ranges between 300 and 700 years with an average recurrence interval of about 500 years (PG&E, 2003).

Based on our kinematic model of the fault zone and trench data documenting no late Quaternary surface faulting, we conclude that the ISFSI site will behave as it has for the past 80,000 years and continue to move up and to the southwest above the hanging wall ramp of the Buhne Point fault without surface faulting for tens of thousands of years. The rate of this movement is a function of the slip rate on the Buhne Point fault. The displacement on the Buhne Point fault per event is conservatively estimated to be one quarter of the total displacement on the Little Salmon fault zone because the main fault in the zone is the Bay Entrance fault; the Buhne point fault is a secondary strand. The estimated slip rate for the Little Salmon fault zone as a whole is 8 to 13 mm/yr and measured individual coseismic displacements range from 3½ to 4½ meters. Because the fault has several strands the coseismic displacements may not represent the full displacement, Hence for the source characterization, a range of 4.5 to 8 m was selected to span the uncertainty and this is used herein (PG&E, 2003). As a secondary strand the Buhne Point fault would have less displacement, possibly one fourth the total, giving a slip rate of 2 to 3 mm/yr and a slip per event of about 0.8 to 1.3 meters along the fault.

2.2 POTENTIAL FOR SURFACE FAULTING IN 10,000 YEARS

Reverse and thrust faulting has many different surface expressions from underlying structural relationships as illustrated in Figure 2-7. The style of faulting at the ISFSI site is the form shown in Figure 2-7b. Using the model, the predicted position of the ISFSI site over time periods longer than the 50-year assumed life of the ISFSI is illustrated in Figure 2-8, a schematic representation of two models discussed below. For a 100-year scenario, the maximum total movement of the site would be about 1 meter if an earthquake on the Cascadia subduction zone and Little Salmon fault zone or independently on the Little Salmon fault zone occurred during that time. This is essentially no change from existing conditions. Over a 1,000-year time period the site may experience 2 to 3 earthquake events, and thus up

to 2 to 3½ meters of cumulative dip-slip displacement would occur on the Buhne Point fault. Like the 100-year scenario, the 1000-year scenario is not significantly different from the existing conditions. For a 10,000-year time span the total movement would be about 20 events with a cumulative fault displacement of about 20 to 40 meters displacement (35 meters is used on Figure 2-8). Because 10,000 years is only about 12 percent of the total age of Buhne Hill as a geomorphic feature, the expected conditions at that time would be the same as the current conditions. Small displacements of a few inches may occur in the hanging wall in these time frames, similar to the small offsets seen in the trenches to the south of the ISFSI.

2.3 POTENTIAL FOR SURFACE FAULTING IN 100,000 YEARS

In order to evaluate likely future positions of the ISFSI site over time periods in excess of about 10,000 years, we propose two end-member models for the kinematic development of the Buhne Point fault (Figure 2-8). The first end-member model assumes that a thrust "flat" develops at the tip of the thrust ramp at or near the ground surface (Figure 2-8a). As displacement accumulates on the fault, material in the hanging wall passes through an axial surface tied to the ramp-flat transition and develops an antiformal fore limb above the growing thrust "flat" in the hanging wall. The preliminary geometry shown in Figure 2-8a does not conserve area or line length, but is intended to show gross development of a fault-bend fold as a consequence of this process. We note that this end-member model does not account for erosion at the thrust front, nor does it provide a complete kinematic or mechanical description of material flow through the forelimb axial surface.

A second end-member model assumes that surface and coastal erosion will provide an erosional limit to the development of topography in front of the tip of the Buhne Point fault ramp (Figure 2-8b). In this model, the present angle of the southwest-facing slope is maintained at 32 degrees, the slope inclination that is stable at present (Page, 2002). In this model, material is displaced up the thrust ramp and eroded as it intersects the "erosional limit" line on the figure.

The time frame for the 100,000-year surface faulting potential scenario is comparable to the time that has passed since the terrace at Buhne Hill formed. We thus infer that Buhne Hill has already experienced about 200 to 300 events in its 80,000-year life span. The total potential fault displacement in the next 100,000 years would be 200 to 400 meters (350 meters used on Figure 2-8) distributed over 200 events. In the first end-member model described above, the ISFSI would remain above the thrust ramp of the fault-bend fold for most of the time with little potential for differential displacement of the site. However, in 50,000 to 100,000 years from now the ISFSI would be carried through the axial surface that projects from the bend in the thrust fault (Figure 2-8a). This would cause significant down-to-the-southwest tilting of the ground beneath the vault accompanied by fracturing and faulting with small offsets in the soft soils below the vault.

In such a long time period, the Buhne Point fault might change geometry and the fault tip would likely shift farther to the southwest surfacing beyond the collapsing front. It is very unlikely that the fault would rupture up beneath the ISFSI, but if it did so the potential surface displacement would be on the order of a meter.

In scenarios where the potential coseismic displacement is very small (i.e., a few inches), the reinforced concrete vault in which the ISFSI is placed would not be damaged from surface faulting. The cracking and offsets would deform the soft sediments around the resistant vault. Any cumulative minor tilting of the vault would not change the relative position of the cask in the vault. Hence there is no significant damage to the ISFSI in scenarios up to several tens of thousands of years.

In the second end-member model (Figure 2-8b), the ISFSI would move up and to the southwest parallel to the fault ramp for about 130 meters until it reaches the "erosional limit" line. At that point, the ISFSI would be at the edge of the slope high above the bay and would be susceptible to erosion and translation downslope like a large block of rock. Given slip rate for the fault, the ISFSI would reach the "erosional limit" line in about 41,000 years when the ISFSI is on a hill high above sea level as discussed in section 3 below.

2.4 POTENTIAL IMPACTS ON THE ISFSI

In the scenarios where the vault passes through a fault-bend-fold, the vault would be tilted in the 50,000- to 100,000-year time frame, but any fracturing in the soil foundation, including any potentially large offsets in the soils beneath the vault, would not crack the vault and the reinforced vault and casks would remain intact.

Examples from more extreme cases are documented in recent earthquakes, During the 1999 Chi-Chi earthquake in Taiwan many reinforced concrete structures were tilted on the fault-bend fold scarp, but remained relatively undamaged (Photo 2-1). Buildings that were not reinforced or massive enough were fractured as they passed through the fault-bend-fold (Photo 2-2). During the 1999 Kocheli earthquake in Turkey the concrete ammunition bunkers at the naval academy in Goleuk were displaced, rotated and tilted but not broken even though the soft soils, similar to those that comprise Buhne Hill, deformed around it by strike slip fault of over 4 meters (Figure 2-9; Photo 2-3) (Youd and others, eds., 2000).

3.0 IMPLICATION OF FUTURE SEA LEVEL CHANGES AT BUHNE HILL

3.1 INTRODUCTION

A seaward-sloping berm of riprap that is about 15 to 20 feet in front of Red Bluff has protected Buhne Hill from coastal erosion since it was installed in the 1950s and up graded in the 1980s. Prior to this mitigation, wave erosion caused Red Bluff and Buhne Point to retreat an estimated 1300 feet (~400 m) since the 1850s (Page, 2004). Much of this erosion occurred as the result of the opening of the entrance to Humboldt Bay for a deep, stable shipping channel. Although PG&E addressed the potential erosion of Buhne Hill for the next 50 years (Page, 2004), the Coastal Commission raised the concern that future sea level rise and higher and longer duration storm waves—possible outcomes of anticipated global warming—may increase the vulnerability of the ISFSI site to coastal erosion over longer time periods in the event that the site needed to be used beyond the 50 year design life of the ISFSI storage casks.

In an earlier report, PG&E assessed the potential erosion at Buhne Hill for the projected life of the ISFSI, about 50 years (PG&E, 2003). The analyses presented below address possible future changes to the site over time scales from decades to centuries to many thousands of years. A major difference between the 50-year evaluation and evaluations over longer time horizons is the need to anticipate changes in relative sea level, which is a product of local land level change and global sea level change. Our approach involves five components:

1. Assessing local land level change by determining the long-term pattern of tectonic uplift of Buhne Hill and short-term land level changes due to the earthquake cycle,
2. Forecasting global sea level change in a global environment predicted to be warmer than present for the next several centuries to millennia,
3. Characterizing changes in wave heights and patterns that may result from modifications in the strengths and directions of Pacific storms,
4. Reviewing tsunami hazards and maximum run-up heights in the context of relative sea level change, and
5. Analysis of the coastal protection for Buhne Hill as it is affected by the above changes.

Because changes in relative sea level and climate are uncertain and complex to forecast explicitly, we construct and evaluate scenarios of relative sea level change at Buhne Hill that encompass the likely range of future conditions. Based on these scenarios of potential future sea level, storminess, and tsunami run-up, we discuss possible coastal erosion measures and propose methods of coastal protection.

3.2 TECTONIC SETTING AND LAND-LEVEL CHANGE

Buhne Hill is located within the convergent plate boundary between the subducting Gorda Plate and the overriding North America Plate. The two primary tectonic elements that comprise the plate boundary and characterize the region are (1) the offshore Cascadia subduction zone (Figure 3-1) and (2) the onshore fold-and-thrust belt (Figure 3-2) that includes the Little Salmon fault zone (PG&E, 2003). As discussed in section 2, Buhne Hill is located within the hanging wall (up-thrown side) of the Little Salmon fault zone (Figures 2-2 and 2-3). Land-level change at Buhne Hill is affected by the earthquake cycle related to

these two tectonic elements, including abrupt "coseismic" uplift or subsidence during earthquakes and longer term "interseismic" uplift or subsidence between earthquakes. To evaluate future land level change, we construct a relatively simple model that includes both long-term tectonic uplift as recorded by ancient marine terraces and short-term variability in land level resulting from the earthquake cycle on both the Cascadia subduction zone and Little Salmon fault zone.

3.2.1 Long-term uplift

A sequence of uplifted marine terraces is preserved on Humboldt Hill, a linear ridge that extends eastward from Buhne Hill (Figure 2-4). The terraces provide a record of long-term tectonic uplift of the ridge over the past several hundred thousand years. The terraces were formed by wave erosion during past sea level high stands, and thus the highest point of each wave-cut terrace coincides approximately with a former position of mean sea level (paleo-sea level). We estimate the long-term rate of land level change at the proposed ISFSI site by examining the uplifted marine terrace that forms the gently sloping top of Buhne Hill, near the ISFSI site. The long-term rate of tectonic uplift at Buhne Hill is calculated from the age of the terrace, the modern elevation of the terrace at the ISFSI, and the paleo-sea level at the time the terrace was formed. The age, t, of the marine terrace is estimated to be ~80,000 or ~105,000 years old, coinciding with the sea level high stands of marine isotope stages 5a or 5c (PG&E, 2003). The modern height, h_m, of this terrace is about 50 feet above mean sea level. Reconstructions of past sea level high stands from coral reefs in the Caribbean Sea suggest that paleo-sea levels, h_p, during stages 5a and 5c were about 62 ± 16 feet (19 ± 5 m) and 46 ± 13 feet (19±5 m) *below* modern sea level (Potter and others, 2004). The long-term uplift rate, u, of Buhne Hill at the ISFSI site is determined by the equation: $u = (h_m - h_p) / t$. This equation yields uplift rates of 1.4 ± 0.3 feet per thousand years (0.4 ± 0.1 millimeters per year (mm/yr)) assuming the terrace was formed during stage 5a and 0.9 ± 0.2 feet per thousand years (0.3 ± 0.05 mm/yr) assuming the terrace was formed during stage 5c. For this study, we consider the full range of uncertainty in the long-term rate and forecast a future uplift rate of 0.7 to 1.7 feet per thousand years (0.25 to 0.5 mm/yr), with a best estimate of 1.4 feet per thousand years (0.4 mm/yr), the mean rate for an assumed stage 5a terrace. In order to utilize symmetric uncertainties in our calculations, we assume a long-term land level change of 1.2 ± 0.5 feet per thousand years (0.4 ± 0.1 mm/yr) (Figure 3-3).

3.2.2 Short-term land level change

Land level at Buhne Hill is expected to fluctuate about the long-term rate due to the abrupt release of elastic strain energy during earthquakes and the gradual buildup of elastic energy between earthquakes (i.e., the "earthquake cycle"). There are two primary earthquake sources for the ISFSI site that affect short-term land-level changes: the Cascadia subduction zone and the Little Salmon fault zone. For our model of short-term fluctuations in land level, we consider end-member models in which each source is considered to rupture independently in an earthquake. The scenario in which both sources rupture simultaneously (e.g., PG&E, 2003) will yield a result that lies somewhere in between the end-member models.

Cascadia subduction zone - The Cascadia subduction zone, which lies offshore between southern Vancouver Island, British Columbia and northern California, ruptures during large earthquakes on average every 300 to 700 years (PG&E, 2003). Evidence for these

earthquakes includes buried marshes and tsunami deposits at several sites along the coast that record abrupt land subsidence of up to several meters during each earthquake and inundation by large waves generated by sea-floor displacements, respectively (e.g., Clarke and Carver, 1992; Atwater and Hemphill-Haley, 1997; Kelsey and others, 2002; Witter and others, 2003). Elastic dislocation models of the Cascadia subduction zone predict abrupt subsidence along the coast during earthquakes and gradual uplift along the coast between earthquakes as elastic strain energy accumulates (Hyndman and Wang, 1995). This model clearly applies to Washington, Oregon and the California coast north of the Klamath River and is constrained by estimates of present-day vertical uplift of the coast derived from tide-gage data and geodetic leveling (e.g., Mitchell and others, 1994).

Regional present-day uplift rates at the latitude of Humboldt Bay, similar to the uplift to the north, range from about 1.3 feet per century (4 mm/yr) based on leveling surveys tied to the Crescent City tide gage (Mitchell and others, 1994). Another uplift rate in this area is about 0.3 feet per century (1 mm/yr) based on three to seven years of GPS data (Williams, 2002). Thus, as one end-member model for land-level change at Buhne Hill, we anticipate abrupt subsidence of a few meters at the site during a Cascadia subduction zone event, and uplift rates between earthquakes on the order of 1.3 feet per century (4 mm/yr). We note that there is no direct geologic evidence for coseismic subsidence in tidal marshes around the ISFSI site (PG&E, 2003), and that this end member model places a conservative limit on the earthquake cycle tied to the subduction zone.

Little Salmon fault zone - The other end-member model considers fault rupture during an earthquake on the Little Salmon fault zone. Paleoseismic data southeast of Buhne Hill constrain dip-slip displacement, d, across the moderately dipping fault zone to be up to 15 to 26 feet (4.5 to 8 m) per event (PG&E, 2003). Given a fault zone dip, δ, of 45 to 55°, the vertical displacement, v, per event is given by the equation: $v = d \sin(\delta)$. This equation yields vertical displacements of 10.5 to 21 feet (3.2 to 6.5 m) per event. Two alternatives are possible. One assumes that equal portions of hanging wall uplift and footwall subsidence occur, we estimate that an earthquake on the Little Salmon fault zone could produce land-level uplift of about 5 to 10 feet (1.6 to 3.2 m) in the hanging wall, and an equal amount of land-level subsidence in the footwall. The second alternative, which is supported by the lack of evidence of significant uplift or subsidence at Buhne Hill, is that Buhne Hill neither rises nor subsides appreciably during the faulting event with respect to sea level but all the fault displacement is taken in the subsidence of South Bay, including King Salmon.

Scenario - The result of uplift and subsidence from earthquakes on the Cascadia subduction zone and Little Salmon fault zone, whether they occur independently as end member models described above, or occur dependently as described by PG&E (2003), when integrated over several earthquake cycles will produce coastal uplift at Buhne Hill equal to the long term uplift rate recorded by the uplifted marine terrace sequence on Humboldt Hill. For this report, we choose the alternative for short-term land level change at Buhne Hill is characterized by interseismic uplift followed by coseismic subsidence to produce the zig-zag curve on Figure 3-3. The rate of interseismic uplift, u_s, is constrained by the present-day rate of uplift of the Humboldt Bay area of 1.3 feet per century (4 mm/yr) (Mitchell and others, 1994). The magnitude of coseismic subsidence, v_s, is estimated by the equation: $v_s = (u_s - u_l)$

* R, where u_l is the long-term uplift rate of the Buhne Point terrace (1.4 feet/thousand years (0.4 mm/yr)) and R is the recurrence interval between earthquakes. The long-term uplift rate, u_l, accounts for permanent uplift accommodated by slip on the Little Salmon fault zone. Using an average recurrence interval of 500 years for Cascadia earthquakes results in a coseismic subsidence estimate of 5.9 feet (1.8 m). We emphasize that this value of coseismic subsidence is a direct function of the assumed interseismic uplift rate of 1.4 feet per thousand years as published by Mitchell and others (1994). The amount of coseismic subsidence shown in Figure 3-3 (5.9 ft (1.8 m)) assumes an average earthquake recurrence interval of 500 years. The best estimate short-term land level change curve is a simplified version of the earthquake cycle dominated by offshore Cascadia subduction zone megathrust events. The amount of coseismic subsidence at Buhne Hill represents sum of: (1) subsidence caused by the elastic strain release of the offshore subduction zone, and (2) uplift caused by permanent (inelastic) slip on the Little Salmon fault zone. At King Salmon, which is located on the footwall of the Little Salmon fault zone, the amount of coseismic subsidence is expected to be greater because slip on the Little Salmon fault zone will produce subsidence there. Our estimates for coseismic subsidence are consistent with published subsidence estimates derived from elastic dislocation models and geologic evidence of buried marshes that dropped several meters during past Cascadia subduction zone earthquakes (e.g., Hyndman and Wang, 1995; Witter and others, 2002). Lower uplift rates suggested by GPS data (Williams and others, 2002) and geologic data that does not detect evidence for abrupt subsidence near Buhne Hill (PG&E, 2003) suggest that amounts of coseismic subsidence may be much less than our selected estimate, or even negative (i.e., coseismic uplift of Buhne Hill) (G. Carver, personal communication, 2005).

We incorporate the considerable uncertainty in short-term land level change caused by future earthquakes on the offshore subduction zone and the Little Salmon fault zone by adding an error term above and below the long-term uplift curves (Figure 3-3). Because neither the timing nor the exact rupture scenario of future earthquakes is certain, we conservatively assume that at any future point in time, an earthquake may cause land level to subside up to 6.6 feet (2 m) below the minimum long term land level, or an earthquake may cause land level to uplift up to 10 feet (3.2 m) higher than the maximum long term land level (Figure 3-3).

3.3 GLOBAL SEA LEVEL CHANGE

Global sea level is tied closely to global climate, and is the product of numerous variables and their complex interactions. Estimating future sea level change is speculative, and different approaches are required to capture the variability of possible sea level change over different time scales. We approach the goal of characterizing sea level change at the proposed ISFSI site by examining possible changes over the next 100, 1000, 10,000 and 100,000 years. For the 100-year time scale, we rely on forecasted global sea level rise published in the United Nations Intergovernmental Panel for Climate Change report (IPCC, 2001). For time scales of several hundreds to a few thousands of years, we rely on extrapolations of the 100-year forecasts, and modify them based on evaluating the major individual contributors to sea level change such as thermal expansion of sea water, change in mass of the Greenland and Antarctic ice sheets, and change in mass of mountain glaciers (IPCC, 2001).

For time periods longer than a few thousand years, forecasts of sea level change rely on three components:

1. The geologic record of past sea level change (Martinson and others, 1987; Thompson and Goldstein, 2005; Hearty and others, 1999) as a proxy for future sea level change (Figure 3-4a),
2. Numerical models and supporting geologic data that evaluate possible maximum sea level changes from each of the major individual contributors (e.g., IPCC, 2001), and
3. Relationships between past changes in Earth's orbit and glacial-interglacial intervals to predict future changes (Berger and Loutre, 2002) (Figure 3-4b).

Estimates over these longer time periods incorporate the assumption that the Earth remains within the climatic paradigm of the Quaternary Period, characterized by glacial and interglacial intervals that change in phase with variations in Earth's orbit around the sun (Imbrie and others, 1984).

3.3.1 Historical and 21st century climate and sea level change

Human-induced increases in greenhouse gases (mainly carbon dioxide (CO_2,) and methane (CH_4) are partially responsible for the historical rise in the Earth's average temperature, and are believed to contribute to the projected 1.4 to 5.8°C rise in global temperature over the 21st century and beyond (IPCC, 2001) (Figure 3-5a, -b). Although temperature has probably varied by several degrees Celsius over the past 10,000 years (IPCC, 2001), present levels of CO_2 and methane are higher than at any point documented in the past ~420,000 years (Petit and others, 1999), and are projected to increase to about twice the 1990 levels by the end of the 21st century (IPCC, 2001). Although changes caused by global warming are most clearly recorded as temperature increases in high latitude regions, global warming is expected to influence local climates through changes in mean annual temperature, temperature extremes, annual precipitation (i.e., overall wetter or drier climate) and/or changes in the duration, pattern, and intensity of storms (IPCC, 2001).

A major consequence of historical and near-future global warming is global sea level rise, caused primarily by the melting of ice in mountain glaciers and by the expansion of ocean water caused by heating at the ocean surface (IPCC, 2001). During the past century average temperature increased 0.6°C (IPCC, 2001) and global sea level rose as much as 4 to 10 inches (10 to 25 centimeters (cm)) (Gornitz, 1995). Present-day rates are estimated at about zero (Mörner, 2004) to as much as 0.7 to 1.2 inches per decade (1.8 to 3 mm/yr) (Peltier and Tushingham, 1989; Douglas, 1991; 1997). By the year 2100, average temperatures are projected to increase 1.4 to 5.8°C, and sea level is expected to rise globally from about 4 to 35 inches (10 to 90 cm) (Figure 3-5), which implies an average rate of global sea level rise up to four times the twentieth century rate (IPCC, 2001).

3.3.2 Holocene climate and sea level change

For the past 11,000 years or so, the Earth has been in an interglacial interval that has been remarkable for its climatic stability relative to the geologic record of the past ~420,000 years (Petit and others, 1999; Ruddiman, 2003). This relatively stable climate still has had variations on ~1500 year time scales that have included shifts in temperature of a few degrees Celsius at European latitudes (IPCC, 2001). European and North American pollen records,

air bubbles trapped in the Greenland ice sheet, and oxygen isotopes in ocean sediment cores record an early Holocene climate that was warmer (probably by about 2°C globally) than the present day, but the period of maximum warmth differed globally (IPCC, 2001). The early Holocene warm interval occurred near the start of the Holocene in the high latitude regions (about 11,000 to 8,000 years ago) but did not start until about 8,000 years ago across much of North America and Europe (COHMAP, 1988). For much of the middle and late Holocene, global temperatures were cooler than present, though variable on time scales of decades to millennia. The twentieth century was the warmest in the past millennium (IPCC, 2001).

Holocene sea level change is characterized by decreasing rates of sea level rise as the ice sheets adjusted to warm, interglacial conditions and their melt water filled the oceans (Figure 3-6). Sea level during the early Holocene rose rapidly as glaciers and ice sheets melted from their maximum glacial extent (Fairbanks and others, 1989). The average rate of sea level rise between 15,000 and 6,000 years was about 3.3 feet per century (10 mm/yr), although considerable variation in the rate occurred during the early part of the deglaciation processes (IPCC, 2001). During the last ~6,000 years, sea level rise slowed dramatically to rates of about 0.16 feet per century (0.5 mm/yr), and during the last 3,000 years sea level rise occurred at about an average rate of 0.03 to 0.07 feet per century (0.1 to 0.2 mm/yr) (IPCC, 2001). Although geologic evidence indicates a middle Holocene relative sea level that was as much as six feet (2 m) higher than present in low latitude regions (e.g., Blum and others, 2002), this relative sea level high stand is thought to be the result of hydro-isostatic effects and does not represent a global change in sea water volume (e.g., Fleming and others, 1998; Peltier, 2001). For comparison to an area close to the ISFSI and Eureka, relative sea level on the south-central Oregon coast rose gradually at a rate of 0.33 feet per century (~1 mm/yr) over the past 6700 years, and at a rate of 0.1 feet per century (~0.3 mm/yr) over the past 3,000 years, reaching a maximum level at the present day (Witter and others, 2003).

The relative stability of climate and sea level over the past few thousand years contrasts with the measured and projected rapid increases in temperature and sea level from the start of the 20th century into the 21st century. Figure 3-7 shows past and future changes in atmospheric CO_2 concentration, global temperature, and sea level for the time period AD 1000 to AD 2100. The departure from past Holocene stability can be seen around the start of the 20th century, when atmospheric CO_2 concentration and temperature increase (Figure 3-7a and 3-7b). This increase coincides with an order of magnitude increase in sea-level rise, from an estimated 0.1 to 0.2 mm/yr average over the past 3000 years to an estimated ~1.5 mm/yr average in the 20th century (IPCC, 2001) (Figure 3-7c). Twenty-first century estimates of CO_2, temperature, and sea level predict even greater rates of change.

3.3.3 Pleistocene climate and sea level change

Over the past 2.5 million years, Earth's climate has fluctuated between glacial and interglacial intervals, with changes in global temperature, atmospheric greenhouse gas concentrations, glacier and ice sheet extent, and sea level occurring on time scales that range from less than a thousand to hundreds of thousands of years (Imbrie and others, 1984; Petit and others, 1999). Glacial intervals are characterized by cool ocean and atmospheric temperatures, low atmospheric CO_2 and methane concentrations, expanded continental ice sheets in high latitude regions and extensive mountain glaciers (glaciers outside of Greenland

and Antarctica). Interglacial intervals, including the Holocene, have warm atmospheric and ocean temperatures, higher greenhouse gas concentrations, and reduced ice sheet and mountain glacier extents. Temperature changes between full glacial and interglacial conditions were about 20°C over Greenland and about 3°C in the tropics (IPCC, 2001). Rapid changes in temperature are recorded at rates up to 10°C in fifty years over much of the Northern Hemisphere, and up to about 7°C in a decade over Greenland (IPCC, 2001). The Vostok ice core from Antarctica shows almost in-phase changes of temperature, CO_2, and methane through the glacial-interglacial ice age cycles over the past ~420,000 years (Petit and others, 1999).

Long-term records of sea level over the past several hundreds of thousands of years are based primarily on variations in the oxygen isotopic concentration in fossil organisms in marine sediment cores (e.g., Waelbroeck and others, 2002; Siddall and others, 2003) (Figures 3-4a and 3-8). The time scales for these records are constrained by limited radiometric dating of young sediments, correlations with volcanic ashes or and magnetic reversals, and are "orbitally tuned" such that major fluctuations in the oxygen isotope records are matched with predictable changes in the earth's orbit around the sun and the resulting changes in solar insolation (Figure 3-4) (Imbrie and others, 1984). Sea level records show oscillations of hundreds of feet of sea level change between glacial conditions, when sea level drops as water is stored in ice sheets, and interglacial intervals, when sea levels rise as ice sheets melt. At the most recent glacial maximum, about 20,000 years ago, sea level was about 400 feet (120 m) lower than present day (Fairbanks, 1989).

High resolution records suggest that sea level changes up to 115 feet (35 m) occurred at rates of up to 6.6 feet per century (20 mm/yr) during abrupt changes in climate (Siddall and others, 2003). These high rates and rapid fluctuations are more typical during glacial intervals and glacial-interglacial transitions than during full interglacial intervals, but millennial-scale changes of tens of feet (and tens of meters) characterized previous interglacial intervals (Lea and others, 2002; Siddall and others, 2003).

Although sea level proxy data from oxygen isotopes in marine cores provides continuous records of sea level, more precise data for past sea levels at specific points in time come from uplifted coral reefs and marine terraces in environments where tectonic activity is assumed constant (e.g., Chappel, 2002; Potter and others, 2004). Uplifted coral reefs and marine terraces record past sea level high stands that place limits on what has been possible during past intervals of warm climate. The highest sea level over the past ~500,000 years appears to have occurred about 400,000 years ago, during marine isotope stage 11, and reached a maximum height of about 43 to 66 feet (13 to 20 m) above present-day sea level (Hearty and others, 1999; Droxler and others, 2003) (Figure 3-8). A more recent high stand of +13 to +26 feet (+4 to +8 m) occurred during the last interglacial interval, at marine isotope stage 5e, about 125,000 years ago (Thompson and Goldstein, 2005) Figure 3-8). Another similar high stand that consisted of multiple sea level standstills between about +6.6 to +20 feet (+2 to +6 m) occurred during the prior interglacial interval (marine isotope stage 7) about 190,000 to 220,000 years ago (Thompson and Goldstein, 2005) (Figure 3-8). Peak rates of sea level rise were about 3.3 feet per century (10 mm/yr) during previous interglacial

intervals (Thompson and Goldstein, 2005), although the uncertainties of these peak rates are unclear.

The largest contributors to major sea level changes over the Pleistocene have been the North American ice sheets (Laurentide, Cordilleran, and Greenland, of which only the Greenland ice sheet partially remains), the Fennoscandian ice sheet (which likely melted in the first half of the Holocene), and the Antarctic ice sheets, which consist of the East Antarctic ice sheet and the much smaller West Antarctic ice sheet (IPCC, 2001). The majority of the ~400 feet (120 m) of sea level rise since the last glacial maximum 20,000 years ago was due to the melting of the North American ice sheets. The water stored in the three remaining ice sheets is equal to about 250 feet (~80 m) of sea level rise.

3.4 ESTIMATES OF FUTURE SEA LEVEL CHANGE

Estimates of future sea level changes are divided into several time periods short time scales of 10 to 100 years, intermediate time scales of about 1,000 years, and long time scales of 10,000 to 100,000 years. These are discussed below.

3.4.1 Short (10- to 100-year) time scales

The main limitations for forecasting sea level change over short time scales are the variability in sea level change that exists both spatially and temporally around the globe, and the ability for numerical models to accurately predict and sum the contributions to sea level change from individual sources. The variability of sea level due to changes in atmospheric and ocean circulation currently exceeds the amplitude of any background trends at any particular location (Douglas, 1991). Anticipating that variability at Buhne Hill is a challenging task. Quantifying *global* sea level change over the past century has traditionally relied on a subset of globally-distributed tide-gage data in tectonically stable areas with 60 years or more of record (e.g., Douglas, 2001). For the subset of tide-gage records in tectonically "stable" sites, land-level change due to long-term isostatic adjustment of the earth's mantle from full glacial (20,000 years ago) conditions is modeled out (e.g., Peltier and Tushingham, 1989; Peltier, 1999). Although most tide-gage records, after corrections for land-level change, show similar trends over the historical period, the rates of sea level change vary by location. Furthermore, models predict geographical variability in sea level change over the 21st century between zero and twice the global average (Gregory and others, 2001). The models agree that sea level rise is expected to be geographically non-uniform, but they do not agree about the geographical pattern. Thus, the global average of both historic changes in the 20th century and forecasted sea level change over 21st century should be considered only proxies for sea level change near Buhne Point. In other words, a global average forecast of sea level change does not predict precise sea level at a particular location and time, but should indicate a direction of change.

Model predictions of future sea level change over the next century (and beyond) rely on quantifying the effects of global warming on four main contributors (IPCC, 2001):

1. thermal expansion of ocean water from heating of surface ocean water,
2. melting or growth of mountain glaciers,
3. melting or growth of the Greenland ice sheet, and
4. melting or growth of the West and East Antarctic ice sheets.

Because it is uncertain how some contributors affect others, the exact response of global sea level to climate change remains somewhat uncertain (Douglas, 2001). Forecasts based on models that integrate these four primary components (and various other contributors) predict sea level to rise 3.5 to 35 inches (0.09 to 0.88 m) between 1990 and 2100 (IPCC, 2001). This range includes an uncertainty in excess of 10% in estimating future changes in terrestrial storage of water (e.g., in dams) (IPCC, 2001; Gornitz, 2001) (Figure 3-5). The higher values have been received with considerable criticism that question forecasts based on numerical models and not past sea level change (Mörner, 2004). The majority of the modeled rise comes from thermal expansion and melting of mountain glaciers, as most models predict that neither Greenland nor Antarctica will contribute to significant amounts of sea level change over the next 100 years (e.g., Huybrechts and others, 2004).

This study adopts the full range of forecasted global sea level rise over the next 100 years as presented by the IPCC (2001) (Figure 3-5c and 3-12a). The maximum sea level curve shows an increasing rate of sea level rise from 1.4 to 4.1 feet per century (4 to 12 mm/yr). The minimum sea level curve shows an increasing then decreasing rate of sea level rise from 0.2 to 0.3 to 0.2 feet per century (0.6 to 1.0 to 0.5 mm/yr). A best estimate of sea level rise that we consider for this study has a gradually increasing rate of sea level rise from 0.6 to 1.7 feet per century (1.8 to 5.2 mm/yr) (Figure 3-12a). This best estimate curve reflects the median value of the "average model runs" shown on Figure 3-5c. The range of rates of sea level rise encompasses rates that are comparable with and up to about six times greater than the rates measured over the 20th century. The highest predicted rate, 4.1 feet per century (12 mm/yr), is comparable in magnitude to the 3.3 feet per century (10 mm/yr) average rate of sea level rise during deglaciation between 15,000 and 6,000 years ago (Fairbanks, 1989) and the approximate rate of 3.3 feet per century (10 mm/yr) that occurred during interglacial intervals between about 70,000 and 250,000 years ago (Thompson and Goldstein, 2005).

Relative sea level change for the next 50 and 100 years is determined by subtracting forecasted sea level change from predicted land level change (Figure 3-12). For land-level change, we assume a constant rate of interseismic uplift of 1.3 ± 0.3 feet per century (4 ± 1 mm/yr) based on level line surveys published in Mitchell and others (1994). We explicitly assume that no major Cascadia subduction zone or Little Salmon fault zone earthquake will occur during this time period. The resulting relative sea level curves show the ISFSI site at 44.0 ± 0.6 feet elevation by 2050 and at 43.8 ± 1.6 feet by the year 2100 A.D. The relative sea level curves show that, over the next century and barring any change in land level due to a major earthquake, the rate of interseismic uplift at Buhne Point will keep up with expected sea level rise. If a major Cascadia subduction zone event occurs within this time, however, land level may abruptly drop by up to about 6 feet (~2 m).

3.4.2 Intermediate (1000-year) time scales

Predictions of sea level over time scales of thousands of years rely on estimating the contributions of thermal expansion, melting of mountain glaciers, and changes in ice stored in the Greenland and Antarctic ice sheets. Because these systems are large, their responses to climatic perturbations occurring today and in the near future would be expressed over several

centuries to millennia. Below, we summarize the major individual components that could contribute to sea level change over the next few thousands of years.

Thermal expansion – The rate of sea level rise due to thermal expansion of ocean water is predicted to be 1.6 to 6.6 feet (0.5 to 2.0 m) to 3.3 to 13 feet (1 to 4 m) for atmospheric CO_2 levels that are two and four times pre-industrial levels, respectively (IPCC, 2001). This contribution to sea level rise is predicted to reach half its total value in about 500 years and will take several thousand years to reach the full value.

Mountain glaciers – Melting of mountain glaciers due to global warming will contribute a significant, if not major component of sea level rise over the next century. Mountain glaciers cumulatively contain about 1.5 feet (0.5 m) of total sea level equivalent, and currently are in a state of general retreat and loss of mass (e.g., Arendt and others, 2002). With continued global warming, most of the world's mountain glaciers likely will continue to lose mass over the next several thousands of years.

Greenland ice sheet – Although the Greenland ice sheet is the most vulnerable of the Earth's ice sheets to climatic warming (IPCC, 2001), its contribution to future sea level change is highly uncertain. The Greenland ice sheet contains enough ice to raise sea level by 20 to 23 feet (6 to 7 m) (IPCC, 2001). At its relatively low latitude, the Greenland ice sheet is susceptible to melting given moderate increases in summer temperatures. Small increases in temperature, however, result in increased accumulation of snow during the winter, which may partially offset the increased summer melting. Glacier mass balance calculations suggest that a "mid-range" scenario of 5.5°C warming over Greenland will produce about 10 feet (3 m) of sea level rise over about 1000 years, and an 8°C warming will produce about 20 feet (6 m) of sea level rise, essentially eliminating the ice sheet over several thousands of years. Evidence from ice cores and sediment cores is consistent with partial melting of the Greenland ice sheet during the last interglacial period about 125,000 years ago, with a plausible contribution of 13 to 18 feet (4 to 5.5 m) to sea level (Cuffey and Marshall, 2000). This contributed to the oxygen isotope stage 5e sea level high stand of about 20 ± 6 feet (6 ± 2 m) above present-day sea level 125,000 years ago.

West Antarctic ice sheet – The West Antarctic ice sheet contains enough ice to raise sea level by about 13 to 20 feet (4 to 6 m) (Oppenheimer, 1998). The base of the ice sheet rests below sea level, and the outer margins of the ice sheet are floating ice shelves that extend seaward. These conditions make the West Antarctic ice sheet susceptible to changes in ice dynamics due to changes in sea level and ocean temperature. Analysis of sediment cores and geophysical data suggests that the ice sheet has repeatedly advanced and retreated over the ocean floor during the Quaternary period, including a major retreat about 400,000 years ago (Scherer and others, 1998). Evidence for such instability in the face of 20th century climate change has led several authors to conclude that the ice sheet is susceptible to rapid melting and retreat in short time periods (reviewed in Oppenheimer, 1998). Currently, however, there is considerable consensus that major loss of the ice sheet is unlikely during the 21st century, and significant contributions to sea level change likely will require time scales of thousands of years (IPCC, 2001). Conservative estimates suggest that the West Antarctic ice sheet could melt at rates corresponding to 0.9 mm/yr of sea level rise, which projects to

disappearance of the ice sheet in 4000 to 7000 years (Bindschadler, 1998). Total melting of both Greenland and the West Antarctic ice sheet would be required to reproduce the +43 to +66 foot (+13 to +20 m) sea level high stand that may have occurred about 400,000 years ago (Hearty and others, 1999; Droxler et al,. 2003).

East Antarctic ice sheet – Although the East Antarctic ice sheet contains enough ice to raise sea level by about 200 feet (60 m), the ice sheet has persisted for as long as 20 million years (Oppenheimer, 1998), and is unlikely to lose any significant mass in the foreseeable future. The threshold for loss of mass of the ice sheet requires a temperature warming above 20°C, an amount well beyond forecasted levels (IPCC, 2001). A warming of the ocean and atmosphere near the East Antarctic ice sheet will likely cause an increase in mass due to increased snow fall, which would contribute to short and long-term draw-downs of sea level. This increase in East Antarctic ice sheet mass balance may partly offset sea level rise from other sources. However, it is also possible that sea level rise could cause melting around the margins of the ice sheet that may contribute to short-term sea level rise. Some net melting of the East Antarctic ice sheet probably was necessary to achieve the +66 foot (+20 m) sea level about 400,000 years ago as suggested by Hearty and others (1999).

Forecast over the next 1000 years – For our maximum sea level projection, we assume a maximum sea level rise over the 21st century as forecasted by IPCC (2001), followed by an average rate of sea level rise of about 3.3 feet per century (~10 mm/yr) from the end of the 21st century to the end of the next millennium (Figure 3-9). The average rate is consistent with the maximum rates during interglacial intervals in the geologic record (Thompson and Goldstein, 2005). The sustained high rate reflects initial high rates of thermal expansion and meltwater from glacial ice, followed by high rates of melting of the Greenland and West Antarctic ice sheets that would probably lag behind the near-term abrupt rise in global temperatures (IPCC, 2001). The maximum sea level curve over the next 1000 years allows for partial melting of both Greenland and the West Antarctic ice sheets, negligible contribution from the East Antarctic ice sheet, significant sea level rise caused by thermal expansion of ocean water, and melting of the majority of ice presently stored in mountain glaciers.

Our minimum sea level scenario assumes a linear increase of sea level of about 0.26 feet per century (~0.8 mm/yr), comparable to the minimum average rate forecast over the next 100 years (IPCC, 2001). The minimum curve allows for sea-level rise from more limited melting of both Greenland and West Antarctica ice and a negligible change to an increase in mass balance of the East Antarctic ice sheet. The minimum curve also allows for limited thermal expansion of sea water and limited melting of mountain glacier ice.

Our best estimate for sea level change over the next 1000 years follows our 100-year forecast based on the median rate of sea level rise of IPCC (2001) (Section 3.4.1), then shows a gradually decreasing rate of sea level rise from 1.7 feet per century (5.2 mm/yr) to 1.0 feet per century (3.0 mm/yr) (Figure 3-9). The best estimate curve allows for considerable thermal expansion and melting of mountain glacier ice in the short term followed by later melting of the Greenland and West Antarctic ice sheets that is moderated by sea level drawdown by an increase in snowfall and mass balance of the East Antarctic ice sheet.

3.4.3 Long-term (10,000- to 100,000-year) time scales

Over time scales beyond several thousands of years, forecasting sea level change is not accomplished by integrated numerical models but rather is constrained by considering past variations in sea level and maximum sea level high stands recorded in the geologic record over the past ~500,000 years (Thompson and Goldstein, 2005; Cutler and others, 2003; Siddall and others, 2003), and by placing limits on the maximum likely contributions from each ice sheet, plus the relatively minor contributions from thermal expansion and mountain glaciers. Thus, our forecasts of sea level change at Buhne Hill rely on considering the possible magnitudes and duration of the present interglacial, the start of the next glacial interval, and future glacial-interglacial cycles. Two major factors to consider over the next 10,000 years and longer are: (1) the probability that most fossil fuels will be depleted over the next several thousand years, and that the vast ocean system will have absorbed much of the excess human-induced atmospheric CO_2 and cause global cooling (Ruddiman, 2003), and (2) variations in Earth's orbit and resulting solar insolation will cause more- and less-favorable conditions for initiation of glacial intervals in the future (Berger and Loutre, 2002).

It is uncertain when the present interglacial interval will end and the next glacial interval (and start of major sea level lowering) will begin. Most interglacial (or interstadial) intervals over the past million years or so have lasted on the order of 5,000 to 10,000 years, with a maximum interglacial interval of about 30,000 years occurring about 400,000 years ago (Droxler and others, 2003). The ends of past interglacial and the onset of past glacial intervals have coincided with decreasing levels of solar radiation that are approaching minimum values on the 22,000 year orbit cycle (Berger and Loutre, 2002) (Figure 3-4b), and a lowering of atmospheric CO_2 levels (Petit and others, 1999). Presently, the solar radiation on Earth is decreasing towards a low point in the 22,000-year cycle, which is predicted to occur in about 3000 years (Berger and Loutre, 2002). The present, therefore, is an appropriate opportunity for the next glacial interval to begin (Figure 3-4b). Instead of indications of continued global cooling recorded in the 18th and 19th centuries and a lowering of atmospheric CO_2, however, global warming and CO_2 increases typify the 20th century and the present climate. Based on future orbital and solar radiation variations and present-day CO_2 levels, there is a compelling hypothesis that suggests Earth is bypassing the present "opportunity" to begin the next glacial interval (Berger and Loutre, 2002; Archer and Ganopolski, 2005). Although uncertain, the present window of opportunity to begin the next glacial interval may last for another 3000 years (Figure II-4b). Although it is possible that most fossil carbon reserves will be depleted within the next few hundred years, excess greenhouse gas emissions caused by the burning of that fossil carbon likely will persist in the atmosphere for up to several thousand years, as the ocean and land uptake of excess CO_2 is likely to be slow and gradual. If the present opportunity is bypassed, the next minimum in solar intensity likely to initiate another glacial interval (and a major draw down in sea level) may not occur for another 50,000 years, because the amplitudes of the next 22,000-year cycles will be dampened by the effects of longer-term cycles (Berger and Loutre, 2002) (Figure 3-4b).

3.5 RELATIVE SEA LEVEL CHANGE AT BUHNE HILL

3.5.1 100-year forecast

The relative change in sea level at Buhne Hill must account for changes in global sea level change as well as local tectonic land level change. As described above, over the next 100 years global sea level may rise at rates between 0.26 and 4.1 feet per century (0.8 and 12 mm/yr) (Figure 3-12). Simultaneously, local land level at Buhne Hill likely will increase at a short-term rate of about 1.3 ± 0.3 feet per century (4 ± 1 mm/yr). The resulting relative sea level curve predicts Buhne Hill to be about 44 ± 0.6 feet elevation in the year 2050, and about 43.8 ± 1.6 feet above sea level in 2100 A.D. (Figure 3-12).

If a Cascadia and/or Little Salmon fault earthquake occurs in this time period, as it may, then Buhne hill may be subjected to sudden coseismic subsidence of about 6 feet (1.8 m). The town of King Salmon, which is on the footwall of the Little Salmon fault zone, may experience additional subsidence of several more feet. An independent earthquake on the Little Salmon fault zone could result in coseismic uplift of Buhne Hill of several feet.

3.5.2 1000-year forecast

Over the next 1000 years, we project an increase in sea level at rates between 0.26 and 3.3 feet per century (0.8 and 10 mm/yr), with a best estimate rate that decreases to 1.0 feet per century (3.0 mm/yr) (Figure 3-9). The minimum sea level curve produces an increase of 2.6 feet (0.8 m) over 1000 years, which is less than the +16 to +23 foot (+5 to +7 m) sea level that occurred during the last interglacial interval 125,000 years ago. The maximum sea level curve produces an increase of +33 feet (+10 m) over 1000 years, which exceeds the 125,000-year sea level maximum, but is less than the maximum sea level 400,000 years ago. The best estimate sea level curve produces an increase of +12 feet (+3.7 m), slightly less than the last interglacial maximum sea level value.

Land-level change during the next 1000 years will fluctuate around the long-term uplift rate of about 0.12 ± 0.05 feet per century (0.4 ± 0.1 mm/yr), with short-term variations that may include up to 6.6 feet (2 m) of coseismic subsidence or up to 10 feet (3.3 m) of coseismic uplift. 5 to 53 feet above sea level in 1000 years, with a best estimate of 33 feet (Figure 3-9).

3.5.3 10,000-year forecast

Forecasted relative sea level change at the Humboldt Bay ISFSI site over the next 10,000 years is shown in Figure 3-10. Buhne Hill rises at the long-term permanent uplift rate of 0.12 feet per century. The maximum sea level curve rises at a rate of about 3.3 feet per century for the first ~1200 years, then rises more slowly to attain a maximum height of about +66 feet (20 m) above present-day sea level. The maximum height is consistent with the maximum sea level high stand about 400,000 years ago, and represents complete melting of the Greenland and West Antarctic ice sheets, significant sea level rise from thermal expansion of sea water, and slight melting of the East Antarctic ice sheet. This scenario is consistent will long-term projections described in IPCC (2001). The projection shows inundation of Buhne Hill in about 2000 years. The forecasted height of Buhne Hill in 10,000 years is about 15 feet below sea level.

The minimum sea level curve increases at a rate of about 0.3 feet per century, representing lower amounts of thermal expansion, partial melting of the Greenland and West Antarctic ice sheets, and no change to an increase in the mass balance of the East Antarctic ice sheet. The rate of sea level rise is lower than the rate of land level rise, which has the effect of increasing the elevation of the ISFSI. The forecasted height of the ISFSI under the minimum sea level curve scenario is as great as 53 feet above sea level. The minimum sea level curve also shows an "Early glacial onset" alternative curve, which indicates the possible drop in sea level due to onset of the next glacial interval in the next several thousand years. This early onset alternative is indicated to produce a drop in sea level starting at 7000 A.D., several thousand years after a scenario of global cooling and initiation of the next glacial interval. A several thousand year difference in time between global cooling and sea level fall may be expected given the long response time of the massive ice sheets to adjust to changes in climate.

The best estimate se level curve shows a decreasing rate of sea level rise from 3000 A.D. to about 8000 A.D., then a negligible change in sea level to 12,000 A.D (figure 3-10). The rate of sea level rise is less than the long-term rate of land level rise after about 6000 A.D., when the ISFSI is shown to be at minimum elevation of about 21.5 feet. After this time, land-level change is expected to increase at a higher rate than sea-level change, and the ISFSI will attain higher elevations. The best estimate sea level curve follows the path of a delayed onset of the next glacial interval, assuming that Earth will bypass the present opportunity of a solar insolation minimum to initiate the next glacial interval.

None of the curves shows the relatively minor millennial-scale fluctuations of sea level typical of past interglacial climates (Siddall and others, 2003; Thompson and Goldstein, 2005).

3.5.4 100,000-year forecast

Over time intervals of 100,000 years and longer, relative sea level at Buhne Hill will be dominated by large-magnitude sea level changes related to major glacial-interglacial cycles (Figure 3-11). Buhne Hill rises at the long-term permanent uplift rate of 0.12 ± 0.05 feet per century (0.4 ± 0.1 mm/yr). The maximum sea level curve is based on a maximum level of +66 feet (+20 m), and then is shown to stay at higher than present-day levels for about 50,000 years. The minimum sea level curve attains a maximum height of about +20 feet (+6 m). The early onset alternative curve shows a rapid drop in sea level, indicating a return to glacial conditions in about 5000 years. The delayed onset alternative curve indicates a return to glacial conditions in about 50,000 years, consistent with the next low in solar insolation. The delayed onset curve is partially based on Berger and Loutre (2002). The best estimate curve is intermediate between the minimum and maximum curves, and follows the path of the delayed onset curve.

3.6 CONTRIBUTION OF PACIFIC STORMS

Past wave heights off shore of Humboldt Bay are summarized in Page (2004). As discussed in Page (2004) the Eel River Buoy data for the period of record between 1982 through 2003 (National Ocean and Atmospheric Administration, 2004a, 2004b) shows that the maximum wave heights for 1987 and 1988, are 9.8 and 10 meters (32 and 32.5 feet) respectively at the

buoy. These are high but not significantly higher than waves in other years and were exceeded only twice: in 1984 (12 meters; 39 feet) and 1999 (10.7 meters; 35 feet). The jetties at the entrance to Humboldt Bay were built to resist these very large waves but have had to be repaired periodically between 1930 and 1972 with large, 20- to 100-ton concrete blocks, and with 43-ton dolosse (Table 7-11 in Coastal Engineering Research Center, 1984).

Global warming may produce more frequent el-Nino-type conditions in the northern Pacific with an accompanying rise in sea level and future waves may be higher and have different directions because global warming may change the patterns and intensity of the potentially damaging Pacific storms that reach Buhne Hill through the Humboldt Bay channel. All storm waves reaching Red Bluff, including possibly higher and more frequent waves resulting from global warming, would be superimposed on the projected sea levels in the next 100 years shown in Figure 3-12. The consequences are potentially more frequent and larger wave attacks that will increase the potential for storms to damage the riprap at Red Bluff and Buhne Hill. The potential impacts from storm waves are considered slightly more important in the short term, tens of years to 100 years as the projected rise in sea level encroaches the riprap berm protecting Buhne Hill. The added contribution from storms to the erosion potential is small so for the scenarios longer than 100 years because the contribution from storm waves is considered inconsequential.

4.0 TSUNAMI HAZARDS

The tsunami hazard for the ISFSI is discussed in detail in PG&E (2003) and is not a concern for the ISFSI because in the highly unlikely chance that the vault is overtopped the casks would not be damaged by water and the vault is set below grade so impact from large floating objects and debris is not a significant hazard. The expected maximum runup from an event on the Cascadia Subduction zone is 21-36 feet (MLLW) at low tide or 28-43 feet (MLLW) at high tide (PG&E, 2003). Such a tsunami does not reach the 44 foot elevation of the ISFSI (Figure 1-7). We consider this tsunami the maximum runup expected and would be added to postulated future conditions caused by any relative change in sea level as discussed in section 3 above.

The maximum tsunami generated by a Cascadia subduction zone earthquake discussed above has not been exceeded in the past two to four thousand years (the limit of the Holocene geologic record easily accessed) based on the analysis of the numerous paleo tsunami studies that have been completed along the northern California coast (PG&E, 2003) and the Oregon, Washington and British Columbia coasts. For example, multiple sand deposits preserved in a small coastal lake in south-central Oregon provide paleotsunami runup estimates between 16 and 26 feet (5 to 8 m) (Kelsey and others, 2005). In northern Oregon, Peterson and others (1995) concluded that paleotsunami runup at the open coast ranged from 16 to 39 feet with a preferred estimate of 23 to 30 feet. Inspection of the offshore bathymetry west of Oregon and northern California indicates several very large submarine landslides, but these are estimated to be hundreds of thousands of years old (PG&E, 2003; Plafker, oral communication, 2001). A large local landslide that might occur during a Cascadia earthquake would enhance the tectonic tsunami and might rise significantly higher than the ones predicted from a Cascadia earthquake at Buhne Hill. These are postulated to be similar to those known elsewhere in the world such as the 1946 landslide enhanced tsunami from the Aleutian earthquake (PG&E, 2003). Such a tsunami is considered to be rare but possible at Humboldt Bay and Buhne Hill over a time frame of thousands to tens of thousands of years.

A tectonic tsunami similar to the 2004 Sumatran earthquake does not appear to be the type generated by a Cascadia earthquake because none have been recorded in the past few thousand years. Recent investigations of the great 2004 Sumatra earthquake and tsunami show run up heights in the immediate vicinity of the earthquake epicenter (near field) approaching 40 meters (130 feet) (Figure 4-2) (Cluff, Plafker, and Nishenko, unpublished data, 2005; Dengler, 2005). The tsunami also stripped a 10 to 20 meter high zone of trees and vegetation from the coastal hills of southwestern Sumatra for a distance of ~ 250 km (~155 miles) (Photo 4-1). The maximum observed run up height is more than 3 times the postulated maximum run up at Buhne Hill. However, if such an event occurred it would be on time scales of 10,000 to 100,000 years but would severely damage the coastal margin in Humboldt Bay. Potential effects are illustrated by examples from Sumatra. While the majority of non-engineered structures (e.g. residential housing, etc) in the tsunami runup zone were completely destroyed their foundations remained intact as did roads that were at grade with the surrounding land surface (Photos 4-1, 4-2 and 4-3) illustrating the limited damage from base erosion because the surging tsunami runup and backwash had relatively low velocities. Moreover; engineered structures, such as the LaFarge Cement plant at

Lhoknga (Photo 4-4), while damaged, remained standing and are currently being restored for service.

In addition to the destruction from the dynamic water forces generated by the tsunami itself, demolition from the impacts caused by large floating objects, including ships, barges, fuel storage tanks, cars, and other water born debris, occurred throughout the run up zone (Photos 4-3, 4-5 and 4-6). The dynamic force of the tsunami waves at Lhonnga is illustrated by the displacement of tetra-pods weighing more than 30 tons along the dock for the cement plant. These examples show that Buhne Hill will probably be stripped of vegetation and the bluff edges eroded, but the ISFSI which is at grade and more than 80 feet from the bluff edge would not be exposed by erosion or damaged by impacts from floating objects during such a tsunami.

5.0 IMPLICATIONS TO COASTAL PROTECTION AT BUHNE POINT

The assessment of the coastal protection works at Buhne Hill is discussed in some detail by Page (2004). The performance of the existing riprap berm in front of Red Bluff is reevaluated in light of potential long term changes of sea level as discussed below.

5.1 Current Coastal Protection works

As described by Page (2004), Red Bluff and Buhne Hill are protected by a riprap berm (Figure 1-1; Photos 1-1, 5-1. 5-2 and 5-3) Riprap was first placed along the bay shoreline in front of Red Bluff in the 1950s to help arrest wave erosion after PG&E acquired the property. The berm protects all of Buhne Hill, extending southwest for about 3,100 feet from the Northwestern Pacific Railroad's riprap berm on the north to the protective berm placed by the Corps of Engineers in front of the village of King Salmon to the south.

The original riprap, which consisted of silicified, micaceous schist and silicified diorite (maximum lengths 8 ½ feet; median length 6 ½ feet) was eroded during winter storms in the 1980s. In 1989 the riprap berm was completely refurbished by repairing the remnants of the earlier berm and placing additional 4- to 9-ton stones in two layers on the berm. The plan drawings (Figures 5-1 to 5-6) show that the repairs significantly added to the seaward toe of the berm and decreased the seaward slope to 2.5:1 or 2:1 from the steeper older berm. The plans also call for setting 6- to 9-ton stones in a trench on the seaward toe of the berm. The more damaged sections for the 1889 fix are those indicated for repair in the first phases (Figure 5-2). The new riprap consisted of greenish-gray, very hard and resistant, silicified diorite (9 feet in longest dimension) (Photos 5-4 and 5-5). The berm is shaped in cross section as a triangle with the hypotenuse sloping seaward. As measured in 2005 the seaward slope varies between 15 to 30 degrees 3:1 to 4:1) with and average of about 20 degrees (Photo 5-6). The berm is about 20 to 30 feet wide and 5 feet high on the landward side. The foundation of the berm is a layer of naturally occurring fine sand (estimated to be 1 to 3 foot thick) that forms the sand flat in front of Red Bluff (Photos 5-7 and 5-8); the sand layer overlies the wave-cut bench on 'bedrock' that is moderately to well consolidated sand, silt and clay beds of the Pleistocene Hookton Formation. The berm is set 15 to 20 feet in front of the foot of Red Bluff (Photos 5-9 and 5-10). This set back allows for repairs to be made easily if the berm is damaged and permit easy public access along the coast.

The riprap berm as designed and constructed should withstand waves about 12 to 13 feet high, assuming an average slope of about 20 degrees, and an average stone as 7 tons, with a unit weight similar to basalt, 170 pounds per cubic foot (calculation 7-116 as recommended by the Coastal Engineering Research Center, 1984). And indeed since the augmentation of the riprap berm in 1989, a period of typical waves is recorded off shore, including relatively high waves in 1999, the riprap has remained stable and performed well. Several areas of minor erosion of the foundation materials are evident behind and beneath the berm (Photos 5-10 and 5-11). None of these are of concern at this time. Minor settlement is evident in the several blocks of riprap that have toppled from the steep landward side of the berm toward Buhne Hill and a few blocks of riprap have been displaced and lie in front of the berm (Photos 5-4, 5-7 and 5-12).

5.2 Damage from storms, tsunamis and earthquake events

As stated in Page (2004) the riprap BERM at Buhne Hill may be damaged in future storms or tsunami events. The implications of possible increased wave heights and increased frequency of storms resulting from global warming to the stability of the riprap berm a Buhne Hill has minimal consequence . The berm may be damaged more frequently than under current conditions but such damage likely would be slight to moderate, similar the damage sustained by the mid 1980s and would be repaired by rebuilding the riprap berm with larger size of the riprap and possibly other improvements to account for the changed wave characteristics and other conditions. Any repairs would be undertaken only after significant damage occurred to the existing berm.

Damage from tsunamis is expected to be minor to extensive depending on the size of the runup surges. If the runup is high enough, the riprap berm may be significantly damaged by the wash and backwash of the tsunami surges and the vegetation will probably be stripped from the sides of Buhne Hill similar to what happened during the 2004 Sumatra tsunami, but erosion is expected to be minimal because the tsunami are limited to only a few runups surges and the velocity is relatively slow. If a tsunami is larger than the maximum estimated for the ISFSI and floods the vault, no damage is expected because the casks are designed to be submerged and the vault is at ground level so no floating projectiles will impact the ISFSI. This conclusion is supplemented by the evidence from the 2004 Sumatra tsunami: while numerous houses were washed away by the 2004 Sumatra tsunami, most foundation pads remained intact. If and when a tsunami damages the protective berm or erodes Red Bluff, the riprap and other protection works will be repaired and augmented as needed. This is relatively easily done because of the wide strip between the berm and Red Bluff allow for easy equipment access and room to raise the berm.

An earthquake on Cascadia subduction zone and/or Little Salmon fault zone is expected to produce a small amount of subsidence or uplift of one to two feet of Buhne Hill and the ISFSI site and a simultaneous subsidence of up to 6.6 feet (2 meters) at the village of King Salmon, which lies on the footwall of the Bay Entrance and Buhne Point faults. This will inundate King Salmon and the south side of Buhne Hill and expose this area to erosion from storm waves that will more easily reach the area after the earthquake. The berm may need repairs and be heightened to accommodate the relative rise in sea level from the subsidence of Buhne Hill. Additional protection of the south-facing aspect of Buhne Hill may be required, but this part of the hill is not subject to significant wave erosion. None the less, if significant erosion develops, it can be mitigated by adding a riprap berm at the base of the hill, similar to the existing berm.

5.3 Changed conditions from rise in sea level

As new knowledge about global warming and rise in sea level are gained during the next 100 to 1,000 years, the potential effectiveness of the coastal protection at Buhne Hill will be reassessed. These reassessments will be performed periodically to consider how the projected changes in sea level and variations in storm waves may impact the coastal protection works. Under the minimum sea level rise scenario, tectonic uplift keeps pace with sea level rise. However, if sea level rises significantly with respect to the ISFSI as illustrated under the best and extreme estimated projections (Figure 3-9) the rise will be slow and hence

needed modifications can and will be implemented to continue to protect the ISFSI. The wide area between the existing berm and the bluff allows for the berm to be raised with a minimum effort. Only under the maximum possible scenario in the 10,000-year projection (Figure 3-10) does the ISFSI become inundated by the rise in sea level. If the maximum scenario proves correct a thousand years from now, the casks would be moved to another location.

6.0 REFERENCES

Archer, David; Ganopolski, Andrey, 2005, A movable trigger: Fossil fuel CO_2 and the onset of the next glaciation: *Geochem. Geophys. Geosyst*., Vol. 6, No. 5, Q05003 DOI 10.1029/2004GC000891

Arendt, A.A., Echelmeyer, K.A., Harrison, W.D., Lingle, C.S., and Valentine, V.B., 2002, Rapid wastage of Alaska glaciers and their contribution to rising sea level: *Science*, v. 297, p. 382-386.

Atwater, B.F. and Hemphill-Haley, E., 1997, Recurrence intervals for great earthquakes of the past 3500 years at northeastern Willapa Bay, Washington: U.S. Geological Survey Professional Paper 1576, 108 p.

Berger, A. and Loutre, M.F., An exceptionally long interglacial ahead?: *Science*, v. 297, p. 1287-1288.

Bindschadler, R., 1998, Future of the West Antarctic Ice Sheet: *Science*, v. 282, p. 428-429.

Blum, M.D., Carter, A.E., Zayac, T, and Goble, R., 2002, Middle Holocene sea level and evolution of the Gulf of Mexico coast (USA), *Journal of Coastal Research*, Special Issue 36, pp. 65-80.

COHMAP Members, 1988, Climate changes of the last 18,000 years: observations and model simulations: *Science*, v. 271, p.1043-1052.

Chappell, J., 2002, Sea level changes forced ice breakouts in the last glacial cycle: New results from coral terraces: *Quaternary Science Review*, v. 21, p. 1229-1240.

Chappell, J., Omura, A., Esat, T., McCulloch, M., Pandolfi, J., Ota, Y., and Pillans, B., 1996, Reconciliation of late Quaternary sea levels derived from coral terraces at Huon Peninsula with deep sea oxygen isotope records, *Earth and Planetary Science Letters*, v. 141, p. 227-236.

Chen, J.H., Curran, H.A., White, B., and Wasserburg, G.J., 1991, Precise chronology of the last interglacial period; 234U-230Th data from fossil coral reefs in the Bahamas: Geol. Soc. Am. Bull. v. 103, p. 82-97.

Clarke, S. H., Jr., and G. A. Carver, 1992, Late Holocene tectonics and paleoseismicity, southern Cascadia subduction zone: Science, v. 255, p. 188-192.

Coastal Engineering Research Center, 1984, Shore protection manual: Department of the Army, Waterways Experiment Station, Corps of Engineers; v. 2, pp. 7-202-237.

Cuffey, K.M. and Marshall, S.J., 2000, Substantial contribution to sea-level rise during the last interglacial from the Greenland ice sheet: *Nature*, v. 404, p. 591-594.

Cuffey, K.M., G.D. Clow, R.B. Alley, M. Stuiver, E.D. Waddington, and R.W. Saltus. 1995. Large Arctic temperature change at the Wisconsin-Holocene glacial transition. *Science* v. 270, p. 455-458.

Cutler K.B., Edwards R.L., Taylor F.W., Cheng H., Adkins J., Gallup C.D., Cutler P.M., Burr G.S., Chappell J., and Bloom A.L. (2003). Rapid sea level fall and deep-ocean temperature change since the last interglacial. *Earth and Planetary Science Letters*, v. 206, p. 253-271.

Douglas, B.C., 1991, Global sea level rise: *Journal of Geophysical Research*, v. 96, p. 6981-6992.

Douglas, B.C., 1997. Global sea level rise: a redetermination, *Surveys Geophys*., v. 18, p. 279-292.

Douglas, B.C., 2001, An introduction to sea level, in, Douglas, B.C., Kearney, M.S., and Leatherman, S.P., eds., *Sea Level Rise: History and Consequences*, International Geophysics Series, v. 75, Academic Press, 232 p.

Droxler, A.W., Alley, R.B., Howard, W.R., Poore, R.Z., and Burckle, L.H., 2003, Introduction: Unique and exceptionally long interglacial marine isotope stage 11: window into Earth warm future climate: In, A. Droxler, R. Poore, L. Burckle, and L. Osterman, Eds., *Earth's Climate and Orbital Eccentricity: The Marine Isotope Stage 11 Question*: American Geophysical Union Geophysical Monograph 137, pp. 69-85.

Fairbanks, R.G., 1989. Glacio-eustatic sea level record 0-17,000 years before present: influence of glacial melting rates on Younger Dryas event and deep ocean circulation. *Nature*, 342, 637-642.

Fleming, K., Johnston, P., Zwartz, D., Yokoyama, Y., Lambeck, K., and Chappell, J., 1998, Refining the eustatic sea-level curve since the Last Glacial Maximum using far- and intermediate-field sites: Earth and Planetary Science Letters, v. 163, p. 327-342.

Flück, P., Hyndman, R.D., and Wang, K., 1997, Three-dimensional dislocation model for great earthquakes of the Cascadia subduction zone: Journal of Geophysical Research, v. 102, p. 20,539-20,550.

Gornitz, V., 1995, Sea level rise: A review of recent past and near-future trends: *Earth Surface Processes and Landforms*, v. 20, p. 7-20.

Gornitz, V., 2001, Impoundment, groundwater mining, and other hydrologic transformations: impacts on global sea level rise, *In*, Douglas, B.C., Kearney, M.S., and Leatherman, S.P., Eds., *Sea Level Rise: History and Consequence*: International Geophysics Series, v. 75, Academic Press, p. 97-119.

Gregory, J. M., J. A. Church, G. J. Boer, K. W. Dixon, G. M. Flato, D. R. Jackett, J. A. Lowe, S. P. O'Farrell, E. Roeckner, G. L. Russell, R. J. Stouffer, and M. Winton, 2001, Comparison of results from several AOGCMs for global and regional sea level change 1900-2100: *Climate Dynamics*, v. 18, p. 225-240.

Hearty, P.J., Kindler, P., Cheng, H. and Edwards, R.L., 1999, A +20 m middle Pleistocene sea level high stand (Bermuda and the Bahamas) due to partial collapse of Antarctic ice: *Geology*, v. 27, p.375-378.

Huybrechts, P., Gregory, J., Janssens, I., and Wild, M., 2004, Modeling Antarctic and Greenland volume changes during the 20th and 21st centuries forced by GCM time slice integrations: *Global and Planetary Change*, v. 42, p. 83-105.

Hyndman, R.D. and Wang, K., 1995, The rupture zone of Cascadia great earthquakes from current deformation and the thermal regime: *Journal of Geophysical Research*, v. 100, p. 22,133-22,154.

Imbrie, J., Hays, J.D., Martinson, D.G., McIntyre, A., Mix, A.C., Morley, J.J., Pisias, N.G., Prell, W.L., and Shackleton, N.J., 1984, The orbital theory of Pleistocene climate: Support from a revised chronology of the marine $\delta^{18}O$ record, in Berger, A.L., and others, eds., *Milankovich and Climate*: Hingham, Massachusetts, Riedel Publishing, p. 269-305.

IPCC, 2001, Climate Change: The scientific basis, Third assessment report by the Intergovernmental Panel on Climate Change: Cambridge University Press, Oxford. See especially Cheaper 11: Changes in sea level, p. 641-693. Available online at: http://www.grida.no/climate/ipcc_tar/

Kelsey, H.M., Nelson, A.R., Hemphill-Haley, E., and Witter, R.C., 2005, Tsunami history of an Oregon coastal lake reveals a 4600 yr record of great earthquakes on the Cascadia subduction zone: Geological Society of America Bulletin, v. 117, n.7/8, p. 1009-1032.

Kelsey, H.M., Witter, R.C., and Hemphill-Haley, E., 2002, Plate-boundary earthquakes and tsunamis of the past 5500 years, Sixes River estuary, southern Oregon: Geological Society of America Bulletin, v. 114, p. 298-314.

Lambeck, K. and Bard, E., 2000, Sea-level change along the French Mediterranean coast for the past 30,000 years: Earth and Planetary Science Letters, v. 175, p. 203-222.

Laskar, J., Robutel, P., Joutel, F., Gastineau, M., Correia, A.C.M., Levrard, B., 2004, A long term numerical solution for the insolation quantities of the Earth: Astronomy & Astrophysics, v. 428, p. 261-285, DOI: 10.1051/0004-6361:20041335.

Lea D. W., Martin P. A., Pak D. K., and Spero H. J. (2002) Reconstructing a 350 ky history of sea level using planktonic Mg/Ca and oxygen isotopic records from a Cocos Ridge core. Quat. Sci. Rev. 21(1-3), 283-293.

Martinson, D.G., Pisias, N.G., Hays, J.D., Imbrie, J., Moore, T.C., Shackleton, N.J., 1987, Age dating and the orbital theory of the ice ages: development of high-resolution 0 to 300,000-year chronostratigraphy: Quaternary Research 27, 1–29.

McManus, J. F., Oppo, D. W., Cullen, J. L., and Healey, S. L., 2003, Marine Isotope Stage 11 (MIS 11): Analog for Holocene and future climate? In, A. Droxler, R. Poore, L. Burckle, and L. Osterman, Eds., *Earth's Climate and Orbital Eccentricity: The Marine Isotope Stage 11 Question*: American Geophysical Union Geophysical Monograph 137, pp. 69-85.

Mitchell, C.E., Vincent, P., Weldon, R.J., and Richards, M.A., 1994, Present-day vertical deformation of the Cascadia margin, Pacific Northwest, United States: *Journal of Geophysical Research*, 99, p. 12,257-12,277.

Mörner, N.-A., 2004, Estimating future sea level changes from past records: *Global and Planetary Change*, v. 40, p. 49-54.

National Oceanographic and Atmospheric Administration, 2004a, Website: http://www.ndbc.noaa.gov/station_history.phtml?station=46022

National Oceanographic and Atmospheric Administration, 2004b, website; http://www.ndbc.noaa.gov/measdes.shtml

Oppenheimer, M., 1998, Global warming and the stability of the West Antarctic Ice Sheet: Science, v. 393, p. 325-332.

Page, W.D., 2004, Assessment of Erosion at Buhne Hill, Humboldt Bay ISFSI, Humboldt County, California; PG&E Geosciences Department report, 32p. .

PG&E, 2003, Humboldt Bay ISFSI safety analysis report, December 2003, Section 2.6: report to the Nuclear Regulatory Commission, Washington, D.C.; produced from PG&E (2002), Seismic Hazard Assessment for the Humboldt Bay ISFSI Project: Humboldt Bay ISFSI Project Technical Report TR-HBIR-2002-01, revision 0 – 27 December 2002, Section 3, Regional Geology, 47 p.; Section 4, Site Geology, 49p.; Section 5, 47 p.; Section 8, Surface faulting potential, 26 p.; Section 9, Tsunami hazard, 64p.

Peltier, W.R., 1999, Global sea level rise and glacial isostatic adjustment: *Global and Planetary Change*, v. 20, p. 93-123.

Peltier, W.R. & Tushingham, A.M., 1989. Global sea level rise and the Greenhouse effect: Might they be connected?: *Science*, v. 244, p. 806-810. (2.4 ± 0.9 mm/yr rise in sea level).

Peterson, C.D., Darienzo, M.E., Doyle, D.D., and Barnett, E., 1995, Evidence for coseismic subsidence and tsunami inundation during the past 3000 years at Siletz Bay, Oregon, in, Priest, G.R., Explanation of mapping methods and use of the tsunami hazard map of the Siletz Bay area, Lincoln County, Oregon: Oregon Department of Geology and Mineral Industries Geological Map Series report.

Petit, J.R., J. Jouzel, D. Raynaud, N.I. Barkov, J.-M. Barnola, I. Basile, M. Benders, J. Chappellaz, M. Davis, G. Delayque, M. Delmotte, V.M. Kotlyakov, M. Legrand, V.Y. Lipenkov, C. Lorius, L. Pépin, C. Ritz, E. Saltzman, and M. Stievenard, 1999, Climate and atmospheric history of the past 420,000 years from the Vostok ice core, Antarctica: *Nature*, v. 399, pp. 429-436.

Potter, E-K., Esat, T.M., Schellmann, G., Radtke, U., Lambeck, K., and McCulloch, M.T., 2004, Suborbital-period sea-level oscillations during marine isotope substages 5a and 5c: Earth and Planetary Science Letters, v. 225, p. 191-204.

Ruddiman, W.F., 2003, The anthropogenic greenhouse era began thousands of years ago: *Climate Change*, v. 61, p. 261-293.

Scherer, R.P., Aldahan, A., Tulaczyk, S., Possnert, G., Engelhardt, H., and Kamb, B., 1998, Pleistocene collapse of the West Antarctic ice sheet: *Science*, v. 281, p. 82-85.

Shackleton, N.J.. 2000. The 100,000-year ice-age cycle identified and found to lag temperature, carbon dioxide, and orbital eccentricity: *Science* v. 289, p. 1897-1902.

Siddall M., E.J. Rohling, A. Almogi-Labin, Ch. Hemleben, D. Meischner, I. Schmelzer, & D.A. Smeed (2003). Sea level fluctuations during the last glacial cycle. Nature, 423, 583-588.

Stirling, C.H., Esat, T.M., McCulloch, M.T., and Lambeck, K., 1995, High-precision U-series dating of corals from Western Australia and implications for the timing and duration of the last interglacial: Earth and Planetary Science Letters, v. 135, p.

Stirling, C.H., Esat, T.M., Lambeck, K., and McCulloch, M.T., 1998, Timing and duration of the last interglacial; evidence for a restricted interval of widespread coral reef growth: Earth and Planetary Science Letters, v. 160, p. 745-762.

Thompson, W.G. and Goldstein, S.L., 2005, Open-system coral ages reveal persistent suborbital sea level cycles: *Science*, v. 308, p. 401-404.

Waelbroeck, C., Labeyrie, L., Michel, E., Duplessy, J.C., McManus, J.F., Lambeck, K., Balbon, E., and Labracherie, M., 2002, Sea-level and deep water temperature changes derived from benthic foraminifera isotopic records: Quaternary Science Reviews, v. 21, 295-305.

Williams, T.B., 2002, The Geodetic Signature of Modern Deformation (1993-2002) within the Southern Cascadia Margin, Northwestern California: unpublished M.S. Thesis, Humboldt State University, Department of Geology, 102 p.

Witter, R.C., Kelsey, H.M., and Hemphill-Haley, E., 2003, Great Cascadia earthquakes and tsunamis of the past 6700 years, Coquille River estuary, southern coastal Oregon: *Geological Society of America Bulletin*, v. 115, pp. 1289-1306. Wright, H.E., J.E. Kutzbach, T. Webb III, W.F. Ruddiman, F.A. Street-Perrott, and P.J. Bartlein, eds. (1993). Global Climates since the Last Glacial Maximum, University of Minnesota Press, Minneapolis, MN, 569 pp.

Youd, T.L., Bardet, J-P, and Bray, J.D., eds., 2000, Supplement to Volume 16 Kocaeli, Turkey, earthquake of August, 17, 1999, reconnaissance report: Earthquake Spectrra 2000-03, 461p.

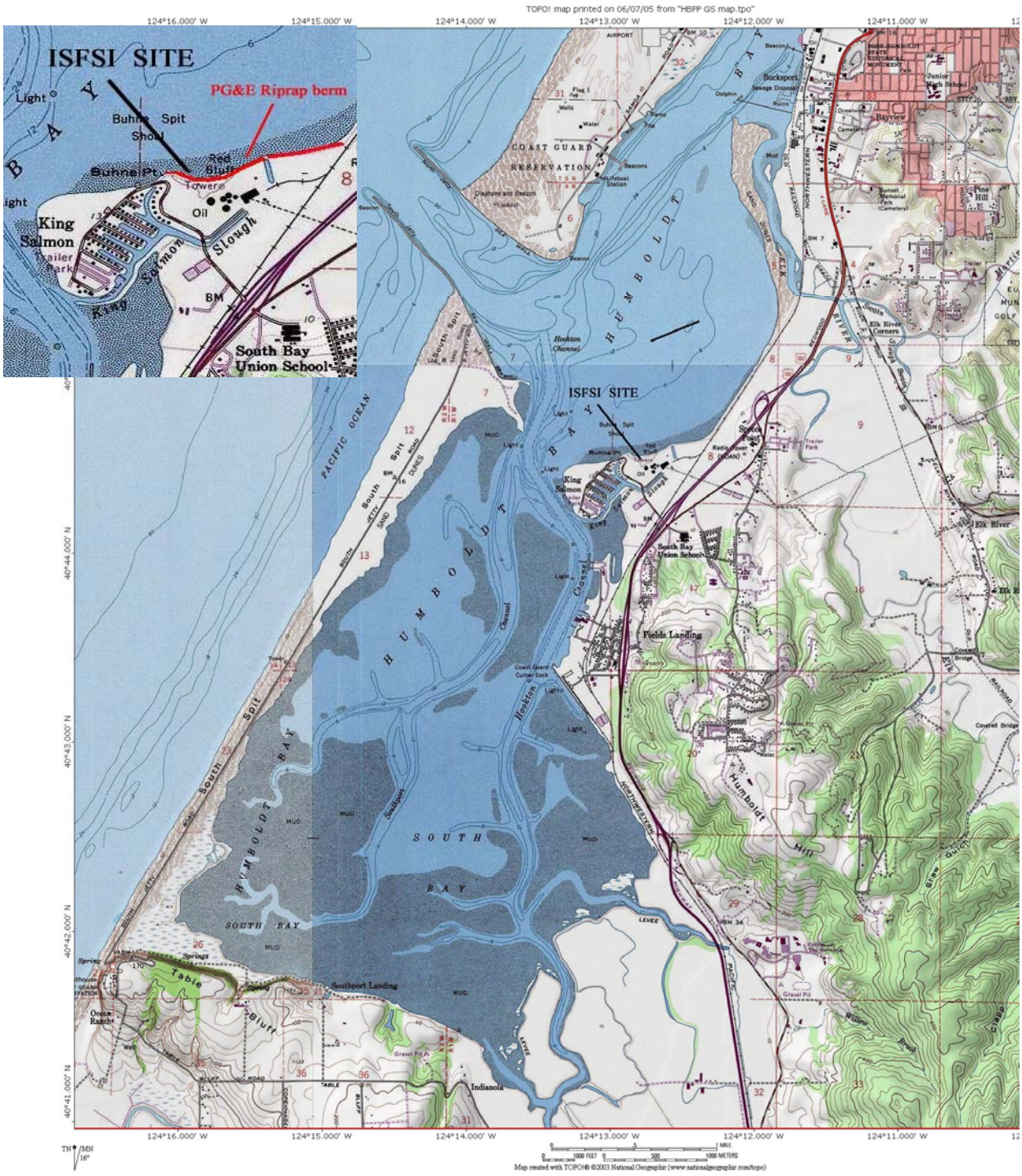

Figure 1-1 Location Map of ISFSI site at Buhne Hill in Humboldt Bay

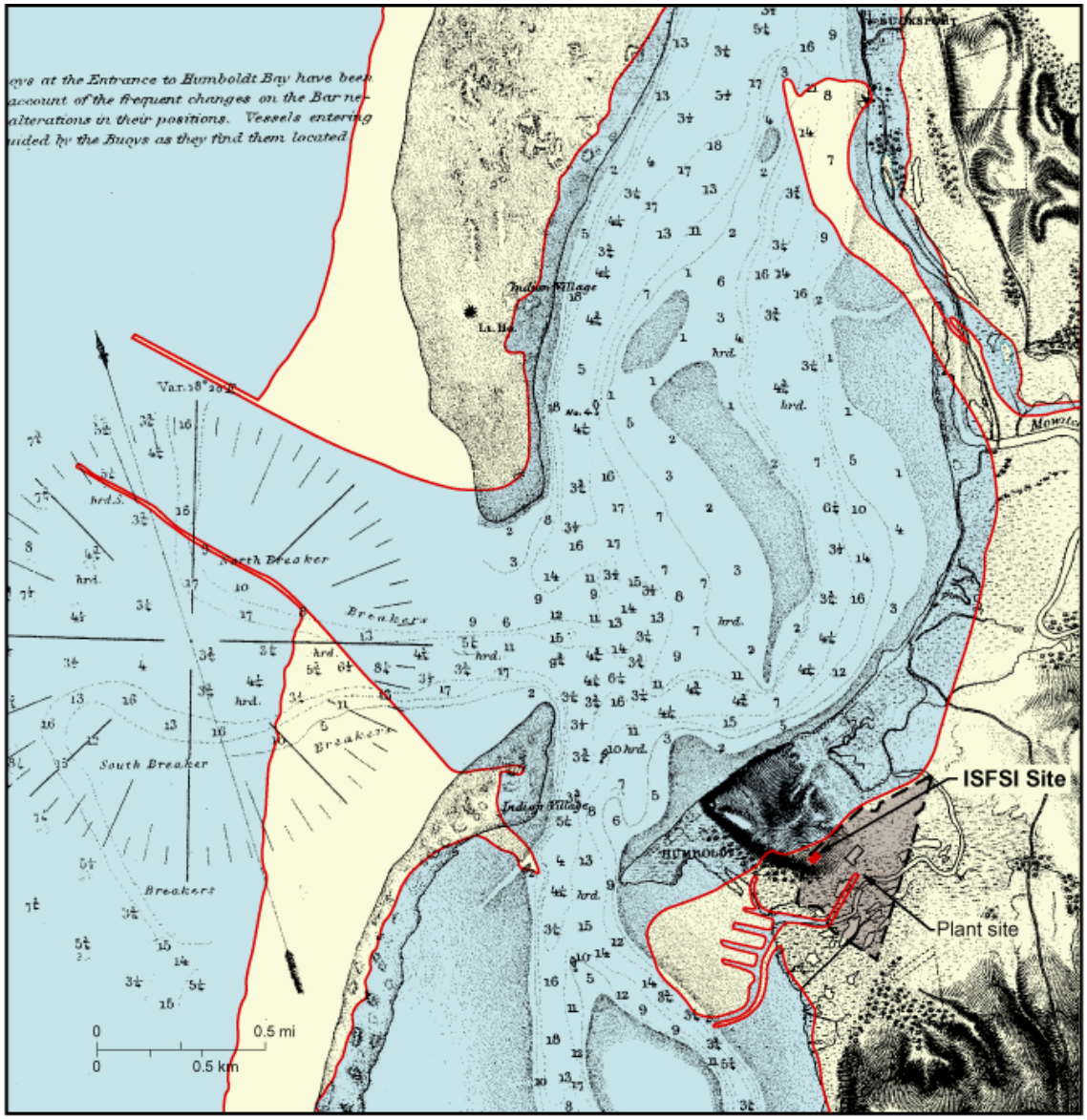

Preliminary Survey of Humboldt Bay, California, U.S. Coast Survey, 1858 (edition of 1879), (original scale 1:30,000) (aids to navigation corrected to 1885). Depths are in feet below mean lower low water to lowest dotted line, then in fathoms. Red line delineates present shoreline and jetties from USGS Fields Landing 7.5 minute Quadrangle (1989). Brown area is plant site.

(SAR Figure 2.6-117)

Figure 1-2 Retreat of Red Bluff in Humboldt Bay since 1858

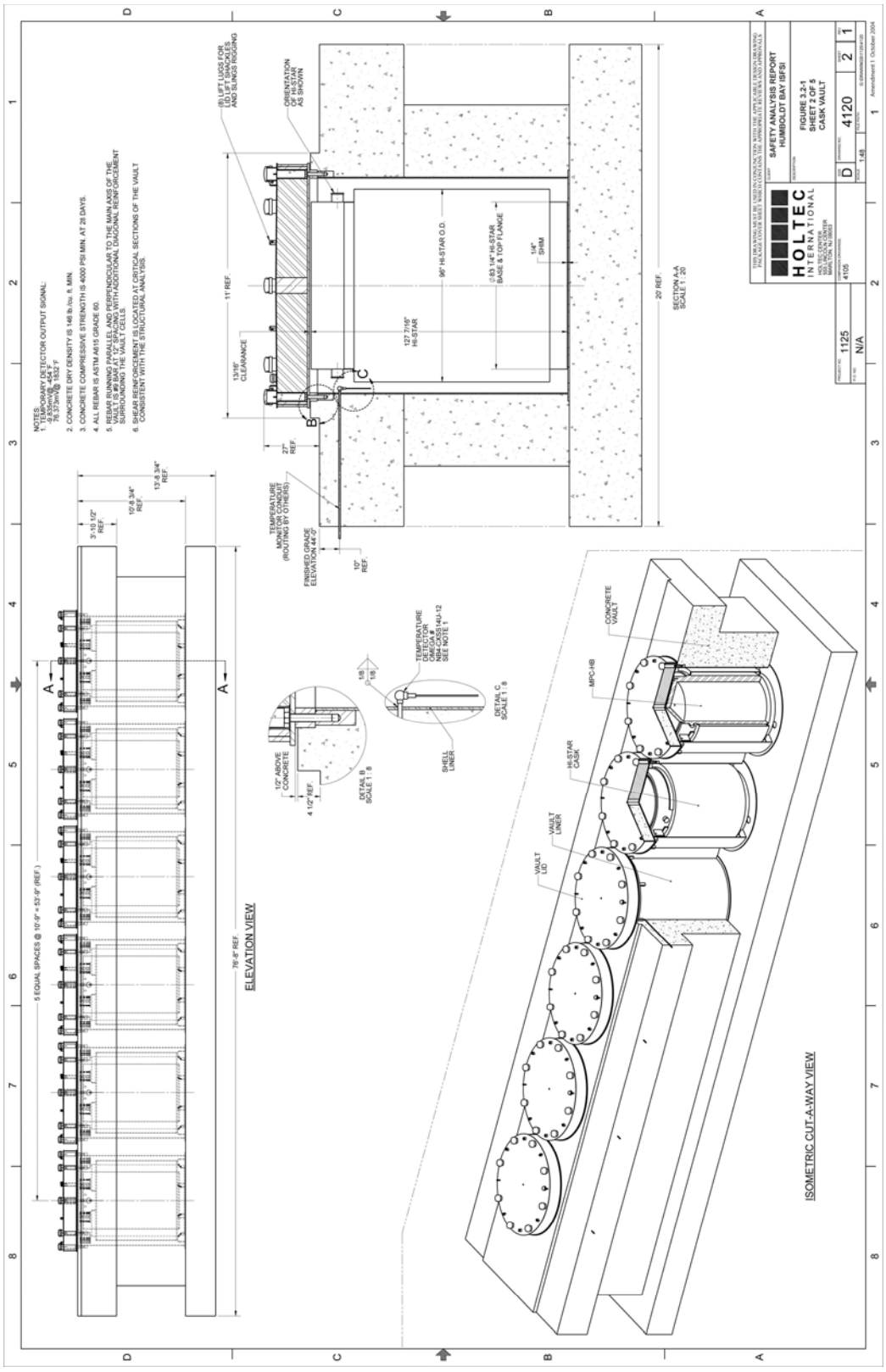

Figure 1-3 Diagram of vault for containing casks

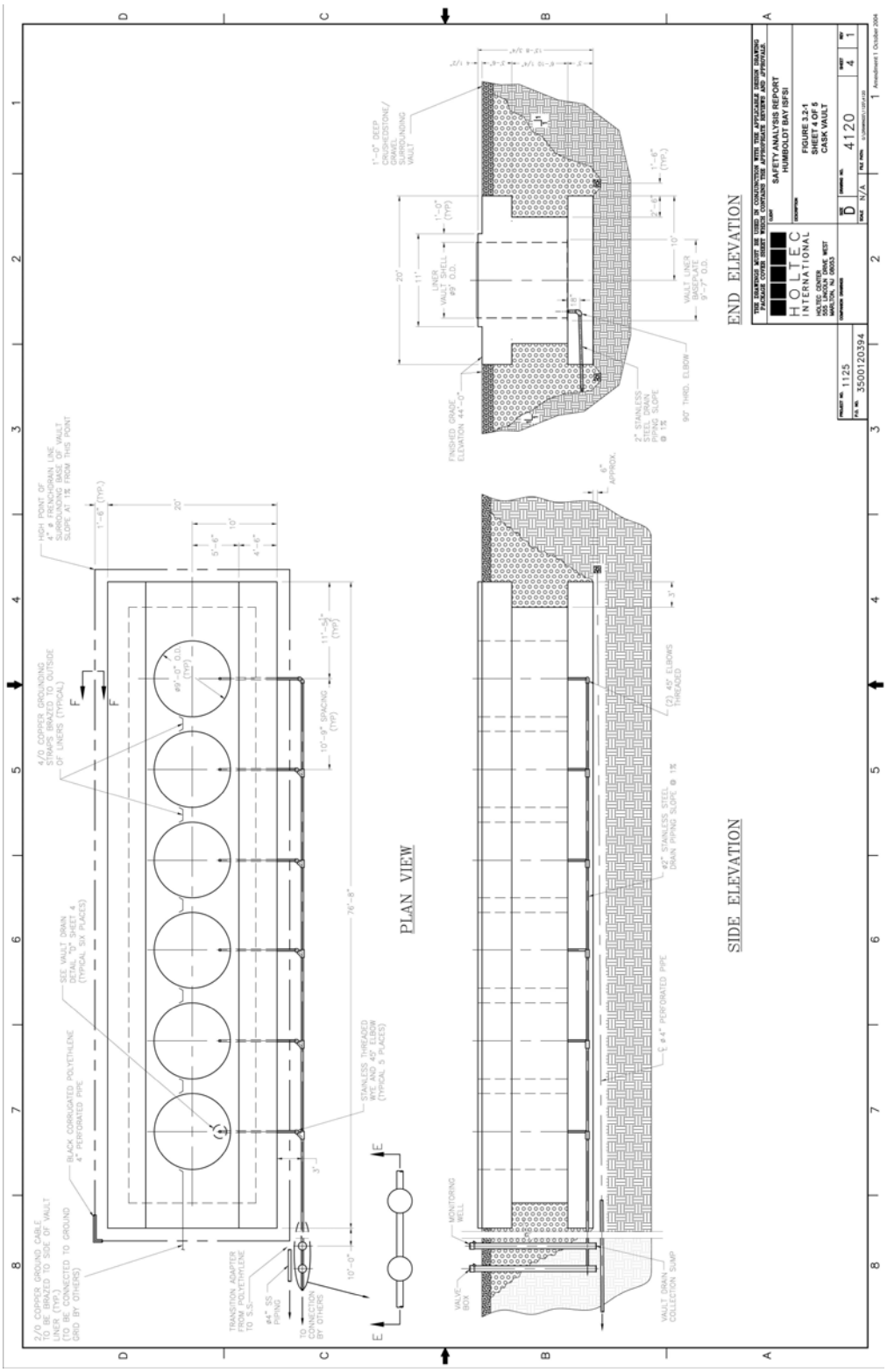

Figure 1-4 Placement of cask vault with top set at ground surface

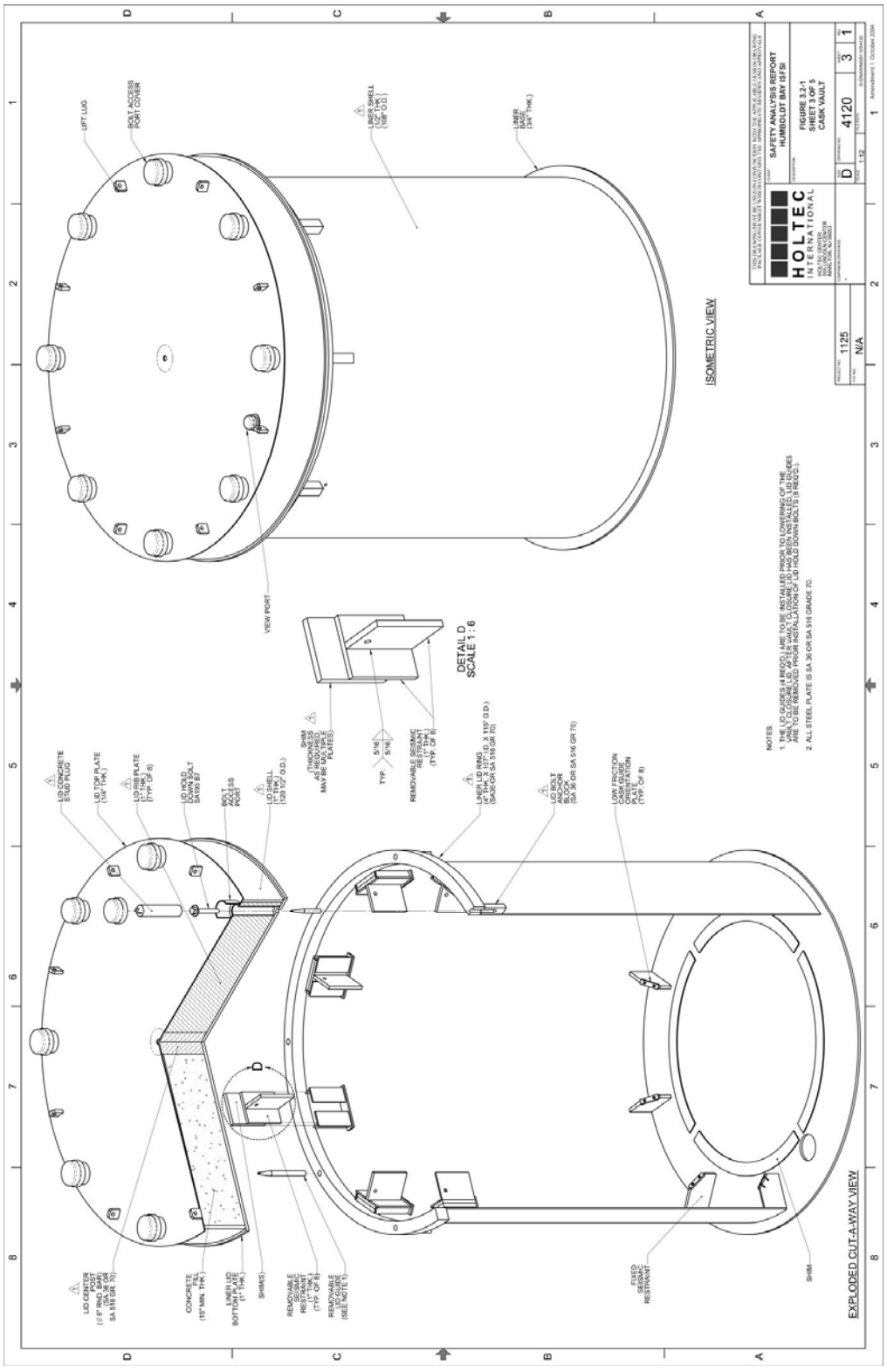

Figure 1-5 Diagram of vault cells that will contain the casks

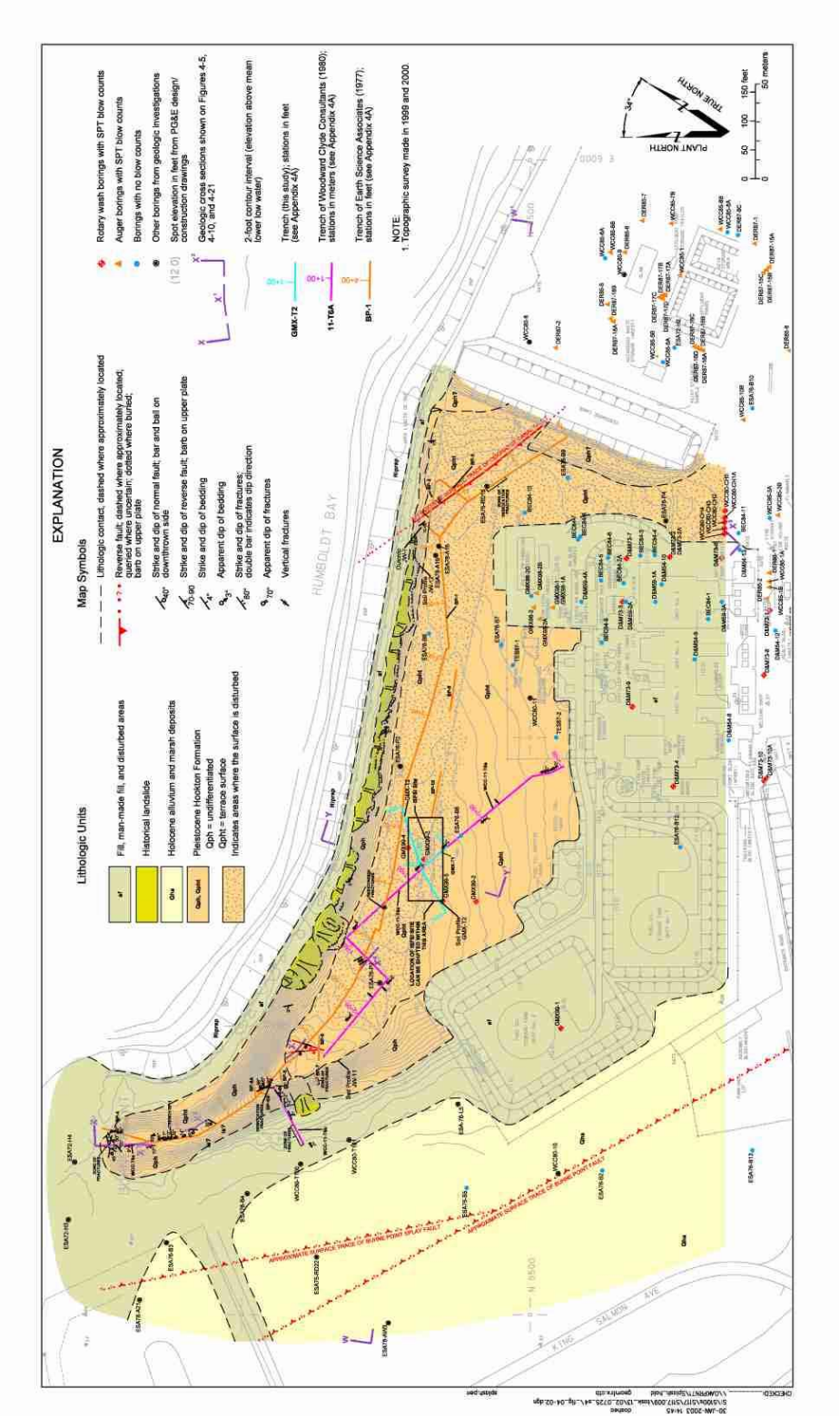

Red Bluff is the north facing side (SAR Figure 2.6-31)

Figure 1-6 Geologic map of Buhne Hill

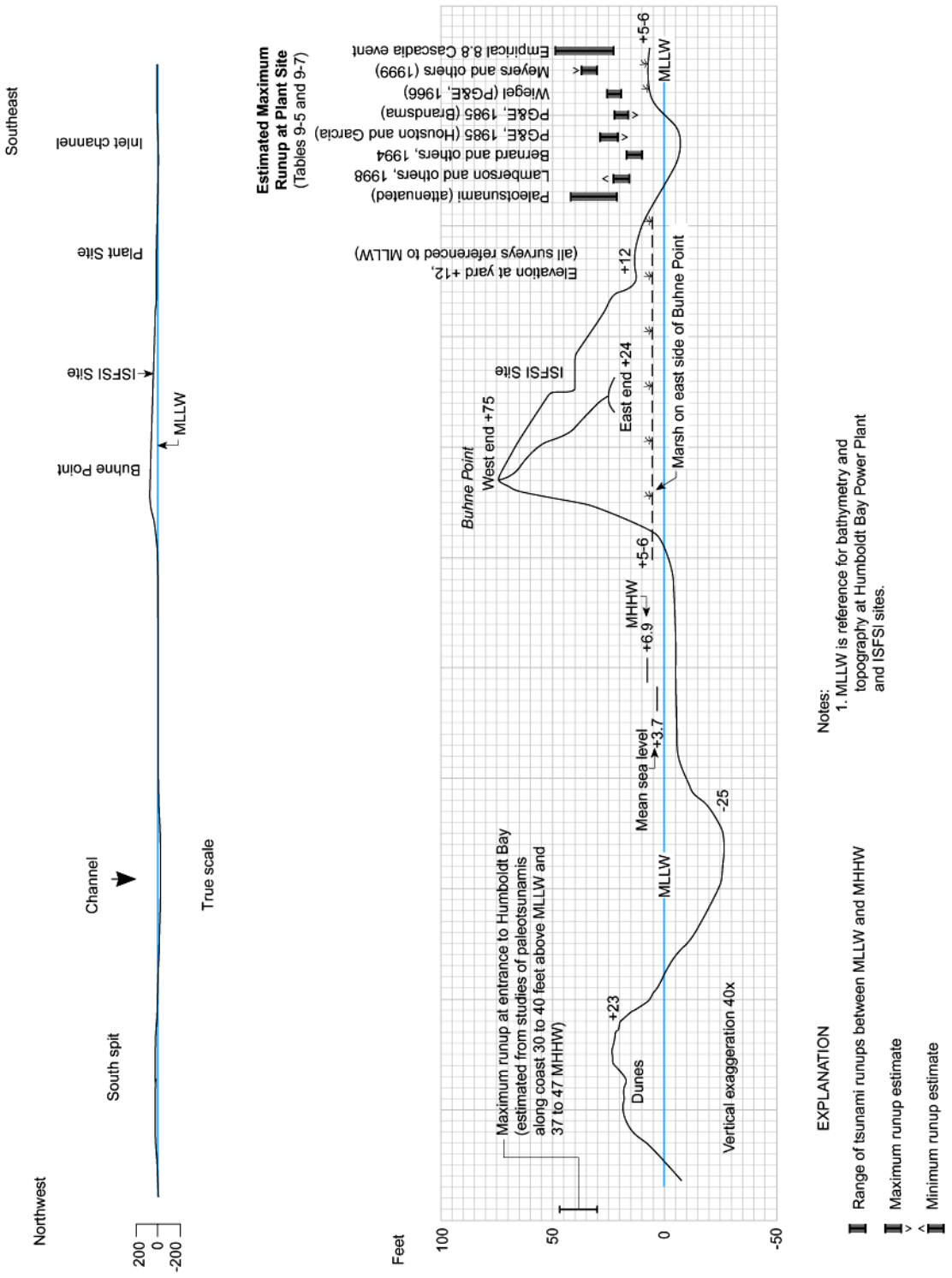

(SAR Figure 2.6-120)

Figure 1-7 Schematic cross section of Buhne Hill showing estimated runup heights of potential Cascadia tsunami

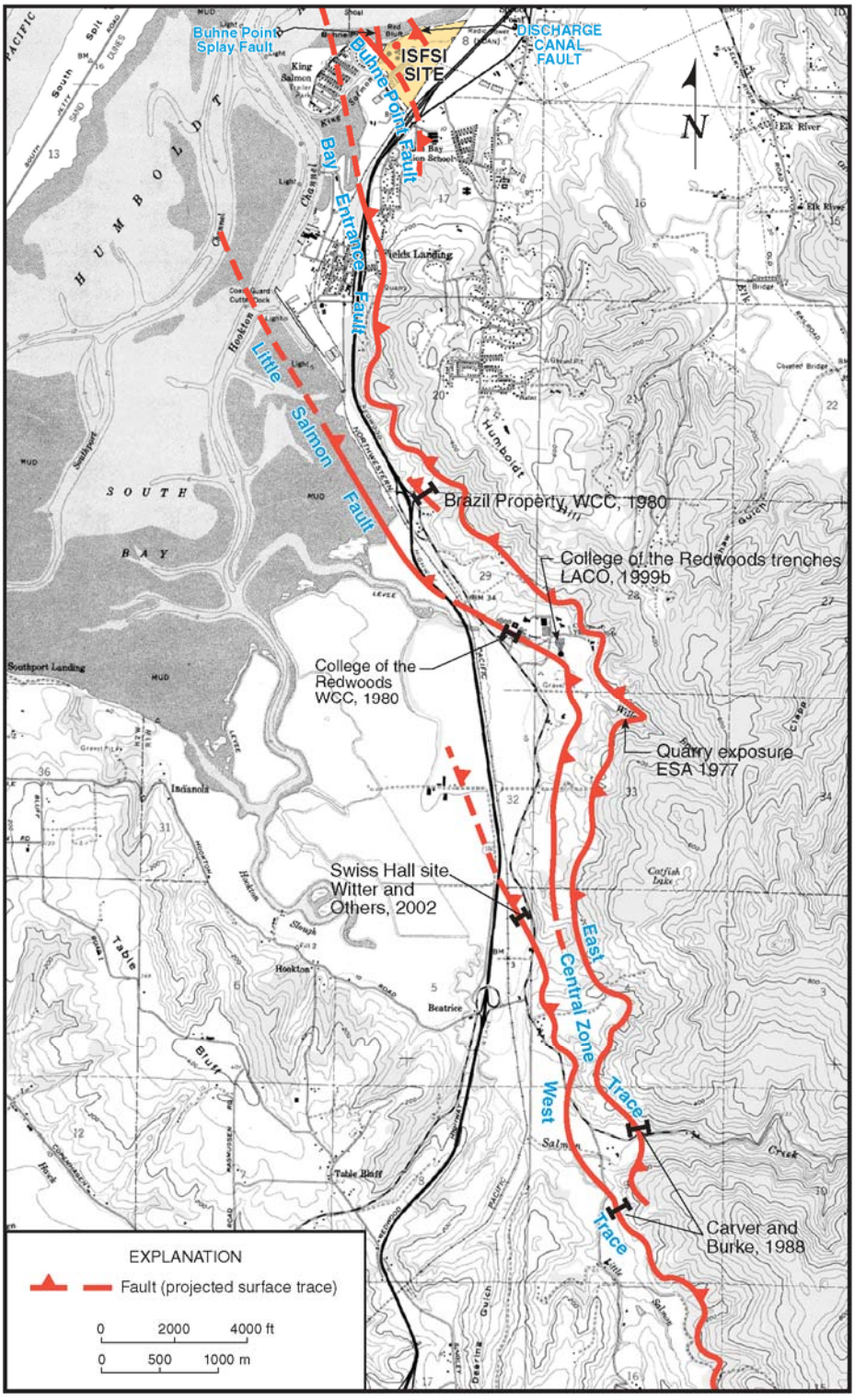

(SAR Figure 2.6-18)

Figure 2-1 Surface traces of the Little Salmon fault zone south of the ISFSI site

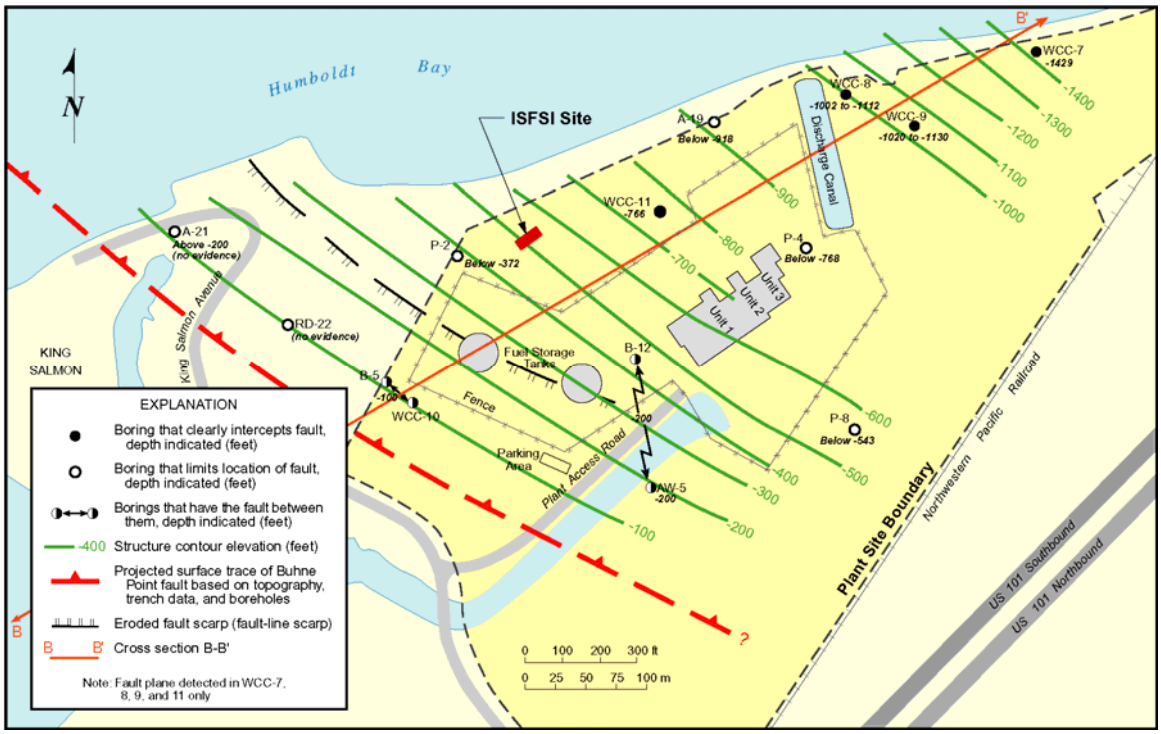

(SAR Figure 2.6-50)

Figure 2-2 Structure contour map on Buhne Point fault

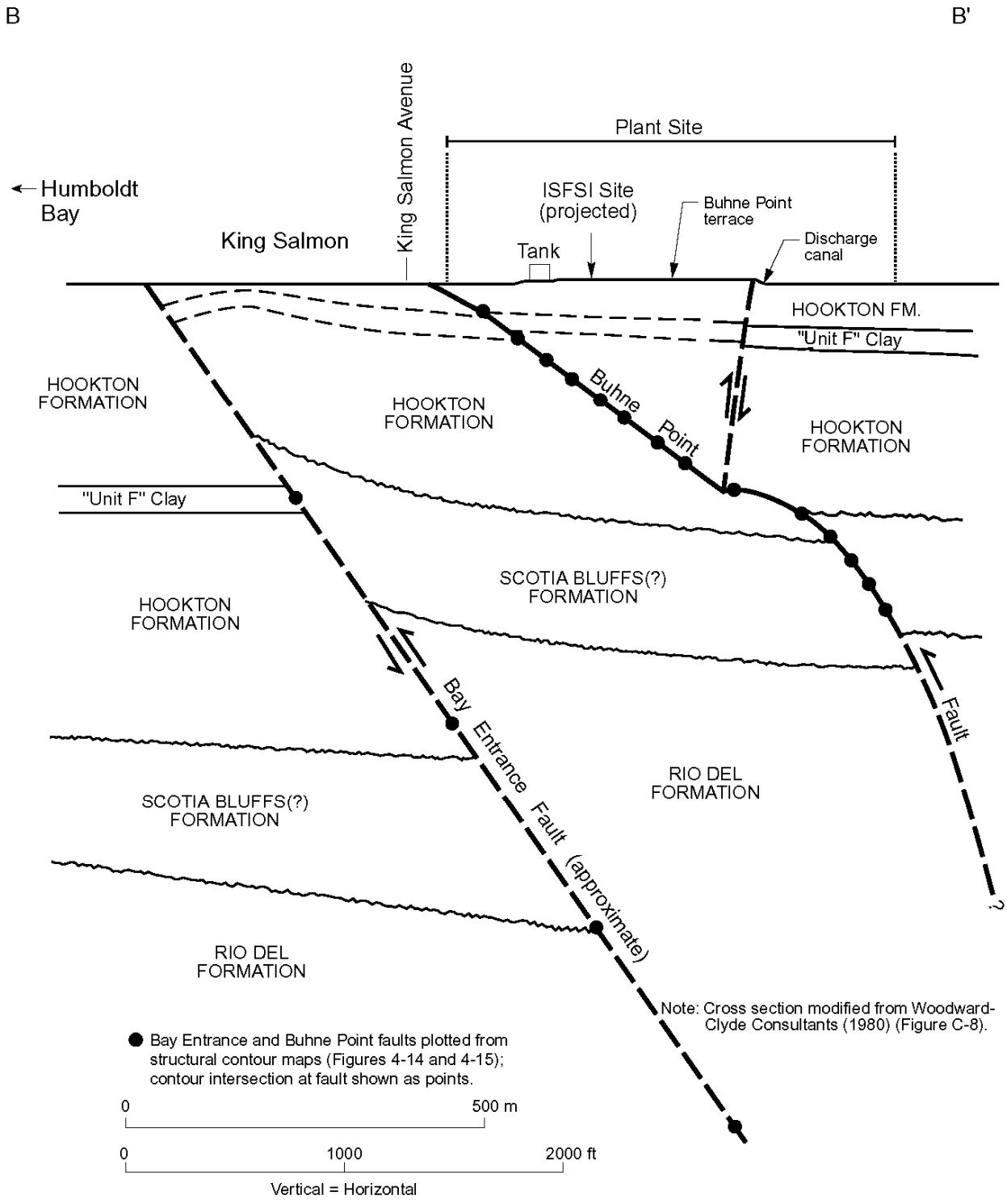

(SAR Figure 2.6-47)

Figure 2- 3 Cross section B-B’ across the Bay Entrance and Buhne Point faults

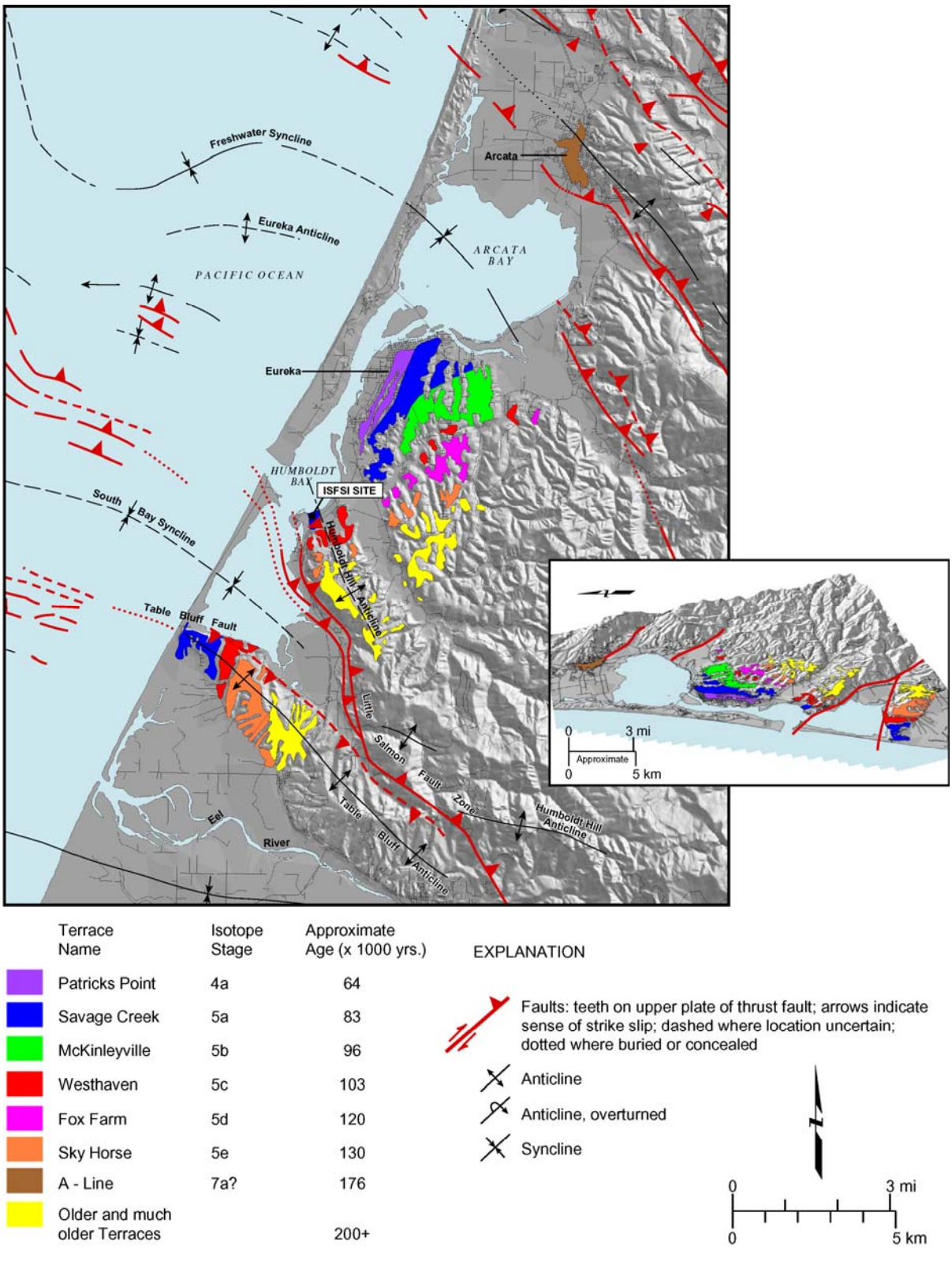

(SAR Figure 2.6-17)

Figure 2-4 Marine terraces around Humboldt Bay

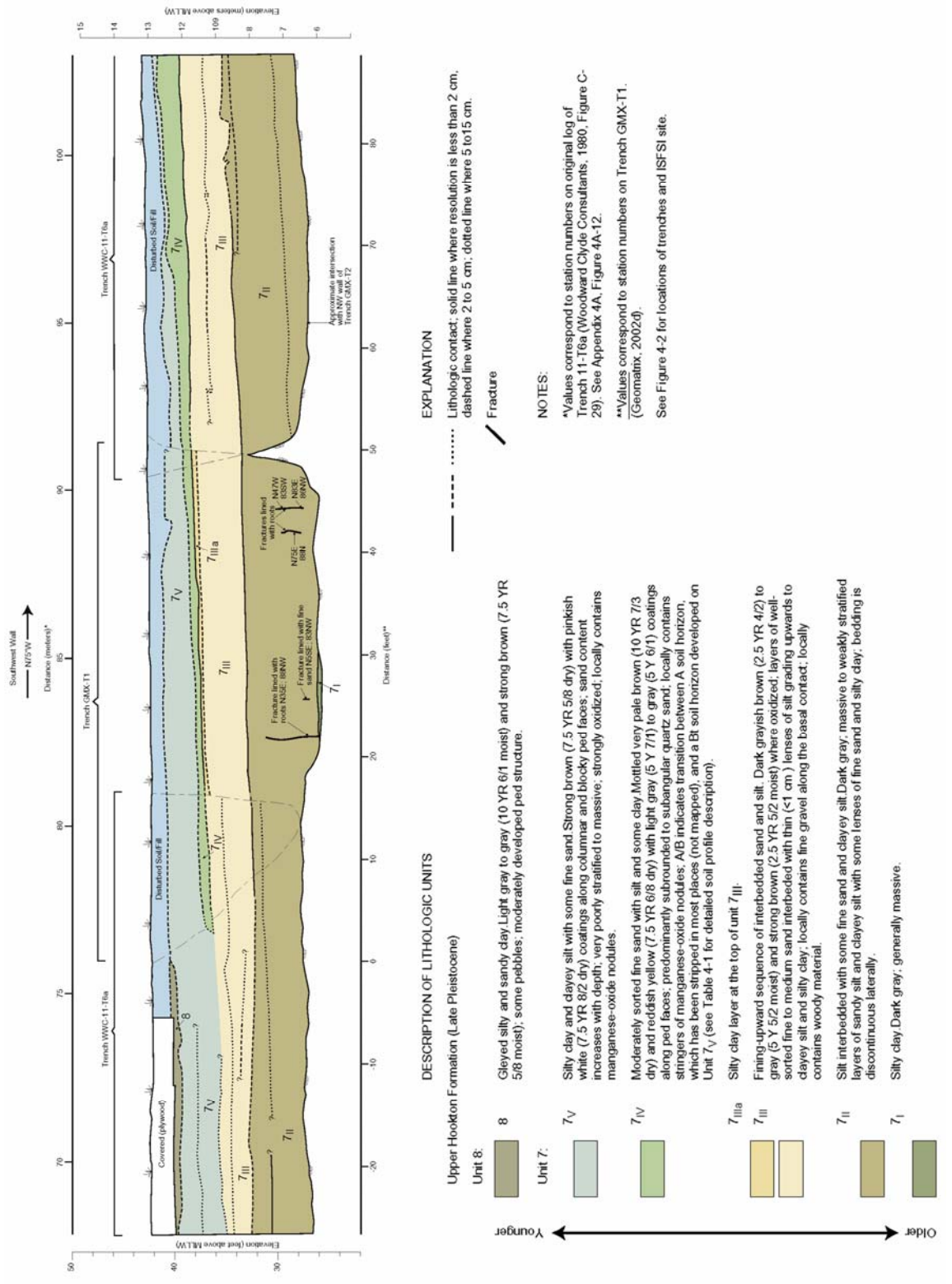

(SAR Figure 2.6-42)

Figure 2-5 Composite log of trenches WCC-11T6a and GMX-T1 on Stage 5a terrace in Hookton Formation

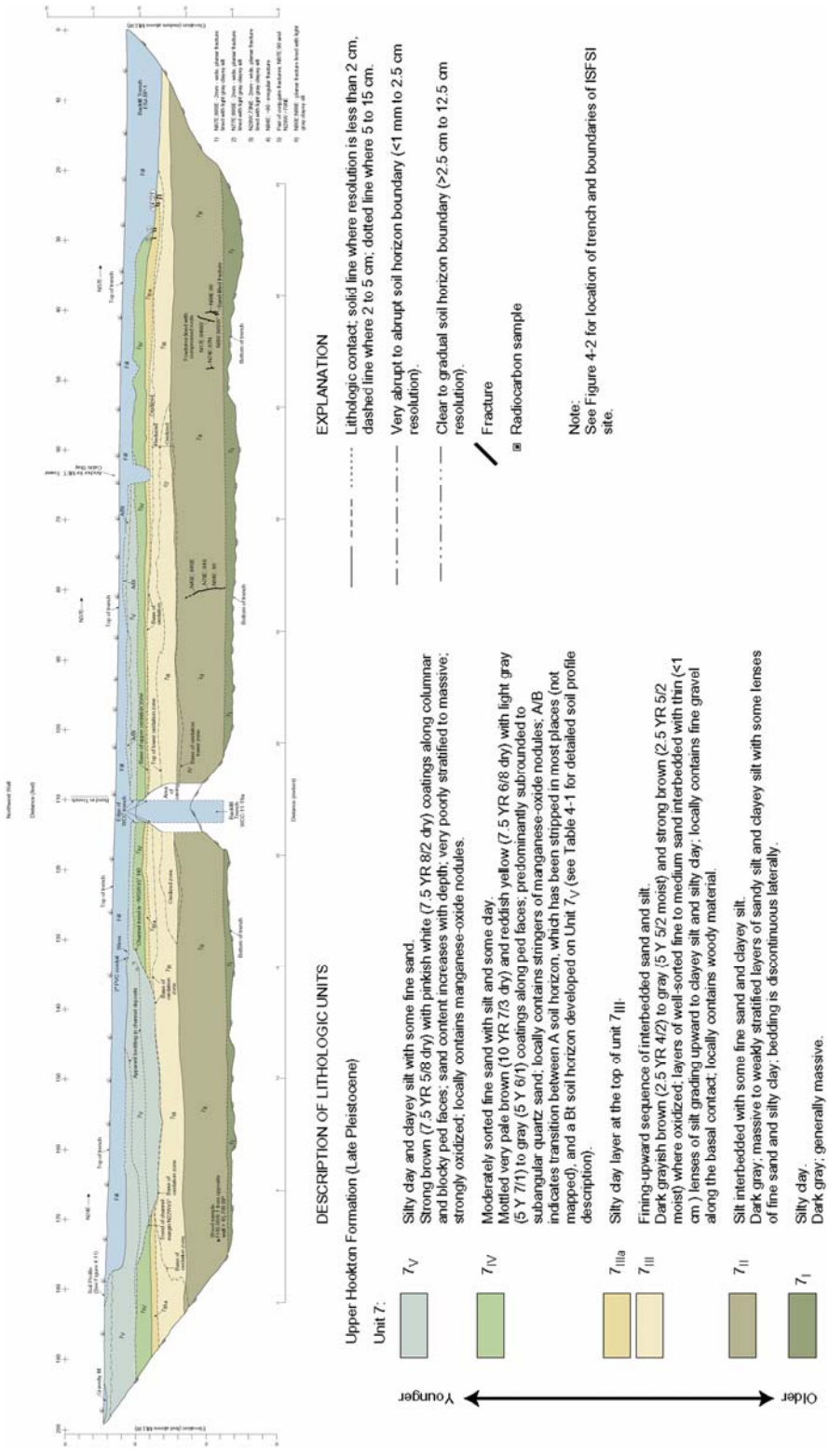

(SAR Figure 2.6-43)

Figure 2-6 Log of trench GMX-T2 on Stage 5a terrace in Hookton Formation

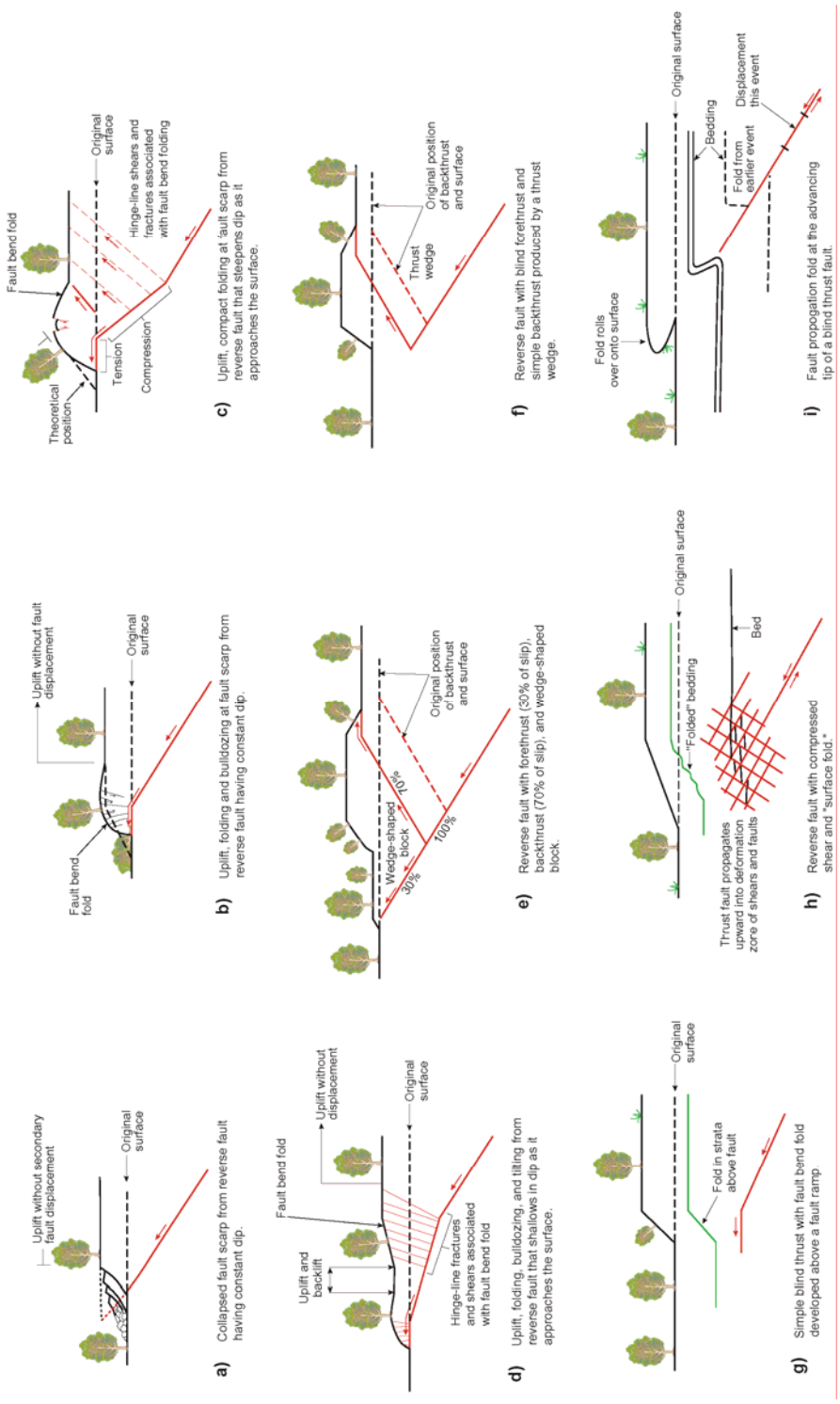

(SAR Figure 2.6-73)

Figure 2-7 Typical types of surface faulting associated with thrust faults

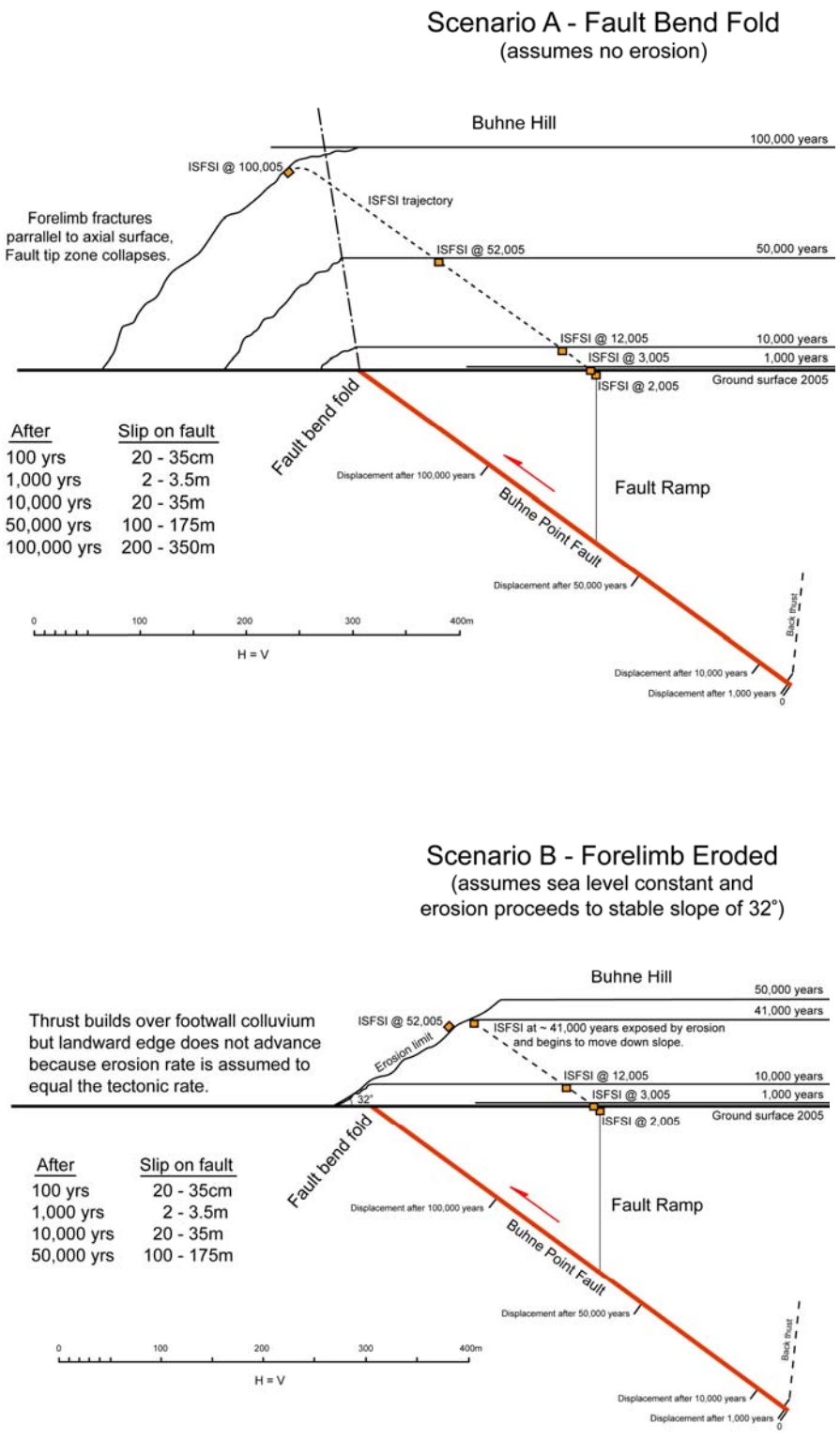

Figure 2-8 Schematic diagrams of the position of the ISFSI after various fault displacements

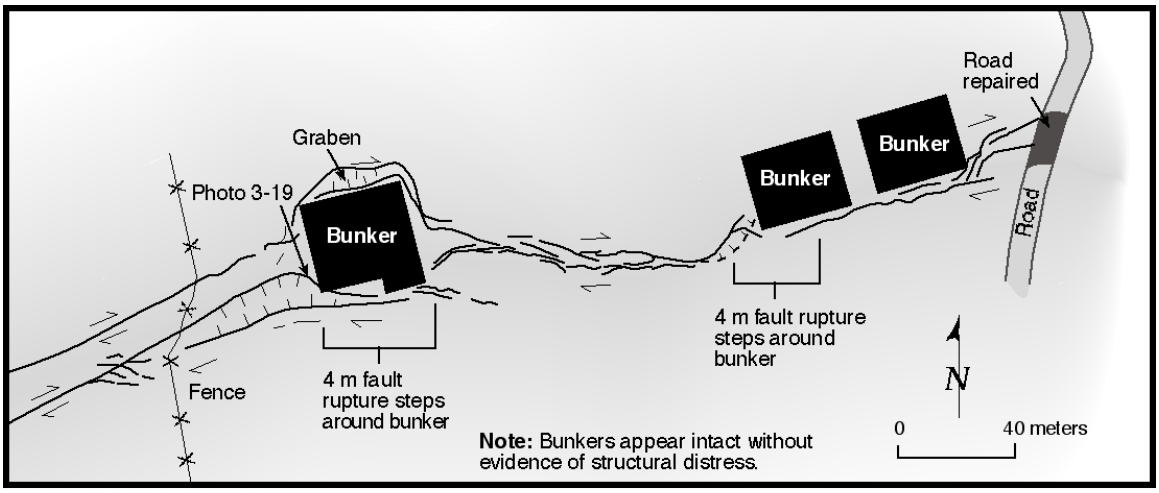

(from Youd and others, eds., 2000)

Figure 2-9 Map of concrete bunkers within the Anatolia fault after the 1999 Kocaeli earthquake, Goleuk, Turkey

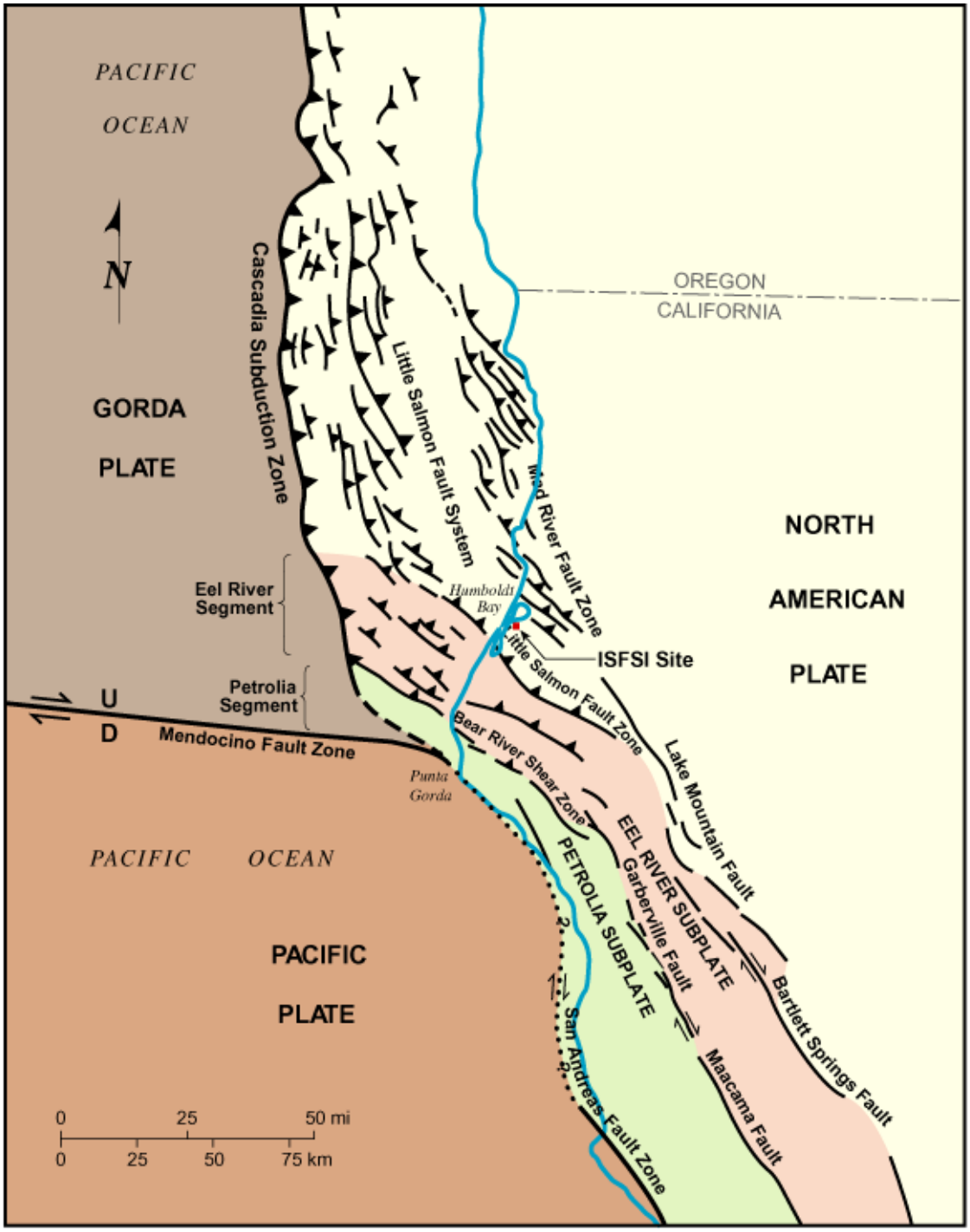

(SAR Figure 2.6-6)

Figure 3-1 Map of the Cascadia subduction zone and major faults in the northwestern California

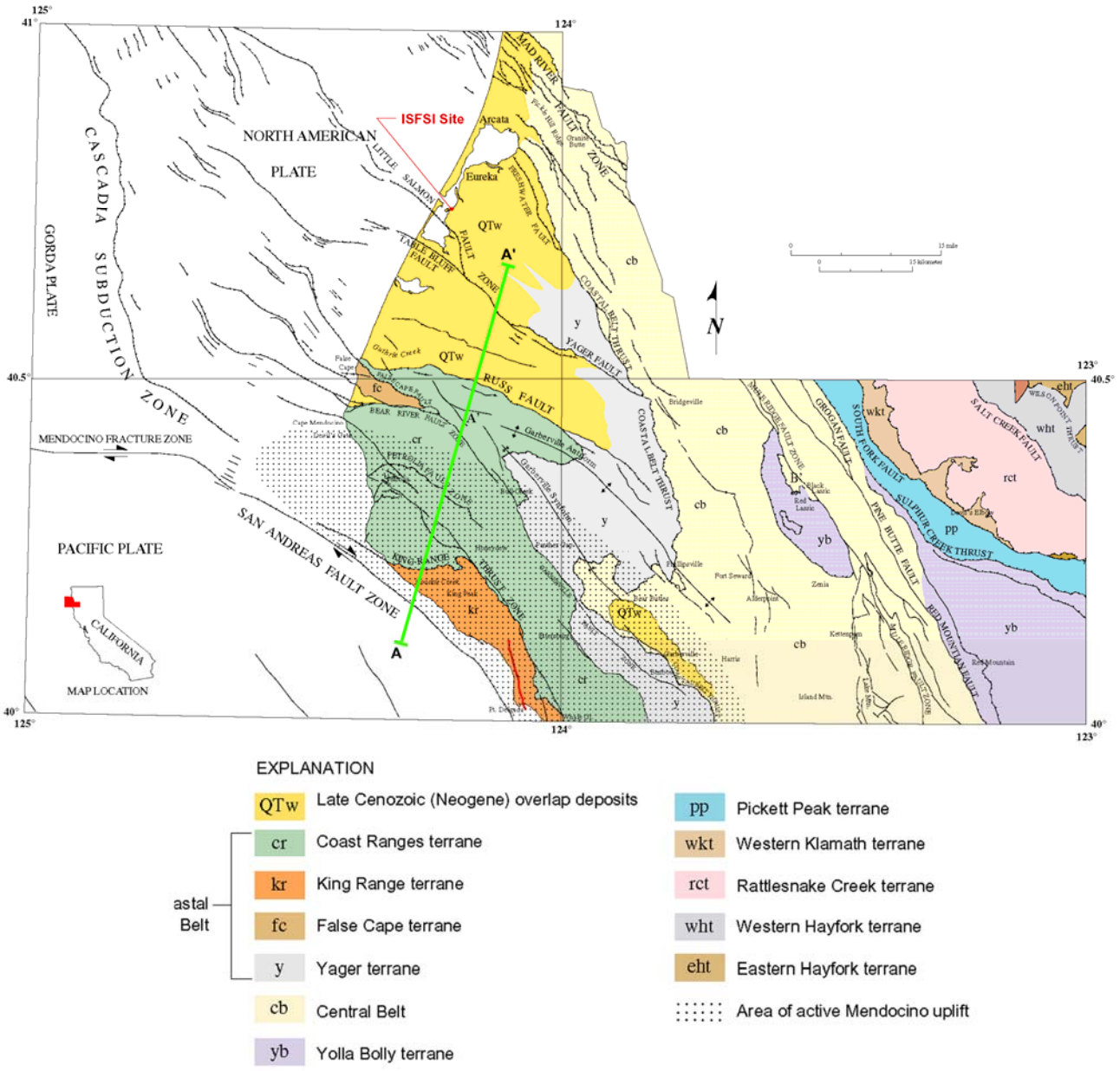

(SAR Figure 2.6-11)

Figure 3-2 Generalized geologic map on the Humboldt Bay region showing principal folds and faults

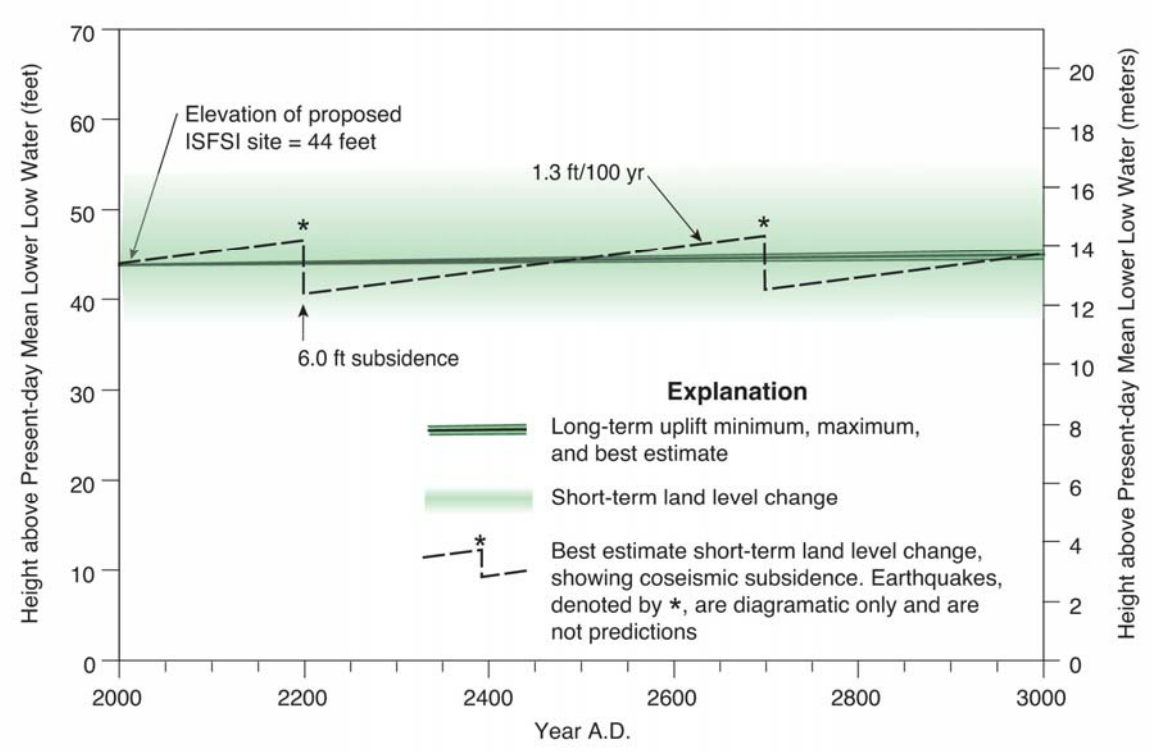

Dashed saw tooth black line represents a conservative estimate of short-term land level change, which has an interseismic uplift rate of 1.3 feet per 100 years (4 mm/yr) interrupted by abrupt subsidence of about 6 feet (1.8 m) during major earthquakes. The solid black lines bounding the dark green background show long-term tectonic uplift at a rate of 0.7 to 1.7 feet per thousand years (0.25 to 0.5 mm/yr) with the center line representing the best estimate rate of 1.4 feet per thousand years (0.4 mm/yr). Uncertainty in short-term changes in land level due to abrupt coseismic uplift or subsidence, or due to gradual interseismic uplift or subsidence, are indicated by the area shaded in light green. Other estimates of interseismic land-level change, based on GPS data (Williams, 2002) and geologic and survey data (G. Carver, personal communication, 2005), are lower, and some data sets suggest low rates of interseismic subsidence. These lower rates suggest lesser amounts of cosesismic subsidence, or even coseismic uplift, at Buhne Hill (G. Carver, personal communication, 2005). Coseismic slip is accommodated by subsidence of South Bay. This alternative lies close to the narrow dark green band for Buhne Hill.

Figure 3-3 Forecasted land-level change at the ISFSI site over the next 1000 years

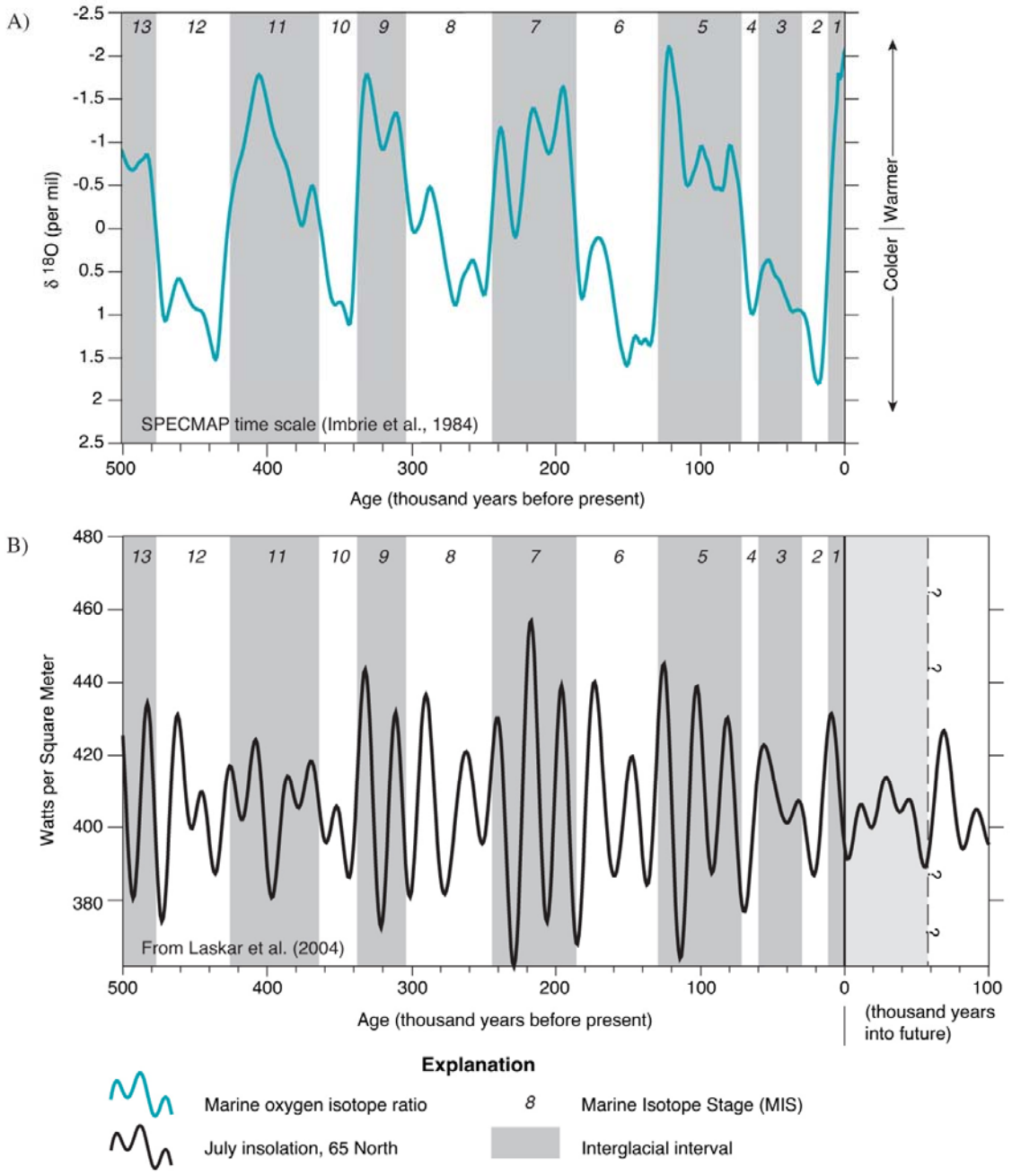

A) Marine oxygen isotope record of deep-sea sediments, from Imbrie and others (1984).

B) Solar insolation curve for 65 degrees North latitude in July. Insolation curve for the next 100,000 years also is shown (from Laskar and others, 2004). Grey shaded areas are major interglacial stages. Typically, several glacial-interglacial substages occur within each major interglacial interval. A possible interglacial - glacial transition in about 50,000 years is indicated by the dashed and queried line.

Figure 3-4 Glacial-interglacial cycles of the past 500,000 years

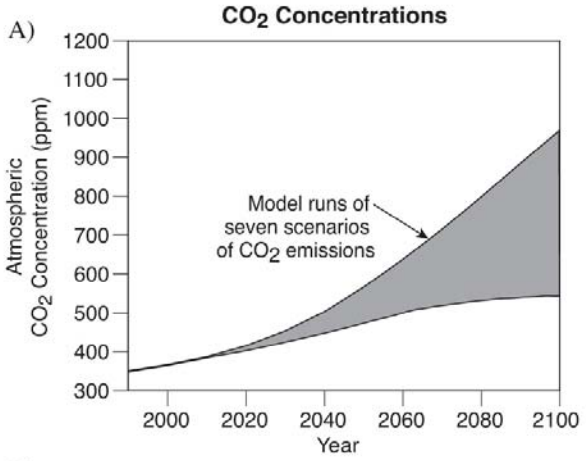

Modified from Figure 3.12, IPCC (2001)

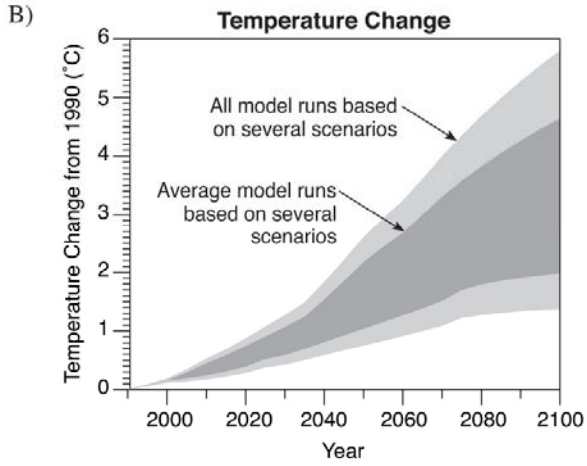

Modified from Figure 9.14, IPCC (2001)

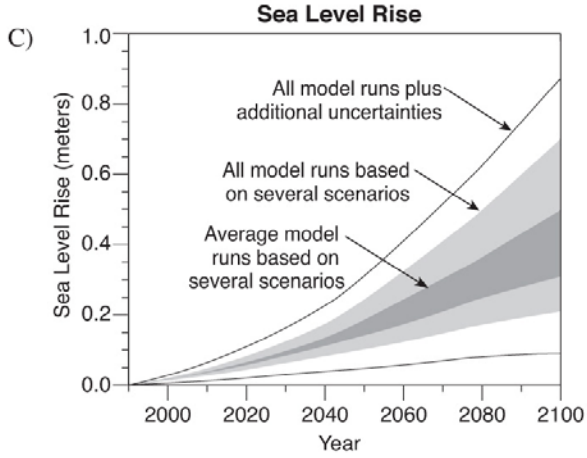

Modified from Figure 11.12, IPCC (2001)

Projected increases in CO_2 emissions are expected to cause increases in global temperature and sea level.
(A) Forecasted rise in atmospheric CO_2 concentration based on seven CO_2 emissions scenarios.
(B) Forecasted rise in global mean annual temperature.
(C) Forecasted rise in global sea level. Outer envelope includes additional uncertainties in meltwater contribution from glaciers and ice sheets not included in the climate models.

Figure 3-5 Forecasted climate change and sea level rise over the next 100 years

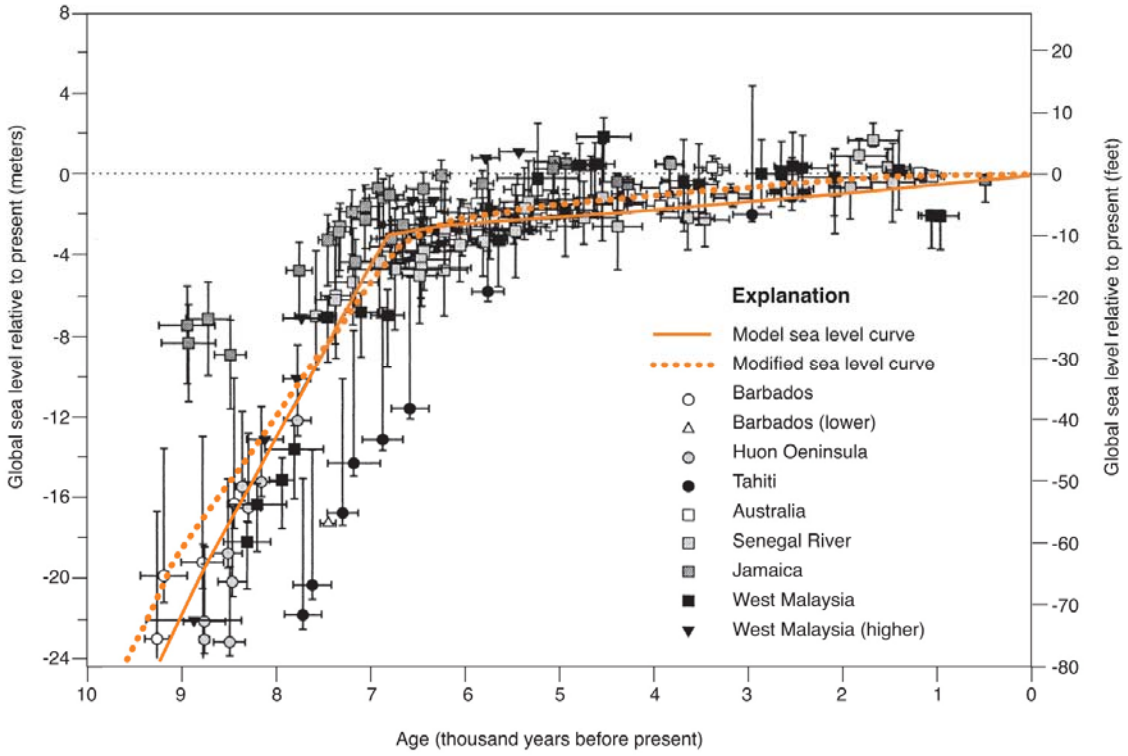

(Modified from Fleming and others, 1998)

Reconstructed sea level curve for the Holocene based on data from coral reefs at several sites around the globe. Solid line is modeled sea level. Dotted line represents a modified sea level curve based on subjective screening of the data.

Figure 3-6 Holocene sea level history

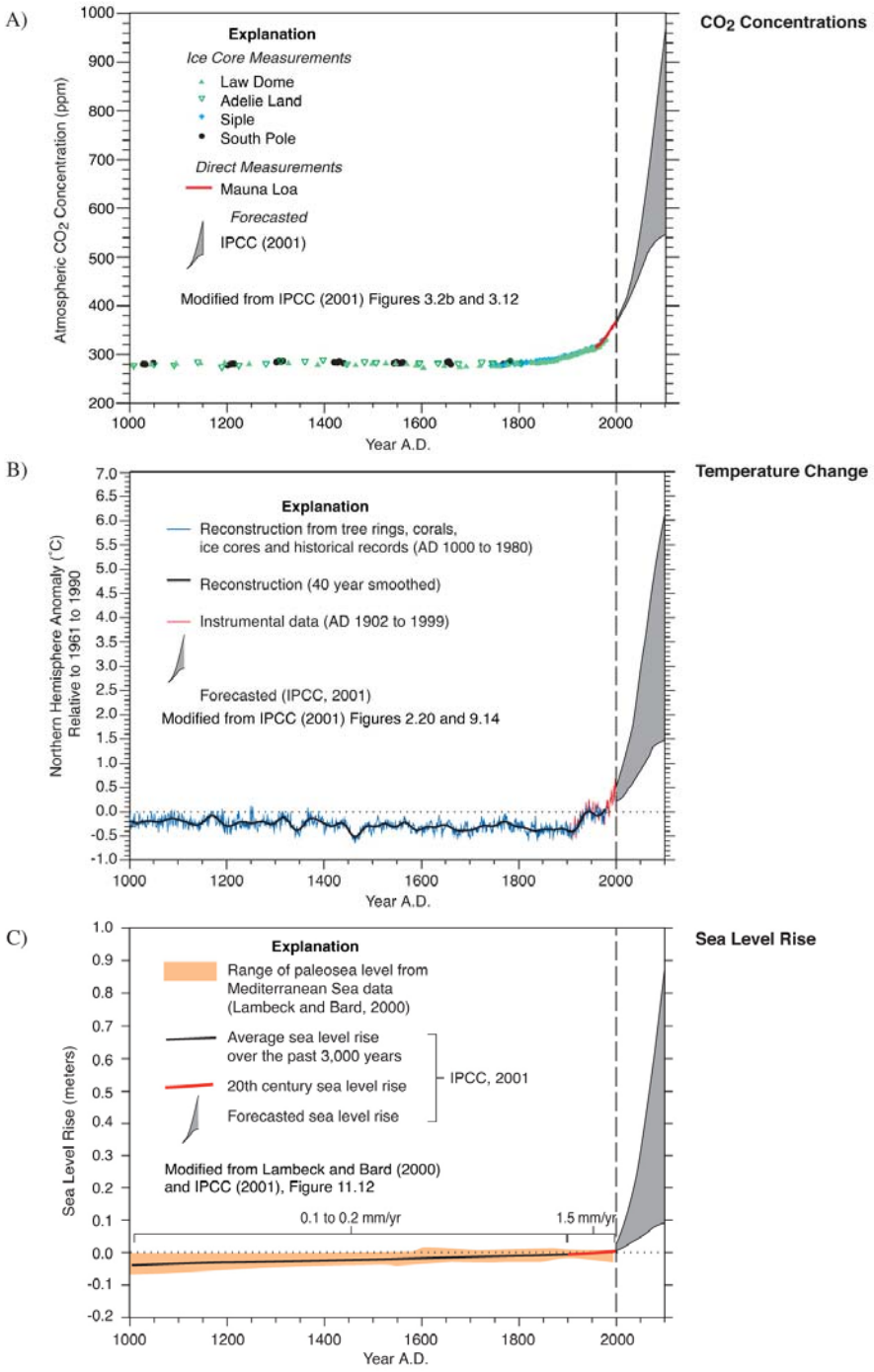

Climate change over the past 1000 years and forecasted for the next 100 years, based on data presented in IPCC (2001).
A) Changes in atmospheric CO_2 concentration.
B) Changes in northern hemisphere temperature.
C) Changes in global sea level.

Figure 3-7 Climate change over the past 1000 years and forecasted for the next 100 years

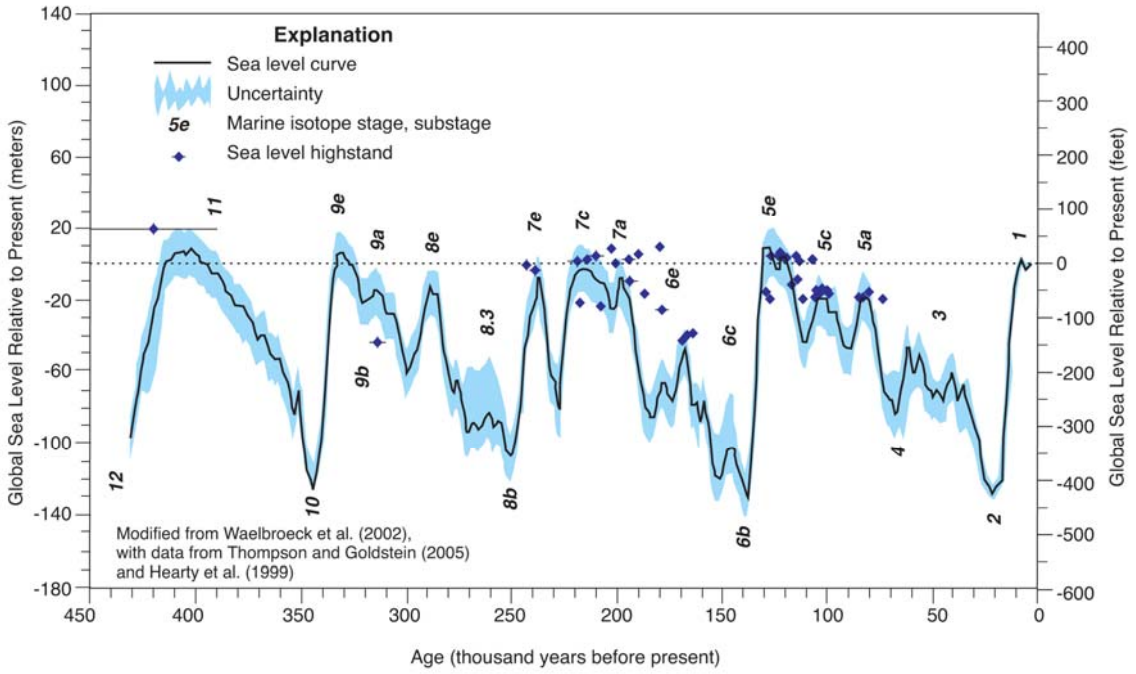

(Modified from Waelbroeck and others, 2000).

Reconstructed sea level curve, 430,000 years ago to the present. The black sea level curve with blue shaded uncertainty is a composite of Atlantic and Pacific ocean core data, corrected for changes in ocean temperature. The numbers next to the curve are marine isotope stage and substage names. Symbols with uncertainty bars are sea level highstand data from coral reefs and beach deposits. Curve from Waelbroeck and others (2002) Coral highstand data from Thompson and Goldstein (2005) and references therein, and Hearty and others (1999).

Figure 3-8 Sea level history over the past 500,000 years

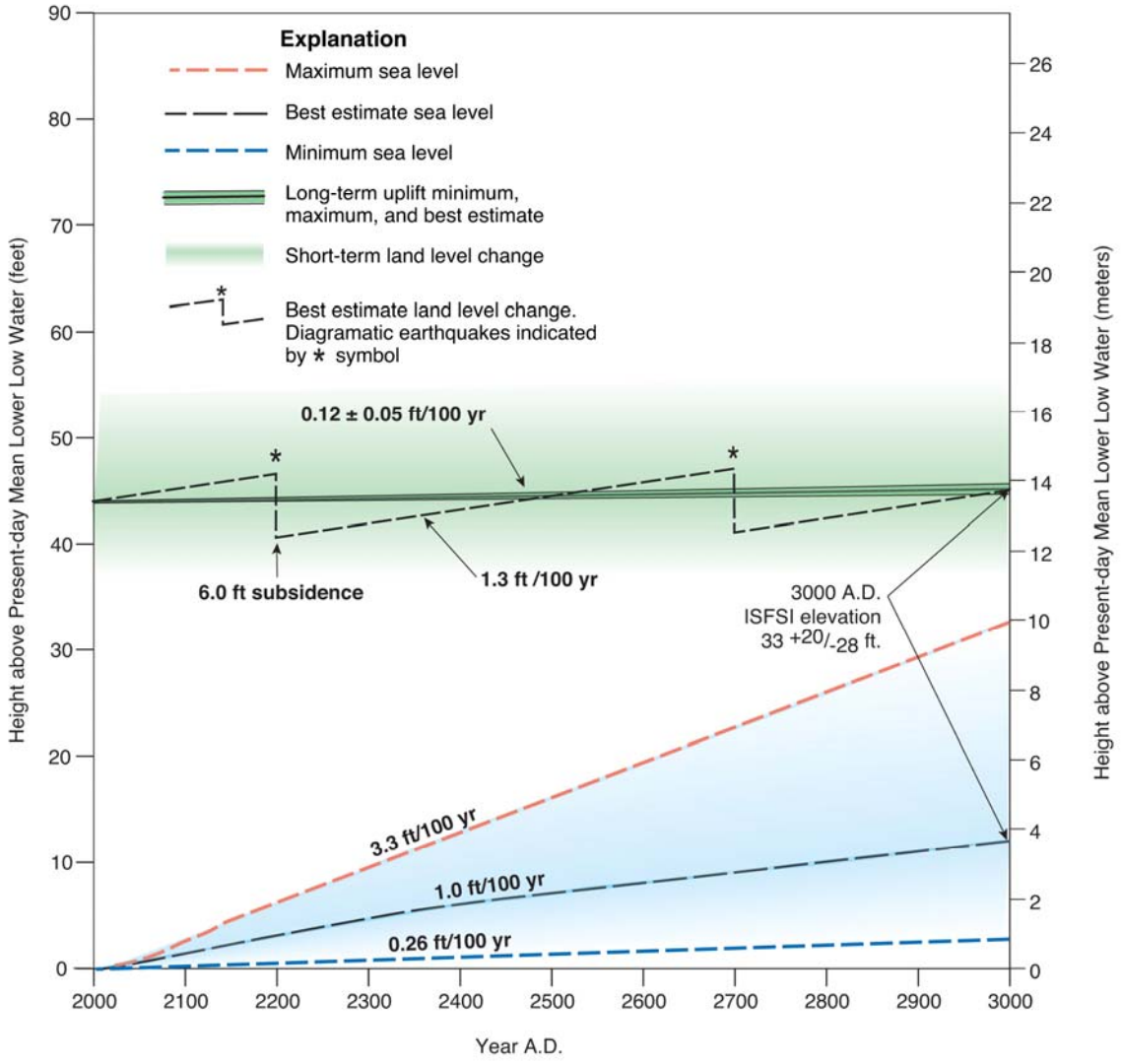

Figure 3-9 Forecasted changes in relative sea level at Buhne Hill over the next 1000 years.

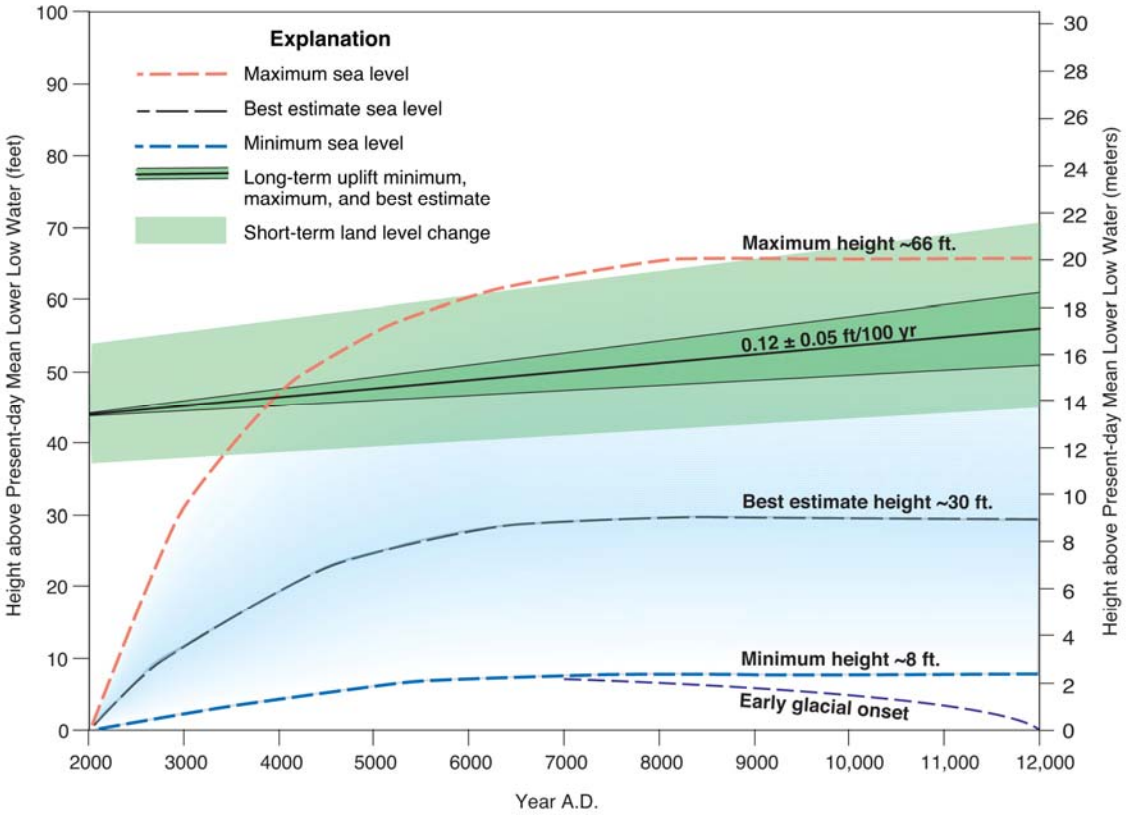

Figure 3-10 Forecasted changes in relative sea level at Buhne Hill over the next 10,000 years

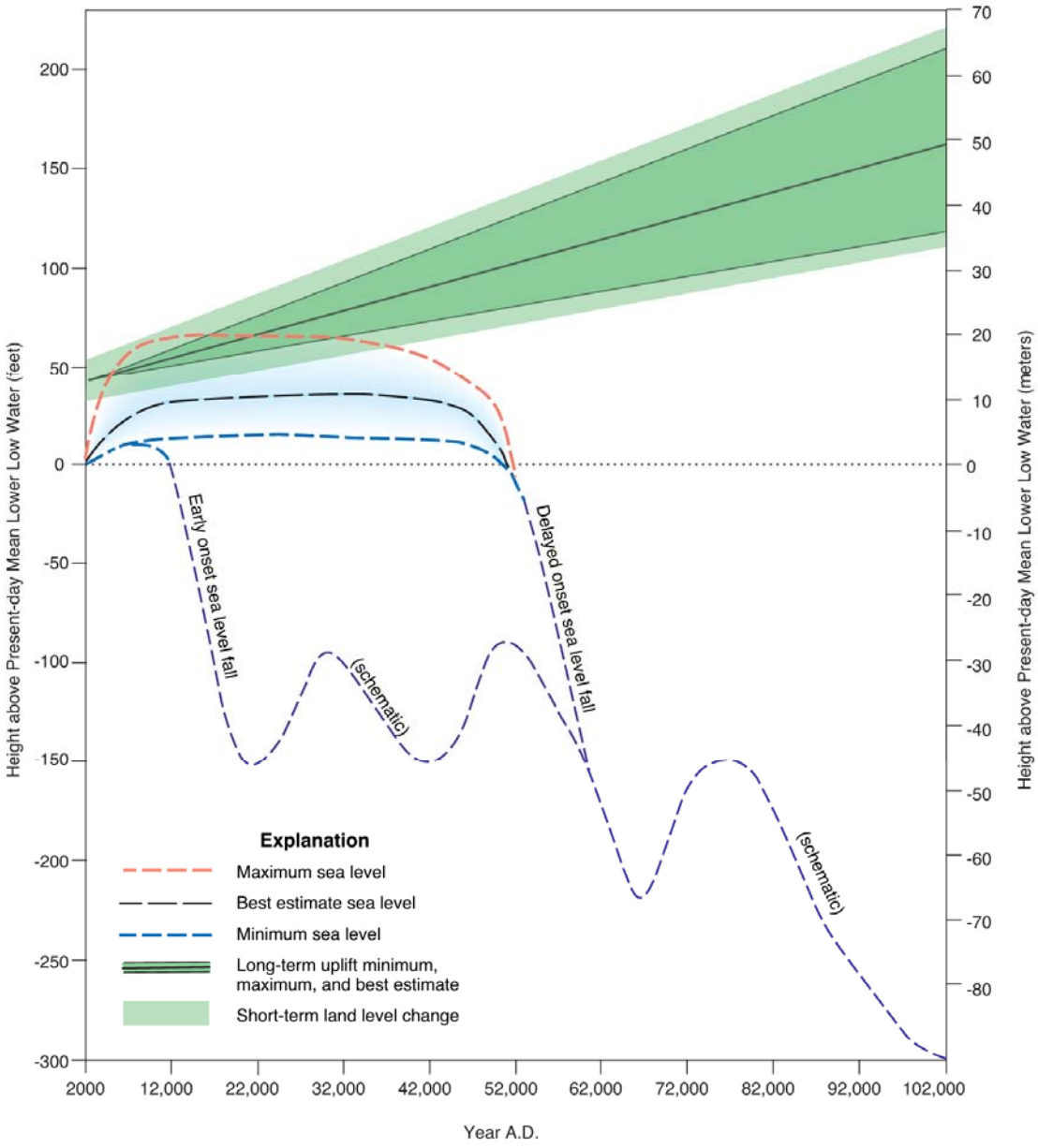

Figure 3-11 Forecasted changes in relative sea level at Buhne Hill over the next 100,000 years.

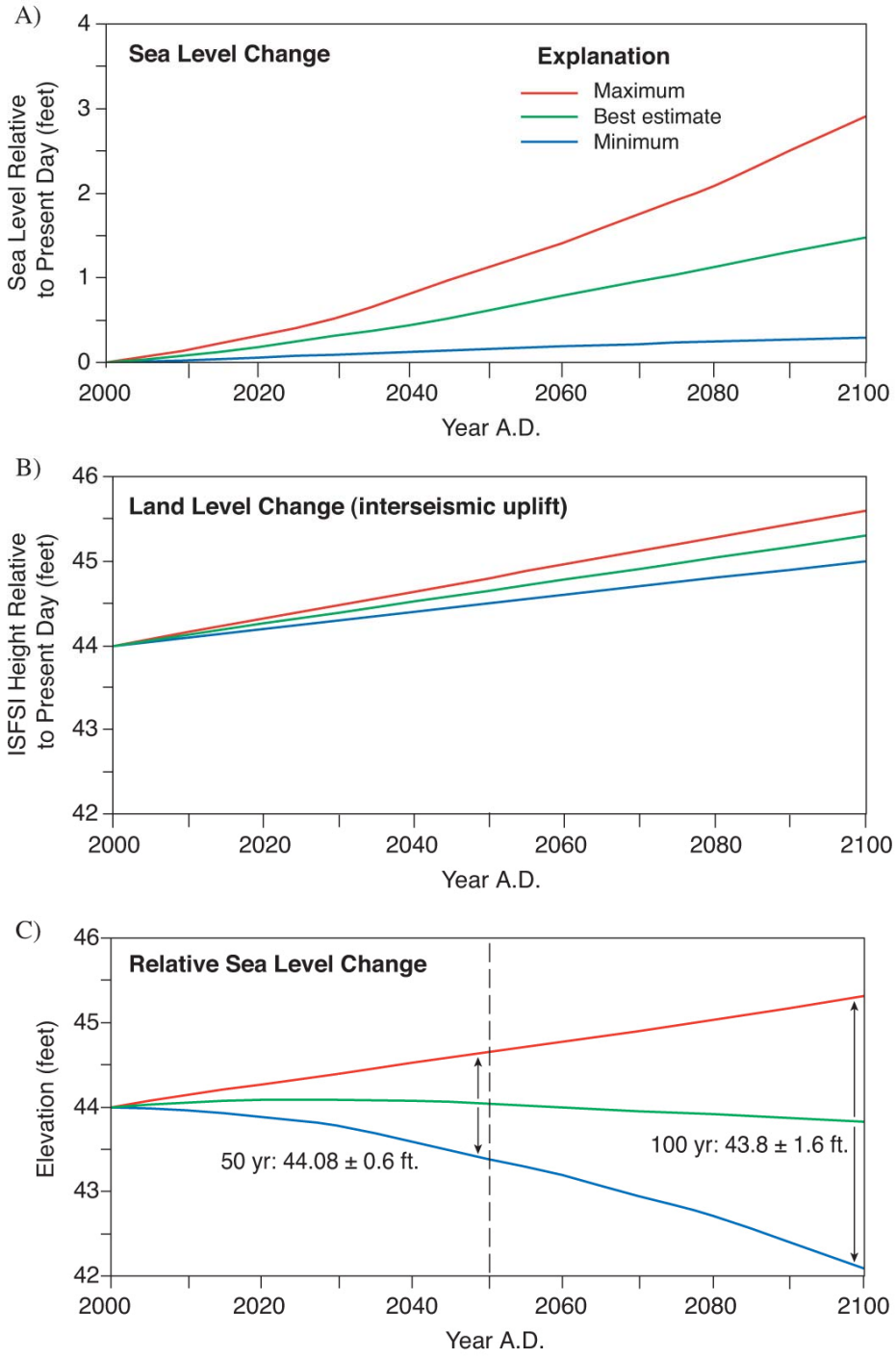

A) Forecasted sea level change from IPCC (2001).
B) Forecasted land level change based on interseismic uplift rates from Mitchell and others (1994).
C) Relative sea level change calculated as the difference between land level and sea level.
The curves assume no major earthquake on the Cascadia subduction zone or Little Salmon fault zone over this time period.

Figure 3-12 Forecasted changes in relative sea level at Buhne Hill over the next 100 years

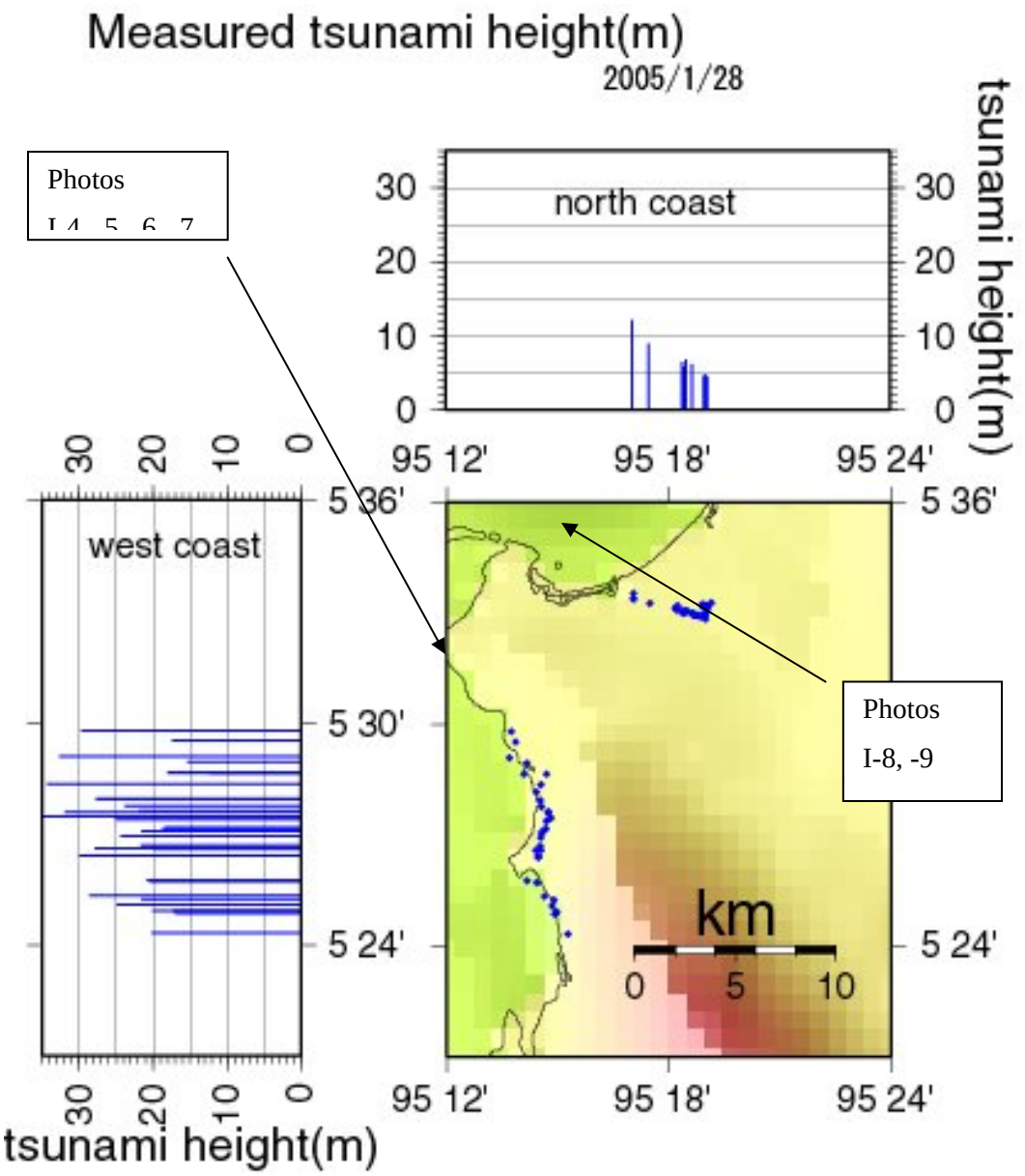

(modified from Dengler, 2005)

Figure 4-1 Map of observed coastal run up values for the December 26, 2004 Sumatra tsunami

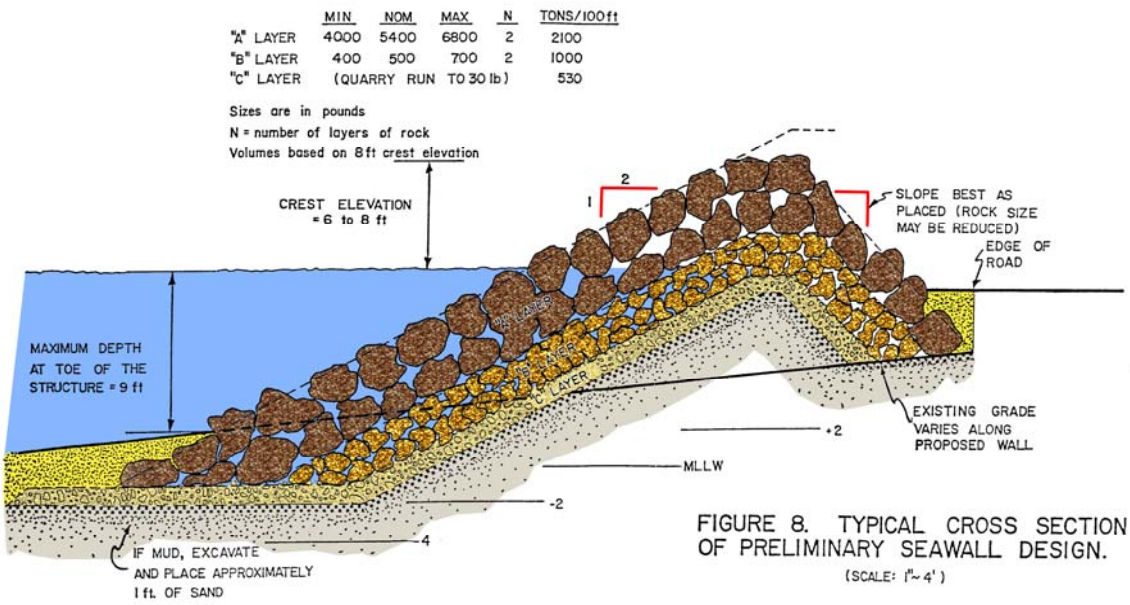

FIGURE 8. TYPICAL CROSS SECTION OF PRELIMINARY SEAWALL DESIGN.
(SCALE: 1"~4')

Field inspection of the berm in 2005 indicates that the berm was placed close to existing grade on a thin layer of bay sand (sand flat) that covers the underlying consolidated sand, silt and clay beds of the Pleistocene Hookton Formation.

Figures 5-1 Schematic diagram of general design for Red Bluff berm 1989 repair

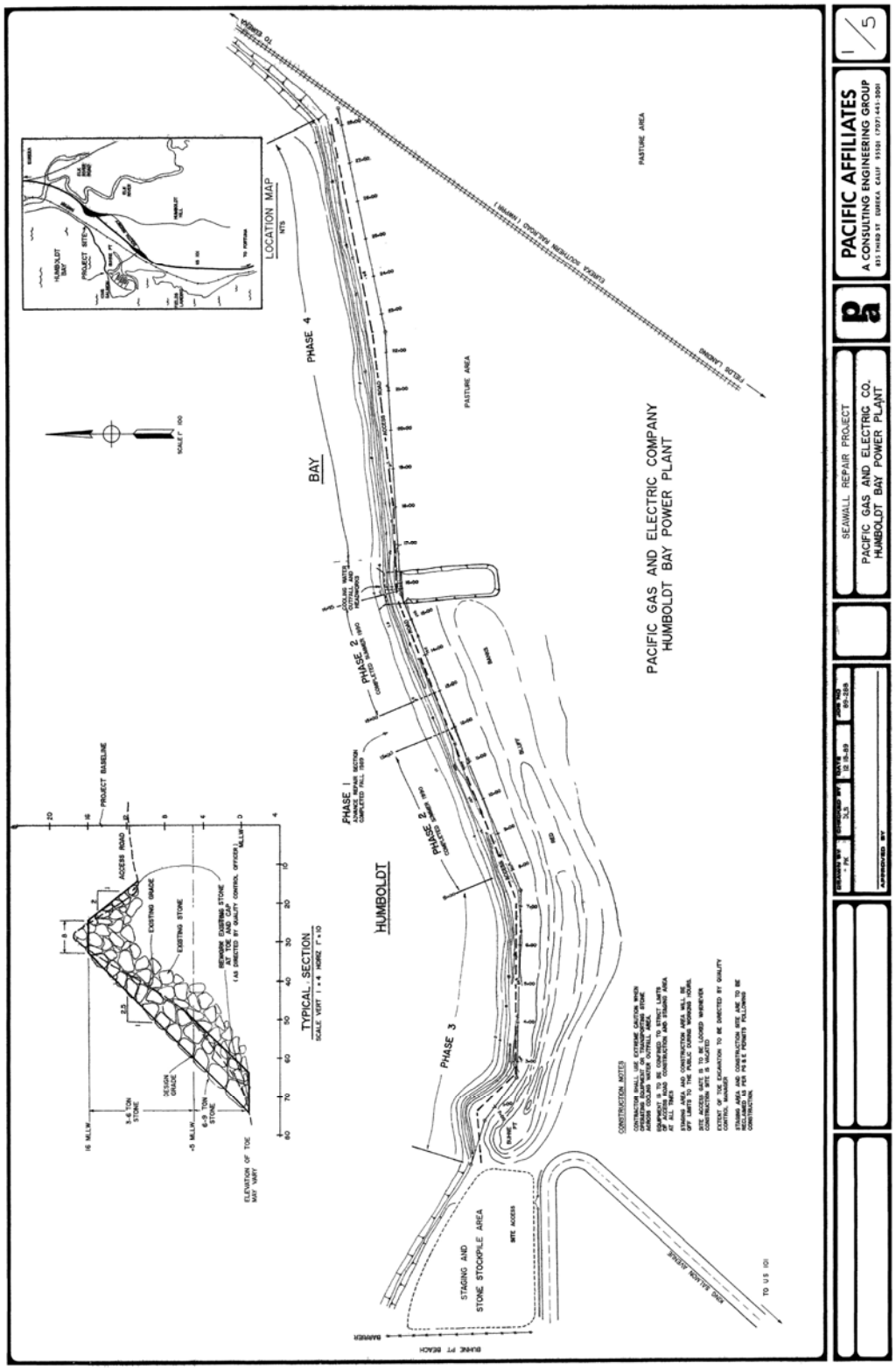

Figure 5-2 Design plan, page 1, for 1989 repairs to Red Bluff berm

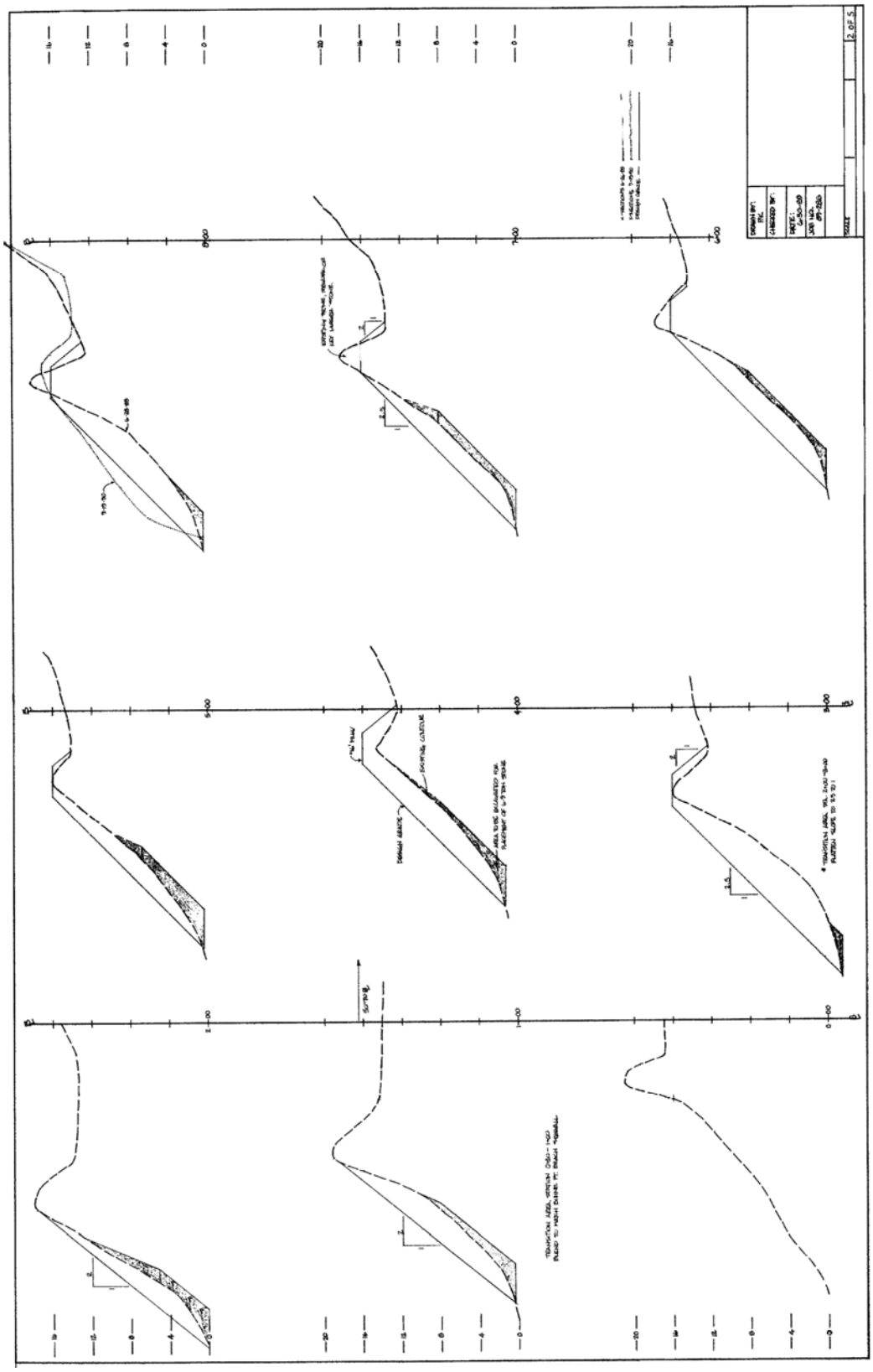

Figure 5-3 Design cross sections, page 2, for 1989 repairs to Red Bluff berm

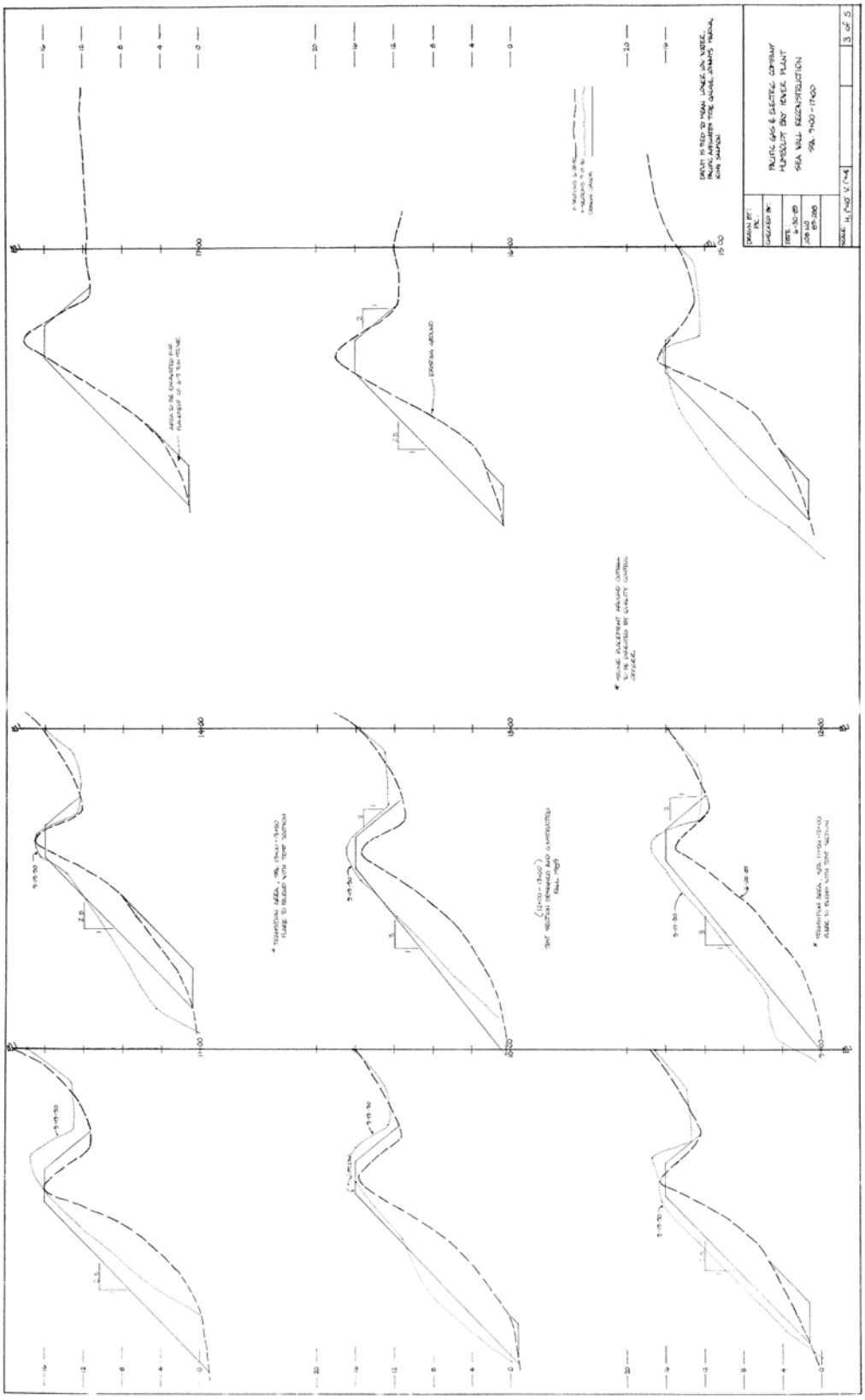

Figure 5-4 Design cross sections, page 3, for 1989 repairs to Red Bluff berm

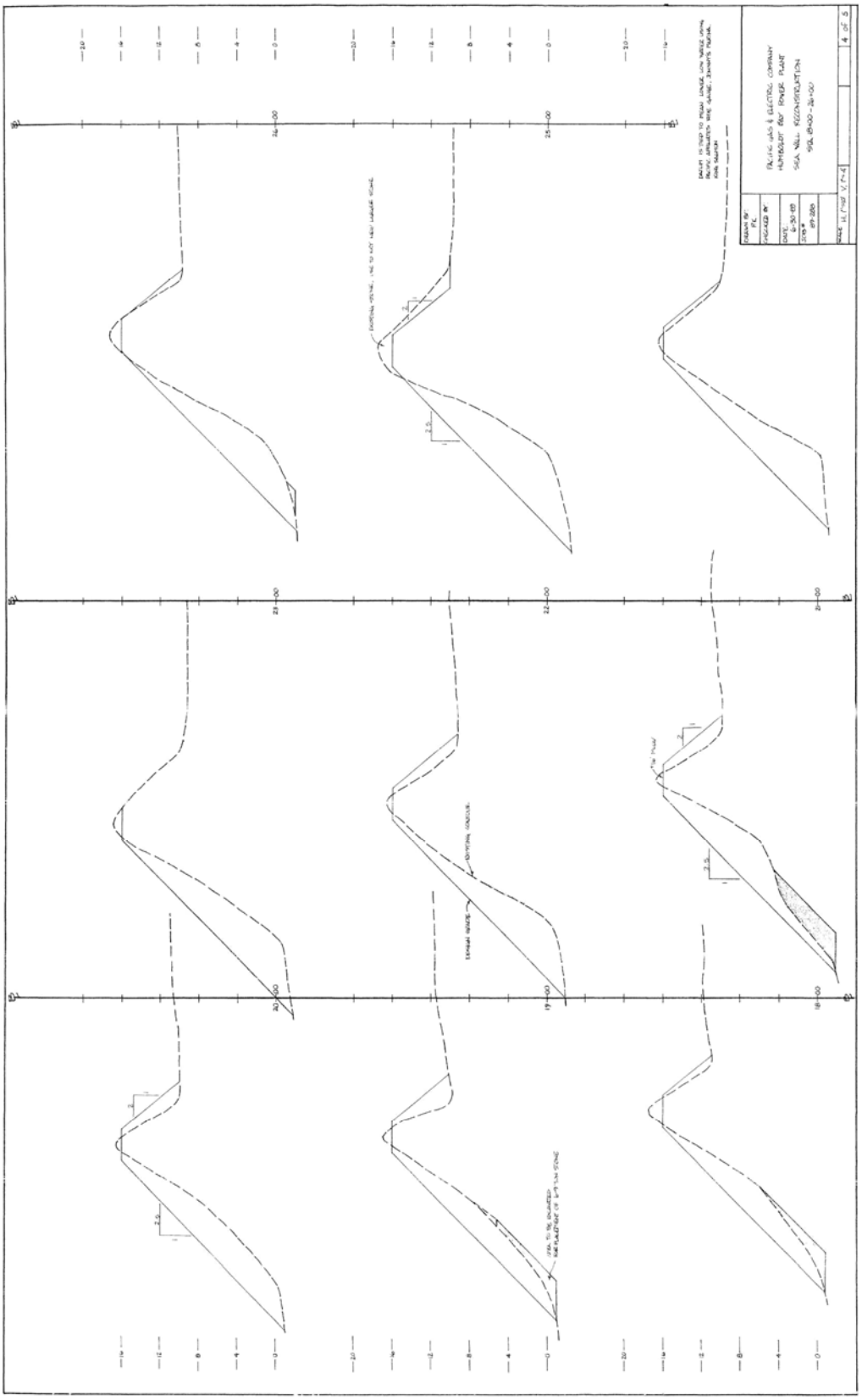

Figure 5-5 Design cross sections, page 4, for 1989 repairs to Red Bluff berm

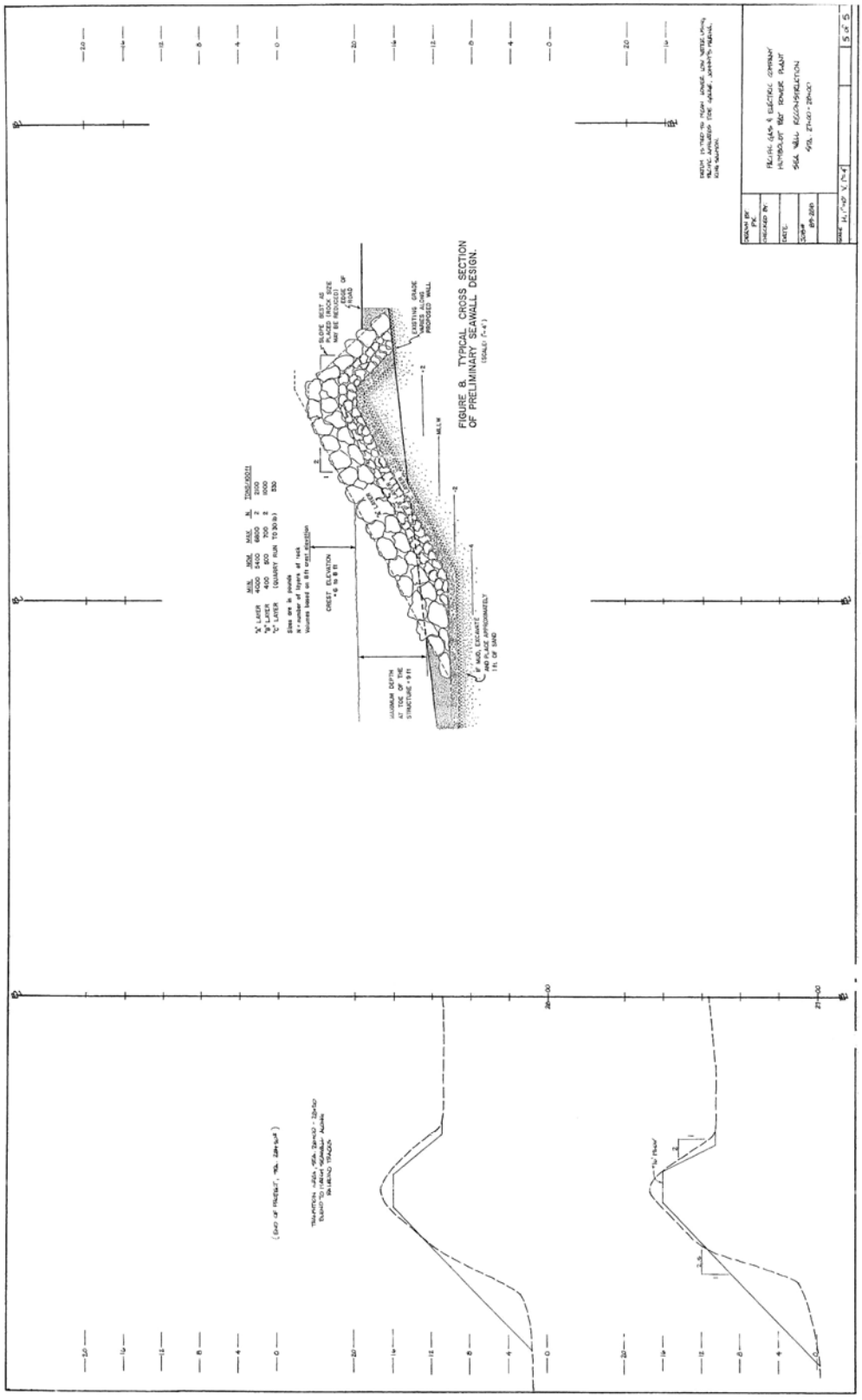

Figure 5-6 Design cross sections, page 5, for 1989 repairs to Red Bluff berm

View to southwest; the ISFSI site is below the 'e' in Buhne Hill (SAR Figure 2.6-29)

Photo 1-1 Aerial view of Buhne Hill and Red Bluff

The rigid reinforced concrete building is tilted on the forelimb at tip of fault-bend fold (WDP 2000)

Photo 2-1 Fault-bed fold with tilted building on Chelungpu fault, near Fengyuan, Taiwan

A) Fault bend fold appears as flexure on the floor of a building destroyed by surface faulting during the 1999 Chi-Chi earthquake.

B) Shears and fractures in wall over the fault bend fold shown above in Photo 8-3A.

(SAR Figure 2.6-81)

Photo 2-2 Fault bed fold and associated fractures on Chelungpu fault, Fengyuan, Taiwan

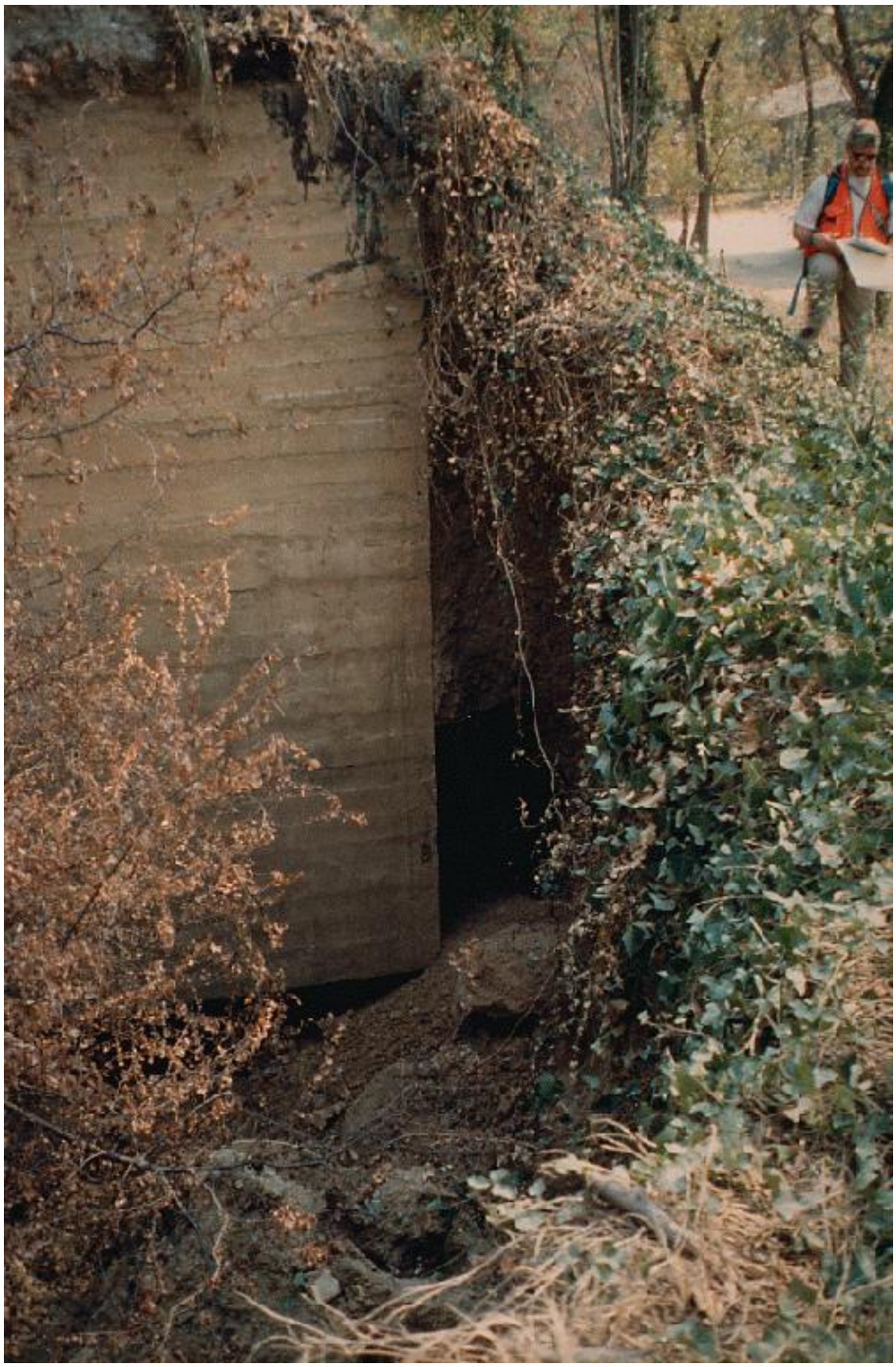

Right lateral displacement of over 2 meters displaced the soil around the bunker. The bunker twisted, but did not crack. (WDP 2000)

Photo 2-3 Soil deformed around concrete bunkers during the 1999 Kocaeli earthquake on the Anatolia fault, Goleuk, Turkey

Cliff face stripped of trees and vegetation from the December 26, tsunami. The average elevation of trim line is ~20 meters along the coast. Note that the road bed and drainage ditch are not eroded or damaged. (SN 5/2005)

Photo 4-1 Tsunami trim line near Lhoknga, Sumatra

The buildings have been swept away but the foundation is intact and has little damage. (SN 5/2005)

Photo 4-2 Building foundation pad in tsunami run up zone north of Lhoknga, Sumatra

LaFarge cement plant is in the background. Tsunami wave run up at this location was measured to be 38.9 meters (~128 feet) (SN 5/2005)

Photo 4-3 Beached coal barge and tug boat along the coastal road in Lhoknga, Sumatra

The curtain walls of the building were damaged, but the superstructure is intact. (SN 5/2005)

Photo 4-4 Tsunami damage to the LaFarge cement plant at Lhoknga, Sumatra

The 10 MW diesel plant was floated 3 km from the coast to its present site by the Dec 26 tsunami.
(SN 5/2005)

Photo 4-5 PLN electric generator barge in center of Banda Aceh, Sumatra

(SN 5/2005)

Photo 4-6 Fishing boat lodged on top of house in Banda Aceh, Sumatra

View to northeast from Buhne Point (WDP 6/25/05)

Photo 5-1 Riprap berm in front of Red Bluff

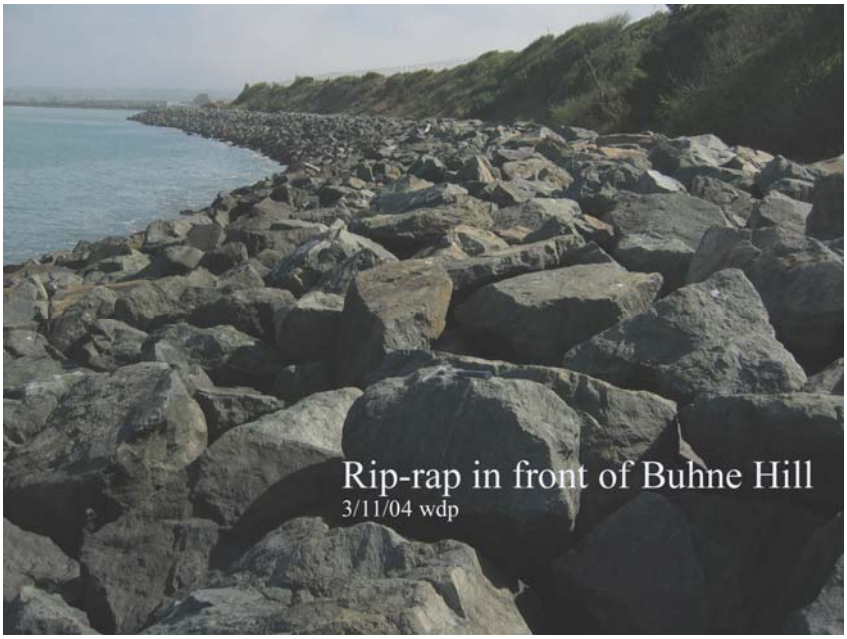

View to northeast (WDP 3/11/04)

Photo 5-2 Typical riprap berm in front of Red Bluff near Buhne Point

View to southwest with Buhne Point in the distance (LSC 5/4/05)

Photo 5-3 Typical riprap berm in front of Red Bluff

View to northeast showing topple block and sand at base in middle distance (WDP 3/11/04)

Photo 5-4 Toe of riprap berm in front of Red Bluff

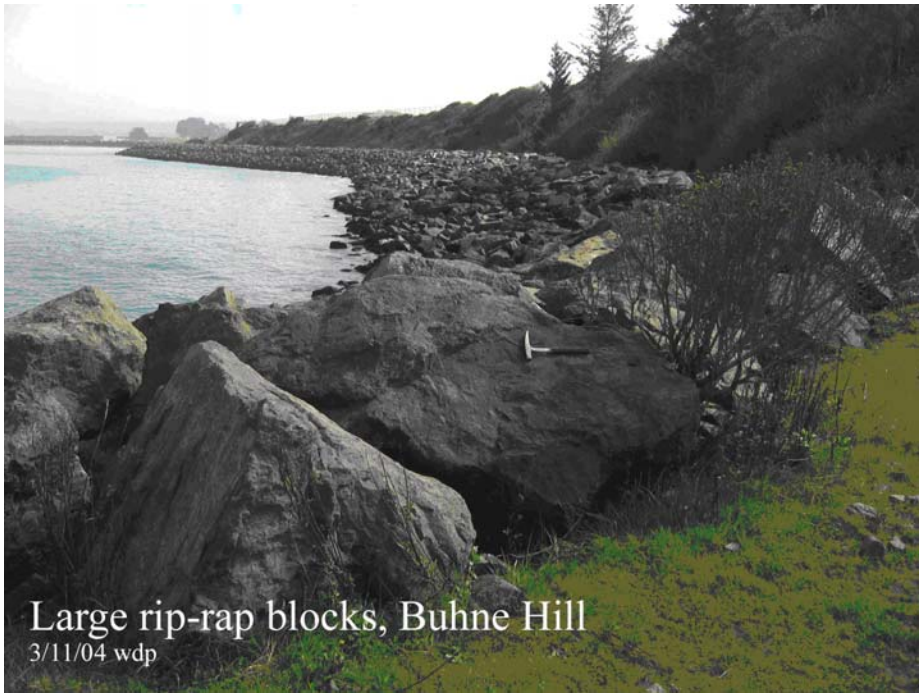

(WDP 3/11/04)

Photo 5-5 Example of large blocks of riprap in berm near Buhne Point

Ron Flick and Walt Crampton are measuring the stones (WDP 6/25/05)

Photo 5-6 Twenty degree slope of riprap in berm in front of Red Bluff

(WDP 6/25/05)

Photo 5-7 Sand layer at base of riprap in berm in front of Red Bluff

(WDP 6/25/05)

Photo 5-8 Close up of sand layer at base of riprap in berm in front of Red Bluff

View to southwest with Buhne Point in the distance (LSC 5/4/05)

Photo 5-9 Area behind riprap berm at Buhne Hill

Swash has eroded local areas in rock along pathway. Buhne Point is in distance. (WDP 3/11/04).

Photo 5-10 Pathway between Red Bluff and the riprap berm

Hookton sandy-silt beds are exposed at feet of Ron Flick and Walt Crampton (WDP 6/25/05)

Photo 5-11 Eroded area from slosh and backwash exposing Hookton Formation

(LSC 5/4/05)

Photo 5-12 Toppled block from riprap berm at eroded area from slosh and backwash